

A THEORETICAL STUDY OF STEREOSELECTIVITY
IN THE DIELS-ALDER REACTION

CENTRE FOR NEWFOUNDLAND STUDIES

**TOTAL OF 10 PAGES ONLY
MAY BE XEROXED**

(Without Author's Permission)

JAMES DIMITRIOS XIDOS



001311



INFORMATION TO USERS

This manuscript has been reproduced from the microfilm master. UMI films the text directly from the original or copy submitted. Thus, some thesis and dissertation copies are in typewriter face, while others may be from any type of computer printer.

The quality of this reproduction is dependent upon the quality of the copy submitted. Broken or indistinct print, colored or poor quality illustrations and photographs, print bleedthrough, substandard margins, and improper alignment can adversely affect reproduction.

In the unlikely event that the author did not send UMI a complete manuscript and there are missing pages, these will be noted. Also, if unauthorized copyright material had to be removed, a note will indicate the deletion.

Oversize materials (e.g., maps, drawings, charts) are reproduced by sectioning the original, beginning at the upper left-hand corner and continuing from left to right in equal sections with small overlaps.

Photographs included in the original manuscript have been reproduced xerographically in this copy. Higher quality 6" x 9" black and white photographic prints are available for any photographs or illustrations appearing in this copy for an additional charge. Contact UMI directly to order.

Bell & Howell Information and Learning
300 North Zeeb Road, Ann Arbor, MI 48106-1346 USA

UMI[®]
800-521-0600



National Library
of Canada

Acquisitions and
Bibliographic Services

395 Wellington Street
Ottawa ON K1A 0N4
Canada

Bibliothèque nationale
du Canada

Acquisitions et
services bibliographiques

395, rue Wellington
Ottawa ON K1A 0N4
Canada

Your file / Votre référence

Our file / Notre référence

The author has granted a non-exclusive licence allowing the National Library of Canada to reproduce, loan, distribute or sell copies of this thesis in microform, paper or electronic formats.

The author retains ownership of the copyright in this thesis. Neither the thesis nor substantial extracts from it may be printed or otherwise reproduced without the author's permission.

L'auteur a accordé une licence non exclusive permettant à la Bibliothèque nationale du Canada de reproduire, prêter, distribuer ou vendre des copies de cette thèse sous la forme de microfiche/film, de reproduction sur papier ou sur format électronique.

L'auteur conserve la propriété du droit d'auteur qui protège cette thèse. Ni la thèse ni des extraits substantiels de celle-ci ne doivent être imprimés ou autrement reproduits sans son autorisation.

0-612-47505-0

Canada

**A Theoretical Study of Stereoselectivity
in the Diels-Alder Reaction**

by

James Dimitrios Xidos
B.Sc. (Chemistry and Applied Mathematics)

A thesis submitted to the
School of Graduate Studies
in partial fulfilment of the
requirements for the degree of
Doctor of Philosophy

Department of Chemistry
Memorial University of Newfoundland

July 30, 1999

St. John's

Newfoundland

©

Abstract

The control of stereochemistry in chemical reactions is a primary concern for synthetic organic chemists. The Diels-Alder reaction often provides good yields of a single stereoisomer. However, the reasons for this stereoselectivity are not always obvious.

The Diels-Alder reaction of 5-substituted-1,3-cyclopentadienes has been the focus of considerable debate. 1,3-Cyclopentadienes substituted at the C₅ position with OR, NRR', and F yielded 100% *syn* addition products, while substitution with CH₃, SR and Cl yielded mixtures of the products of *syn* and *anti* addition, and substitution with Si(CH₃)₃, Br, SePh and I yielded primarily *anti* addition products. Explanations in the literature for the preferential *syn* addition of some dienes usually involved electronic phenomena.

The degree of facial selectivity for the Diels-Alder reactions of 5-substituted-1,3-cyclopentadienes with a variety of dienophiles can be predicted correctly at the *ab initio* HF/6-31G(d) level. It has been determined that the energy required to deform the diene into its *syn* transition state geometry is the primary factor controlling facial selectivity in these reactions. This energy is related to the amount of angular change about C₅ of the diene in the *syn* transition state. Facial selectivity roughly correlates with empirical measures of the size of the C₅ substituent.

The size of the bond between C₅ and its substituent (C₅-X bond) has been defined to be the second moment, evaluated at the centroid of charge of the C₅-X bond, of the localized molecular orbital which describes the C₅-X bond. This measure of size correlates with facial selectivity. The C₅-O, C₅-N and C₅-F bonds are predicted to be smaller than the C₅-H bond.

A substituent factor has been defined by dividing the value of size by the distance between C_5 and the centroid of charge. The substituent factor correlates excellently with facial selectivity. Thus, facial selectivity can be fully accounted for based on steric arguments. An additional electrostatic repulsion has been shown to exist for *syn* addition of 1,3-cyclopentadienes substituted with halogen atoms, $C\equiv N$ or $C\equiv CH$, with 1,2,4-triazoline-3,5-dione.

Protonation of the C_3 -substituent is predicted to stabilize the *anti* addition transition state, resulting in more *anti* addition product. Deprotonation of the C_3 -substituent is predicted to stabilize the *syn* addition transition state, and to destabilize the *anti* addition transition state, thus increasing the proportion of *syn* addition product.

The reaction of 3-substituted-1,2-cyclopropenes with 1,3-butadiene is predicted to yield, in most cases, mainly the product of *endo-anti* addition, with a lesser amount of the product of *exo-anti* addition. It is suggested that *endo-syn* and *exo-syn* additions are disfavoured due to steric hindrance between the diene and the C_3 -substituent of the dienophile. The preference for *endo-anti* addition is primarily due to a favourable interaction between the methylene hydrogen of 3-substituted-1,2-cyclopropene and 1,3-butadiene. This interaction becomes less favourable as the electronegativity of the C_3 -substituent increases.

The substituent factor correlates well with both steric hindrance and electronegativity. It is transferable to other systems, and correlates with geometric trends.

Acknowledgments

I would like to extend my most sincere appreciation to my supervisors, Dr. D. Jean Burnell and Dr. Raymond A. Poirier, for their instruction, guidance, discussions and support during the course of my research work, and for their faith in my capabilities.

I would like to acknowledge Dr. Cory C. Pye for his contributions to this research, for his helpful instruction and discussions, and for his friendship. I would also like to acknowledge the complementary experimental study performed by Dr. Lori C. Burry, Mr. Johnathon E. Letourneau and Mr. Mark A. Wellman. I would like to express my appreciation to Dr. C. Robert Lucas for allowing me to use his office during the writing of this thesis. I extend special thanks to Dr. Graham J. Bodwell for his comments and suggestions concerning this thesis.

I would like to express my gratitude to Mr. Randy Dodge, Mr. Paul Fardy, Mr. Alan Goulding, and Mr. Gilbert Wong of the Department of Computing and Communications for their assistance in the computational aspects of this study. I would like to acknowledge Ms. Diane Burke and Ms. Tammy Gosse who assisted me with most of the calculations and who tabulated much of the data for the study presented in Section 4 of this thesis.

The submission of this thesis ends ten years of study at Memorial University of Newfoundland. I would like to extend my most sincere appreciation to all of the faculty, staff, and students who enlightened my life during my tenure. Special thanks are extended to Dr. Peter Golding.

I would like to extend my warmest thanks to my wife Lisa and to my three children, Matthew, Meghan and Nicholas, for their love, patience and understanding. I dedicate this thesis to them.

Financial support from Memorial University, Dr. D. Jean Burnell and Dr. Raymond A. Poirier is gratefully appreciated.

Table of Contents

Abstract	ii
Acknowledgments	iv
Table of Contents	vi
List of Tables	viii
List of Figures	xiv
List of Abbreviations and Symbols	xx
1. Stereoselectivity in the Diels-Alder Reaction	1
1.1 Introduction	1
1.2 <i>Syn/anti</i> Stereoselectivity	5
1.2.1 The Facial Selectivity Hypotheses	11
1.3 <i>Endo/exo</i> Stereoselectivity	19
2. Facial Selectivity in the Diels-Alder Reactions of	
5-Substituted-1,3-Cyclopentadienes	27
2.1 A Systematic Experimental and Theoretical Study	27
2.2 The <i>ab initio</i> Study	31
2.2.1 Facial Selectivity Model	32
2.2.2 Computational Methods	35
2.3 Activation Barriers and Energies of Reaction	38
2.4 The Search for an Electronic Effect	49

2.5 Geometry	70
2.6 Partitioning Activation Energy	81
2.7 Size and Steric Hindrance	100
2.8 What is Ξ_{CX} Measuring?	122
3. Facial Selectivity of Protonated and Deprotonated	
5-Substituted-1,3-Cyclopentadienes	126
3.1 Computational Method	126
3.2 Activation Energy and its Components	128
3.3 Geometry and Electronic Structure	137
3.4 Steric Hindrance	146
4. Stereoselectivity in the Diels-Alder Reaction of 1,3-Butadiene and 3-Substituted	
Cyclopropene	150
4.1 Computational Method	150
4.2 Activation Energy and its Components	153
4.3 The Destabilization of the <i>endo-syn</i> and <i>exo-syn</i> Transition States	166
4.4 <i>Endo-anti</i> versus <i>exo-anti</i> Stereoselectivity	171
4.5 Reactivity of 3-Substituted-1,2-Cyclopropenes	176
5. Conclusions and Future Work	191
References	196
Appendix	202

List of Tables

2.1	Experimental facial selectivities for the Diels-Alder reaction of CpX with NPM, PTAD and tetracyanoethene	28
2.2	Experimental facial selectivities for the Diels-Alder reaction of CpCl ₃ X with the listed dienophiles	29
2.3	Experimental facial selectivities for the Diels-Alder reaction of CpMe ₃ X with the listed dienophiles	30
2.4	The relationship between $ \Delta\Delta E_{act} $ and facial selectivity	39
2.5	TS conformation, activation energy, calculated and experimental facial selectivity for the reaction of CpX and ethene	40
2.6	TS conformation, activation energy, calculated and experimental facial selectivity for the reaction of CpX and ethyne	41
2.7	TS conformation, activation energy, calculated and experimental facial selectivity for <i>endo</i> addition of CpX to maleimide	42
2.8	TS conformation, activation energy, calculated and experimental facial selectivity for <i>endo</i> addition of CpX to TAD	43
2.9	Activation energy, calculated facial selectivity and calculated total percent <i>exo</i> addition for the <i>exo</i> addition reaction of CpX to maleimide and TAD	44
2.10	Energies of reaction for the given reactions	47
2.11	Ranges of ΔE_{act} for <i>syn</i> and <i>anti</i> addition reactions	48
2.12	Mulliken atomic charge on the sp ² carbons of CpX in its GS and its <i>syn</i> and <i>anti</i> TS's for the reaction with ethene	54
2.13	Bond orders for CpX in the GS and the <i>syn</i> and <i>anti</i> TS's for the reaction with ethene	55
2.14	Maximum and minimum geometry changes in transforming the GS reactants to their TS structures for the reaction of CpX and ethene	76

2.15	$\Delta\Theta_{\text{Total}}$ and facial selectivity for the reaction of CpX with ethene	78
2.16	Energy data for <i>syn</i> and <i>anti</i> addition of CpX and ethene	83
2.17	Energy data for <i>syn</i> and <i>anti</i> addition of CpX and ethyne	84
2.18	Energy data for <i>syn</i> and <i>anti</i> addition of CpX and maleimide	85
2.19	Energy data for <i>syn</i> and <i>anti</i> addition of CpX and TAD	86
2.20	Values of S_{CX} , R_{CX} and Ξ_{CX} derived for GS CpX	112
3.1	A comparison of facial selectivity and level of theory for the reaction of CpCl and ethene	128
3.2	Energies for the Diels-Alder reaction of CpX and ethene, evaluated at 6-31++G(d)//6-31++G(d)	129
3.3	$\Delta E_{\text{isodesmic}}$ for the reaction pictured in Figure 3.2	132
3.4	Ranges of ΔE_{act} for the reaction of CpX and ethene, evaluated at 6-31++G(d)//6-31++G(d)	132
3.5	Sums of the Mulliken net atomic charges resident on the dienophile in the TS	136
3.6	Bond lengths for CpX, evaluated at 6-31++G(d)//6-31++G(d)	138
3.7	Angles for CpX, evaluated at 6-31++G(d)//6-31++G(d)	139
3.8	Maximum and minimum geometry changes in transforming the GS reactants to their TS structures for the reaction of neutral, protonated and deprotonated CpX and ethene	141
3.9	$\Delta\Theta_{\text{Total}}$ evaluated for the reaction of neutral and ionic CpX with ethene	142
3.10	Mulliken net atomic charges on X^{\pm} in CpX and in the <i>syn</i> and <i>anti</i> TS's for the reaction of CpX and ethene	144
3.11	S_{CX} ($e\text{\AA}^2$), R_{CX} (\AA), and Ξ_{CX} ($e\text{\AA}$), evaluated at 6-31G(d)//6-31++G(d)	147

4.1	Energy data and percent (i) for <i>endo</i> additions of CprX and Bdiene	154
4.2	Energy data and percent (i) for <i>exo</i> additions of CprX and Bdiene	155
4.3	Energies relative to the corresponding value for <i>endo-anti</i> addition	156
4.4	$\Delta E_{\text{isodesmic}}$ for the isodesmic reactions defined in Figure 4.7	165
4.5	Maximum and minimum changes in geometry between <i>endo-anti</i> and <i>endo-syn</i> TS structures and the corresponding value in CprX, and minimum and maximum values of other TS parameters	167
4.6	Maximum and minimum changes in geometry between <i>exo-anti</i> and <i>exo-syn</i> TS structures and the corresponding value in CprX, and minimum and maximum values of other TS parameters	168
4.7	$\Delta\Theta_{\text{Total}}$ (degrees) evaluated for the reaction of CprX and Bdiene	169
4.8	Values of S_{CX} , R_{CX} and Ξ_{CX} evaluated for CprX, and Ξ_{CX} evaluated for CpX	176
4.9	$\Delta E_{\text{isodesmic}}$ for the reaction pictured in Figure 4.16	189
A.1	Total energies for CpX	203
A.2	Total energies for the syn addition TS for the reaction of CpX and ethene, evaluated at 6-31G(d)//6-31G(d)	204
A.3	Total energies for the anti addition TS for the reaction of CpX and ethene, evaluated at 6-31G(d)//6-31G(d)	205
A.4	Total energies for the TS's for the reaction of CpX and ethyne, evaluated at 6-31G(d)//6-31G(d)	206
A.5	Total energies for the <i>endo</i> addition TS's for the reaction of CpX and maleimide, evaluated at 6-31G(d)//6-31G(d)	207
A.6	Total energies for the <i>endo</i> addition TS's for the reaction of CpX and TAD, evaluated at 6-31G(d)//6-31G(d)	208
A.7	Total energies for the <i>exo</i> addition TS's for the reaction of CpX and maleimide, evaluated at 6-31G(d)//6-31G(d)	209

A.8	Total energies for the <i>exo</i> addition TS's for the reaction of CpX and TAD, evaluated at 6-31G(d)//6-31G(d)	209
A.9	Total energies for the TS's for the reaction of CpX and ethene, evaluated at 6-31++G(d)//6-31++G(d)	210
A.10	Total energies for GS dienophiles	211
A.11	Total energies for the products of the given reactions, evaluated at 6-31G(d)//6-31G(d)	211
A.12	Total energies for CprX, evaluated at 6-31++G(d)//6-31++G(d)	211
A.13	Total energies for the <i>endo</i> addition TS's for the reaction of CprX and Bdiene, evaluated at 6-31++G(d)//6-31++G(d)	212
A.14	Total energies for the <i>exo</i> addition TS's for the reaction of CprX and Bdiene, evaluated at 6-31++G(d)//6-31++G(d)	213
A.15	Bond lengths for CpX, evaluated at 6-31G(d)//6-31G(d)	214
A.16	Angles for CpX, evaluated at 6-31G(d)//6-31G(d)	215
A.17	Bond lengths for CpX, evaluated at 6-31++G(d)//6-31++G(d)	216
A.18	Angles for CpX, evaluated at 6-31++G(d)//6-31++G(d)	217
A.19	Bond lengths for the <i>syn</i> TS structure for the reaction of CpX and ethene, evaluated at 6-31G(d)//6-31G(d)	218
A.20	Angles for the diene portion of the <i>syn</i> TS structure for the reaction of CpX and ethene, evaluated at 6-31G(d)//6-31G(d)	219
A.21	Dienophile angles and angles of approach for the <i>syn</i> TS for the reaction of CpX and ethene, evaluated at 6-31G(d)//6-31G(d)	220
A.22	Bond lengths for the <i>anti</i> TS structure for the reaction of CpX and ethene, evaluated at 6-31G(d)//6-31G(d)	221
A.23	Angles for the diene portion of the <i>anti</i> TS structure for the reaction of CpX and ethene, evaluated at 6-31G(d)//6-31G(d)	222

A.24	Dienophile angles and angles of approach for the <i>anti</i> TS for the reaction of CpX and ethene, evaluated at 6-31G(d)//6-31G(d)	223
A.25	Bond lengths for the TS structures for the reaction of CpX and ethene, evaluated at 6-31++G(d)//6-31++G(d)	224
A.26	Angles for the diene portion for the TS structures for the reaction of CpX and ethene, evaluated at 6-31++G(d)//6-31++G(d)	225
A.27	Dienophile angles and angles of approach (degrees) for the TS's for the reaction of CpX and ethene, evaluated at 6-31++G(d)//6-31++G(d)	226
A.28	Bond lengths for the TS structures for the reaction of CpX and ethyne, evaluated at 6-31G(d)//6-31G(d)	227
A.29	Angles for the diene portion of the TS structures for the reaction of CpX and ethyne, evaluated at 6-31G(d)//6-31G(d)	228
A.30	Dienophile angle and angles of approach for the TS's for the reaction of CpX and ethyne, evaluated at 6-31G(d)//6-31G(d)	229
A.31	Bond lengths for the TS structures for the reaction of CpX and maleimide, evaluated at 6-31G(d)//6-31G(d)	230
A.32	Angles for the diene portion of the TS structures for the reaction of CpX and maleimide, evaluated at 6-31G(d)//6-31G(d)	231
A.33	Dienophile angle and angles of approach for the TS's for the reaction of CpX and maleimide, evaluated at 6-31G(d)//6-31G(d)	232
A.34	Bond lengths for the TS structures for the reaction of CpX and TAD, evaluated at 6-31G(d)//6-31G(d)	233
A.35	Angles for the diene portion of the TS structures for the reaction of CpX and TAD, evaluated at 6-31G(d)//6-31G(d)	234
A.36	Dienophile angle and angles of approach (degrees) for the TS's for the reaction of CpX and TAD, evaluated at 6-31G(d)//6-31G(d)	235
A.37	Bond lengths and angles for CprX, evaluated at 6-31++G(d)//6-31++G(d) ...	236

A.38	Bond lengths for the <i>endo-syn</i> and <i>endo-anti</i> addition TS's for the reaction of CprX and Bdiene	237
A.39	Angles for the <i>endo-syn</i> and <i>endo-anti</i> addition TS's for the reaction of CprX and Bdiene	238
A.40	Bond lengths for the <i>exo-syn</i> and <i>exo-anti</i> addition TS's for the reaction of CprX and Bdiene	239
A.41	Angles for the <i>endo-syn</i> and <i>endo-anti</i> addition TS's for the reaction of CprX and Bdiene	240
A.42	Electronegativity and measures of size	241

List of Figures

1.1	The Diels-Alder reaction of 1,3-butadiene with ethene	2
1.2	FMO theory and the Diels-Alder reaction	3
1.3	The stereoselective power of the Diels-Alder reaction	4
1.4	FMO rationalization of observed regioselectivity	5
1.5	The Diels-Alder reaction of CpX and ethene, illustrating <i>syn</i> and <i>anti</i> stereochemistry	6
1.6	Diels-Alder reactions of CpX which exclusively yield <i>anti</i> addition products ...	8
1.7	Diels-Alder reactions of CpX and derivatives that exclusively yield the product of <i>syn</i> addition	9
1.8	Facial selectivity in the Diels-Alder reaction of CpCl and CpCl ₂ H	10
1.9	Other Diels-Alder reactions that take place with modest facial selectivity	10
1.10	Anh's orbital mixing hypothesis	12
1.11	Fukui's orbital mixing rule	12
1.12	Orbital tilting hypothesis proposed by Paquette and Gleiter	12
1.13	Dienes studied by Brown, Houk, Burnell and Valenta	13
1.14	Caged ether studied by Coxon, Fong, McDonald and Steel	15
1.15	Backside interaction hypothesized by Ishida, Aoyama and Kato	15
1.16	The "Cieplak effect" proposed by Macaulay and Fallis	15
1.17	<i>Endo</i> versus <i>exo</i> stereoselectivity	19
1.18	Secondary orbital overlap	20

1.19	Examples of the subdivisions defined by Gleiter and Böhm	21
1.20	Jursic's SOI between the methylene hydrogen of cyclopropene and the π -system of the diene.	24
2.1	The four dienophiles	34
2.2	Newman projections and a side-on view of the conformation designations	37
2.3	MO plots for CpH	58
2.4	Plots of HOMO for CpF, CpCl and CpBr	59
2.5	MO plots for CpSeH	60
2.6	MO plots of the three types of π_3	61
2.7	Plotted MO's for the TS for the reaction of CpH and ethene	62
2.8	Plotted MO's for the TS for the reaction of CpH and ethyne	63
2.9	Plotted MO's for the <i>endo</i> addition TS for the reaction of CpH and maleimide .	64
2.10	Plotted MO's for the <i>exo</i> addition TS for the reaction of CpH and maleimide ..	65
2.11	Plotted HOMO's for the TS's for the <i>endo</i> and <i>exo</i> additions of CpH and TAD	66
2.12	Plotted MO's for the TS for the <i>endo</i> addition of CpH and TAD	67
2.13	Plotted MO's for the TS for the <i>exo</i> addition of CpH and TAD	68
2.14	ΔE_{act} versus group electronegativity	69
2.15	Graph of the C ₂ -C ₃ bond length versus the average C=C bond length for ground state CpX's	71
2.16	Graph of <i>syn</i> and <i>anti</i> ΔE_{act} versus average C=C bond length for GS CpX's ..	72
2.17	Graph of <i>syn</i> and <i>anti</i> ΔE_{act} versus C ₂ -C ₃ bond length for GS CpX	73

2.18	Definition of Y and Z	74
2.19	The tilting of X-C ₃ -H ₃ triangle about the C ₃ pivot in transforming CpX to its TS geometry	77
2.20	ΔE_{act} versus $\Delta\Theta_{Total}$ for the reaction of CpX and ethene	79
2.21	Pictorial definition of ΔE_{act} , ΔE_{diene}^{def} , $\Delta E_{diphile}^{def}$ and ΔE_{int}	82
2.22	ΔE_{act} versus $\Delta E_{diphile}^{def}$ and ΔE_{int} for the reaction of CpX and ethene	88
2.23	ΔE_{act} versus $\Delta E_{diphile}^{def}$ and ΔE_{int} for the reaction of CpX with ethyne, maleimide and TAD	89
2.24	ΔE_{act} versus ΔE_{int} for the reaction of CpX and TAD	90
2.25	ΔE_{act} versus ΔE_{diene}^{def} for the reaction of CpX and ethene	92
2.26	ΔE_{act} versus ΔE_{diene}^{def} for the reaction of CpX with ethyne and maleimide	93
2.27	ΔE_{act} versus ΔE_{diene}^{def} for the reaction of CpX and TAD	94
2.28	ΔE_{act} versus ΔE_{diene}^{def} for the reaction of CpX and TAD, including second-order saddlepoints for CpOH and CpNH ₂	97
2.29	<i>Syn</i> ΔE_{act} versus van der Waals radius of X ^o for the reaction of CpX and ethene	101
2.30	<i>Syn</i> ΔE_{act} versus Bragg-Slater radius of X ^o (pm) for the reaction of CpX and ethene	101
2.31	Equilibrium used to define <i>n</i> -values	103
2.32	ΔE_{act} versus A-value of X for <i>syn</i> addition of CpX and ethene	104
2.33	ΔE_{act} versus Taft's E _s for X, for <i>syn</i> addition of CpX and ethene	104
2.34	ΔE_{act} versus molar refractivity of X, for <i>syn</i> addition of CpX and ethene	105
2.35	ΔE_{act} versus van der Waals volume of X, for <i>syn</i> addition of CpX and ethene	105

2.36	ΔE_{act} versus n -value of X for <i>syn</i> addition of CpX and ethene	106
2.37	The steric interaction measured by A-values	107
2.38	ΔE_{act} versus S_{CX} for <i>syn</i> addition of CpX and ethene	113
2.39	Bragg-Slater radius versus S_{CX}	114
2.40	ΔE_{act} versus Ξ_{CX} for <i>syn</i> of CpX and ethene	117
2.41	Plot of <i>syn</i> ΔE_{act} versus Ξ_{CX} for the reaction of CpX with ethyne and maleimide	118
2.42	Plot of <i>syn</i> ΔE_{act} versus Ξ_{CX} for the reaction of CpX and TAD	119
2.43	Group electronegativity versus Ξ_{CX}	125
3.1	ΔE_{act} evaluated at 6-31++G(d)//6-31++G(d) versus ΔE_{act} evaluated at 6-31G(d)//6-31G(d)	130
3.2	Isodesmic reaction used to illustrate the effect of ionization on the stability of the Diels-Alder TS	132
3.3	ΔE_{act} versus ΔE_{diene}^{def} for <i>syn</i> and <i>anti</i> addition of CpX^0 , CpX^- and CpX^+	134
3.4	ΔE_{act} versus $\Delta E_{diphile}^{def}$ and ΔE_{int} for <i>syn</i> and <i>anti</i> addition of CpX^- , CpX^0 and CpX^+	135
3.5	ΔE_{act} versus $\Delta\Theta_{Total}$ for <i>syn</i> and <i>anti</i> addition of CpX^0 , CpX^- and CpX^+ with ethene	143
3.6	Hypothesized direction of the dipole moment of the <i>anti</i> addition TS of CpX^- and CpX^+ with ethene	145
3.7	<i>Syn</i> ΔE_{act} versus Ξ_{CX} for <i>syn</i> addition of CpX^0 , CpX^- and CpX^+ with ethene	148
4.1	The four modes of addition for the reaction of CprX and Bdiene	151
4.2	ΔE_{act} versus ΔE_{diene}^{def} for <i>endo-syn</i> and <i>endo-anti</i> addition of CprX and Bdiene	158
4.3	ΔE_{act} versus $\Delta E_{diphile}^{def}$ for <i>endo-syn</i> and <i>endo-anti</i> addition of CprX and Bdiene	159

4.4	ΔE_{act} versus ΔE_{int} for <i>endo-syn</i> and <i>endo-anti</i> addition of CprX and Bdiene .	160
4.5	ΔE_{act} versus ΔE_{diene}^{def} and ΔE_{int} for <i>exo-syn</i> and <i>exo-anti</i> addition of CprX and Bdiene	161
4.6	ΔE_{act} versus ΔE_{diene}^{def} for <i>exo-syn</i> and <i>exo-anti</i> addition of CprX and Bdiene ..	162
4.7	Isodesmic reactions defined for <i>endo</i> and <i>exo</i> addition of CprX and Bdiene ..	165
4.8	Plotted MO's for the <i>endo</i> addition TS for the reaction of CprH and Bdiene ..	172
4.9	Plotted MO's for the <i>exo</i> addition TS for the reaction of CprH and Bdiene ...	173
4.10	$\Delta \Delta E_{int}$ versus C ₃ -H ₃ bond length in GS CprX	175
4.11	Ξ_{CX} evaluated at 6-31G(d)//6-31(d) for CprX versus Ξ_{CX} evaluated at 6-31G(d)//6-31++G(d) for CprX	177
4.12	The average of the C ₁ -C ₃ and the C ₂ -C ₃ bond lengths and the C ₁ =C ₂ bond length of CprX, versus Ξ_{CX}	179
4.13	The C ₃ -H ₃ bond length and the average of the C ₁ -H ₁ and the C ₂ -H ₂ bond lengths of CprX, versus Ξ_{CX}	180
4.14	The C ₁ -C ₃ -C ₃ angle, the average of the C ₁ -C ₂ -C ₃ and C ₂ -C ₁ -C ₃ angles, and the average of the C ₁ -C ₃ -H ₃ and C ₂ -C ₃ -H ₃ angles of CprX, versus Ξ_{CX}	181
4.15	The average of the C ₁ -C ₃ -X and C ₂ -C ₃ -X angles and the H ₃ -C ₃ -X angle of CprX, versus Ξ_{CX}	182
4.16	Incipient bond length versus Ξ_{CX} for the reaction of CprX with Bdiene	184
4.17	π_5 -HOMO and π_A^* -LUMO of CprX, versus Ξ_{CX}	185
4.18	The isodesmic process defined to quantify energetically the substituent effect on CprX	187
4.19	ΔE_{act} versus Ξ_{CX} for <i>endo-anti</i> and <i>exo-anti</i> additions of CprX and Bdiene ..	188
4.20	ΔE_{act} for the reaction of CprX and Bdiene versus $\Delta E_{isodesmic}$ for the reaction pictured in Figure 4.16	189

5.1	TS's for the reactions of CpH with ethene, ethyne, maleimide and TAD, and for the reaction of CprH and Bdiene	193
5.2	Definition of the <i>endo</i> side and the <i>exo</i> side of a Diels-Alder TS	194

List of Abbreviations and Symbols

AC	active centre
AF	active frame
AM1	Austin Method 1
AO	atomic orbital
BSSE	basis set superposition error
CI	configuration interaction
CMO	canonical molecular orbital
CprX	3-substituted-1,2-cyclopropene, where X is the C ₃ substituent
CpX	5-substituted-1,3-cyclopentadiene, where X is the C ₅ substituent
Cp(CH ₃) ₅ X	5-substituted-1,2,3,4,5-pentamethyl-1,3-cyclopentadiene, where X is the C ₅ substituent
CpCl ₅ X	5-substituted-1,2,3,4,5-pentachloro-1,3-cyclopentadiene, where X is the C ₅ substituent
CpX ⁻	deprotonated CpX
CpX ⁰	neutral CpX
CpX ⁺	protonated CpX
DMAD	dimethyl acetylenedicarboxylate
ER	Edmiston-Ruedenberg (localization)
Et	ethyl
FMO	frontier molecular orbital

GS	ground state
HF	Hartree-Fock
HOMO	highest occupied molecular orbital
IF	inactive frame
LMO	localized molecular orbital
LUMO	lowest unoccupied molecular orbital
MA	maleic anhydride
Me	methyl
MNDO	minimum neglect of differential overlap
MO	molecular orbital
MOP	Mulliken overlap population
<i>n</i> -Bu	<i>n</i> -butyl
NPM	<i>N</i> -phenylmaleimide
OC	Davidon's Optimally Conditioned optimization method
Ph	phenyl
PTAD	4-phenyl-1,2,4-triazoline-3,5-dione
QCISD(T)	quadratic configuration interaction, including singles, doubles, and perturbational triple correction
RHF	restricted Hartree-Fock
SCF	self-consistent field
SOI	secondary orbital interaction

SOO	secondary orbital overlap
TAD	1,2,4-triazoline-3,5-dione
TBDMSO	<i>tertiary</i> -butyldimethylsilyl group
TS	transition state
VSEPR	valence-shell electron-pair repulsion
Vy	vinyl group (CH=CH ₂)
X	C ₅ substituent of CpX
X°	atom of X directly bonded to C ₅ of CpX
Y	C ₅ substituent of CpX which faces the dienophile at the TS
Z	C ₅ substituent of CpX which lies anti-periplanar to the dienophile at the TS
ZPE	zero point energy (correction)
ρ	electron density
∇ρ	$\left(\frac{\partial}{\partial x} + \frac{\partial}{\partial y} + \frac{\partial}{\partial z} \right) \rho$
Δ <i>E</i> _{act}	activation energy
Δ <i>E</i> _{diene} ^{def}	diene deformation energy
Δ <i>E</i> _{dophile} ^{def}	dienophile deformation energy
Δ <i>E</i> _{int}	interaction energy
Δ <i>E</i> _{isodesmic}	energy of reaction for an isodesmic process
Δ <i>E</i> _{rxn}	energy of reaction

$\Delta\Theta_{Total}$	total angular change about C_5 of CpX
R_{CX}	distance between C_5 and the centroid of charge of the C_5-X° bond
S_{CX}, S_a	size of the C_5-X° bond, size of LMO α
Ξ_{CX}	steric factor for the C_5-X° bond

1. Stereoselectivity in the Diels-Alder Reaction

1.1 Introduction

In the world of synthetic organic chemistry, the control of stereochemistry in chemical reactions is of paramount concern. For instance, the stereospecific synthesis of pharmaceuticals is of great interest. It has been determined that for some drugs, such as Ibuprofen¹ and Prozac,² one enantiomer is more effective than the racemic mixture. In the case of Thalidomide,¹ the dextrorotatory enantiomer of the drug has the desired sedative properties, while the levorotatory enantiomer is teratogenic.

The production of a single, desired stereoisomer is not a trivial task. Most reactions are not stereospecific, and thus yield mixtures of products that are often difficult to separate. The separation of racemic mixtures is especially problematic, given that enantiomers share the same physical properties. The generation of undesired stereoisomers is an inefficiency that leads to increased labour and cost. Therefore, reactions that produce high yields of a desired stereoisomer are invaluable tools for the synthetic organic chemist. One of the most popular and useful of these is the Diels-Alder reaction.

The Diels-Alder reaction is the most important cycloaddition reaction available to synthetic chemists. Since the investigation of this reaction in the laboratories of German scientists Otto Diels and Kurt Alder³ about 70 years ago, it has been the centre of much attention and controversy. The simplest prototype (Figure 1.1) is the reaction of 1,3-butadiene (the diene) with ethene (the dienophile). This reaction involves the breaking

of the three π -bonds while forming two new σ -bonds that close the ring, and a new π -bond between C₂ and C₃ of the original diene structure. After a lengthy debate in the literature, based on extensive experimental and computational evidence it has been accepted that the single-step concerted reaction pathway is energetically preferred to the competing two-step biradical mechanism for most diene/dienophile systems.⁴

The accepted mechanism for the concerted reaction path is often explained by Frontier Molecular Orbital (FMO) theory.⁵ The reaction usually involves the transfer of electron density from an electron-rich diene to an electron-poor dienophile. The antisymmetric π_A HOMO of the diene is “in phase” with the antisymmetric π_A^* LUMO of the dienophile, facilitating a transfer of electron density through orbital mixing (Figure 1.2b). Alternatively, the LUMO of the diene can mix with the HOMO of the dienophile. This situation is considered to occur when an electron-rich dienophile transfers electron density to an electron-poor diene, and is called inverse-electron-demand (Figure 1.2c).



Figure 1.1 The Diels-Alder reaction of 1,3-butadiene with ethene.

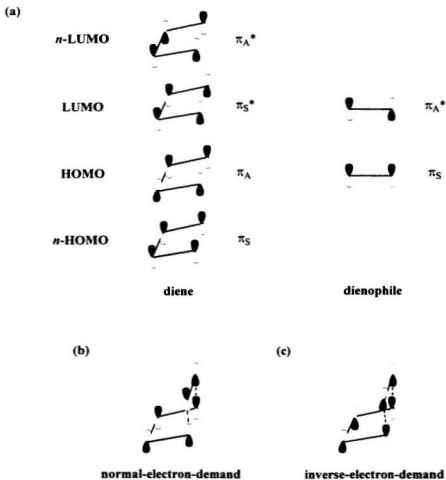


Figure 1.2 FMO theory and the Diels-Alder reaction. (a) π -MO's of diene and dienophile; (b) normal-electron-demand Diels-Alder reaction; (c) inverse-electron-demand Diels-Alder reaction.

Of great importance to synthetic chemists is the stereo- and regiochemistry of the Diels-Alder reaction. All four new sp^3 carbons have the potential to become new stereogenic centres, and if *meso*-compounds are used, even more stereocentres can be generated. The Diels-Alder reaction often gives good yields of a single product. For instance, the Diels-Alder reaction in Figure 1.3 was a key step in an approach to kempene diterpenes.⁶ This reaction could potentially produce eight products: addition to the diene could take place from above or below the plane of the page (*syn* or *anti* addition), with the bulk of the dienophile above or away from the bulk of the diene (*endo* or *exo* addition), and with the dienophile oriented as shown or vertically flipped (yielding two possible regioisomers). Amazingly, this reaction gave a yield of 80%, of which 100% of the isolated Diels-Alder adduct was the single, desired product. The synthetic importance of the Diels-Alder reaction is obvious, since stereo- and regioselectivity are usually predictable and yields are high.

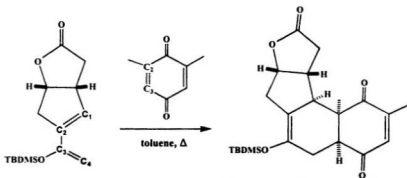


Figure 1.3 The stereoselective power of the Diels-Alder reaction. This reaction gives an 80% yield of only one of the eight possible Diels-Alder products. TBDSO is *t*-butyldimethylsilyl ether.

1.2 *Syn/anti* Stereoselectivity

The stereoselectivity of the Diels-Alder reaction in Figure 1.3 was predicted based on FMO and steric arguments. First, this reaction yielded the product of *endo* addition, which is the observed preference of the majority of dienophiles. This is often attributed to secondary orbital overlap,⁷ although other rationalizations exist (Section 1.3). Second, the dienophile avoids the face bearing the bulky lactone, and instead attacks the less hindered face bearing the hydrogens which point out from the bridge carbons between the two five-membered rings. Finally, it was predicted that C₄ would have the larger p-component in the HOMO of the diene than C₁, while C₃ would have a larger p-component in the LUMO of the dienophile than C₂ (Figure 1.4). These two carbons would have the better overlap, hence the observed regioselectivity. However, while the prediction was correct in this case, the reasoning was flawed. STO-3G//AM1 results predict that the value of the p-components in the LUMO of the dienophile are about the same for the two carbons (0.345 for C₂, 0.338 for C₃). Thus, no regioselectivity should be expected on the basis of FMO arguments.

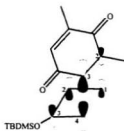


Figure 1.4 FMO rationalization of observed regioselectivity.

Frequently, the stereoselectivity of reactions cannot be predicted easily, and often the rationalizations are questionable. One such case is the controversy associated with facial selectivity of 5-substituted-1,3-cyclopentadienes (denoted CpX, where X is the substituent at C₅ of the diene). Not only are CpX's potent dienes, but they have fewer degrees of freedom than their acyclic counterparts, simplifying both experimental analysis and theoretical study. The reaction of CpX with a dienophile can occur in one of two diastereofacially distinct ways: the dienophile can react on the face of the diene that bears X (*syn* addition), or on the face bearing H₅ (*anti* addition; Figure 1.5).

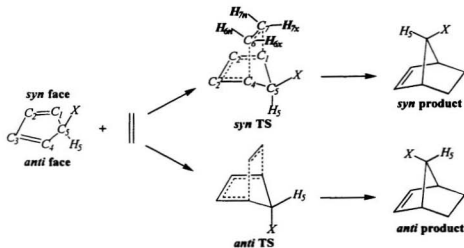


Figure 1.5 Diels-Alder reaction of CpX and ethene, illustrating *syn* and *anti* stereochemistry. TS denotes transition state. The numbering schemes defined above are employed throughout this text.

At first glance, it would be intuitive to predict that the dienophile would prefer to attack the face bearing the smaller group. Hydrogen is considered to be smaller than all other substituents. Thus, the Diels-Alder reaction of CpX would be expected to yield primarily the product of *anti* addition. As anticipated, the Diels-Alder reaction of CpX, where X = Br,⁸ I,⁹ CH₂OCH₃,¹⁰ SePh¹¹ or SiMe₃,¹² yielded 100% *anti* addition product for the reactions displayed in Figure 1.6. However, there are some examples of facial selectivity which seem to defy conventional steric arguments. Reactions involving CpOAc¹³ and CpF¹⁴ yielded exclusively the product of *syn* addition, as did derivatives of CpOH and CpOAc.¹⁵ As well, CpX derivatives bearing OH, OCH₃ or NHAc on C₃ directed addition *syn* to these groups¹⁶ (Figure 1.7). Facial selectivity ranged from 60% to 99% *syn* addition for CpCl⁸ and 1,2,3,4,5-pentachloro-1,3-cyclopentadiene¹⁷ (denoted CpCl₅H; Figure 1.8). On the other hand, CpSPh¹¹ and 1,2,3,4,5-pentamethyl-1,3-cyclopentadiene¹⁸ (denoted Cp(CH₃)₅H) showed little selectivity (Figure 1.9). How could a chlorine atom or an acetoxy group be less sterically demanding than a hydrogen atom? The answer to this question has been considered by several prominent chemists, and has resulted in a lengthy exchange in the literature. Their hypotheses are outlined in the next section.

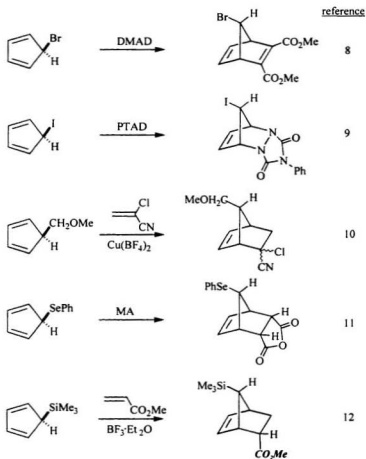


Figure 1.6 Diels-Alder reactions of CpX which exclusively yield *anti* addition products. DMAD denotes dimethyl acetylenedicarboxylate, PTAD denotes 4-phenyl-1,2,4-triazolene-3,5-dione, and MA denotes maleic anhydride.

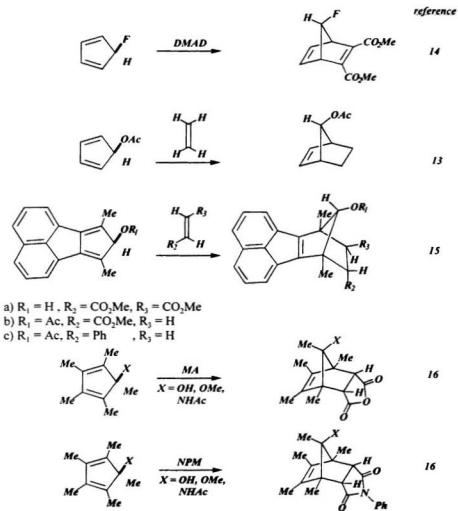


Figure 1.7 Diels-Alder reactions of CpX and derivatives that exclusively yield the product of *syn* addition. NPM abbreviates *N*-phenylmaleimide.

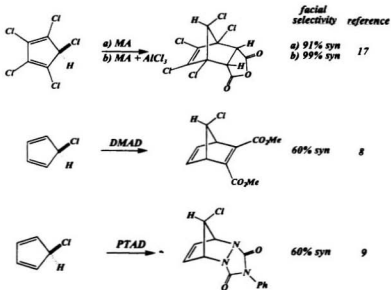


Figure 1.8 Facial selectivity in the Diels-Alder reaction of CpCl and CpCl₃H

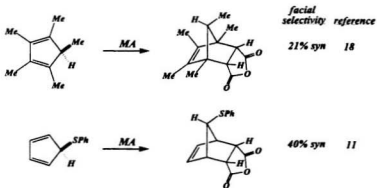


Figure 1.9 Other Diels-Alder reactions that take place with modest facial selectivity.

1.2.1 The Facial Selectivity Hypotheses

The failure of conventional steric arguments to explain these counterintuitive facial selectivities led to the development of rationales based on electronic and hyperconjugative effects. Experimental data involving the Diels-Alder reaction for many CpX derivatives existed. However, the form of the dienes and dienophiles, and the reaction conditions were not consistent. Furthermore, the computational power required to perform *ab initio* studies on the simplest Diels-Alder reactions was not generally available until the late eighties. Thus, most of the hypotheses could not be computationally tested.

In 1969, Williamson, Hsu, Lacko and Youn¹⁹ were among the first to address the question of facial selectivity. They argued that the reaction would occur on the face that, when colliding with a dienophile exhibited the lesser amount of van der Waals repulsion. The predominantly *syn* addition of CpCl₃H to some dienophiles (Figure 1.8) was attributed to attractive van der Waals and London-dispersion forces. The preference for *syn* addition was reported to be greater for more polar dienophiles, indicating a dipole-dipole interaction. Another cited factor was the higher polarizability of chlorine over hydrogen.

In the early seventies, Anh²⁰ suggested that favourable orbital mixing might occur between an antisymmetric orbital on X and the LUMO of the dienophile (Figure 1.10). In 1976, Fukui, Inagaki, and Fujimoto²¹ formally derived the "orbital mixing rule." They postulated that the lone pairs on the heteroatomic C₅ substituent would perturb the π_A -HOMO of the diene, enhancing the reactivity of the *syn* face (Figure 1.11).

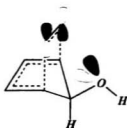


Figure 1.10 Anh's orbital mixing hypothesis.



Figure 1.11 Fukui's orbital mixing rule.



Figure 1.12 Orbital tilting hypothesis proposed by Paquette and Gleiter.

In the early eighties, Paquette and Gleiter²² explained the odd facial preference in the Diels-Alder reactions of isodicyclopentadiene (additions were *syn* to the ethano bridge) using “orbital tilting” arguments. They hypothesized that a strong interaction existed between the π_s -orbital and the σ -orbitals of the carbon framework, resulting in disrotatory “tilting” of the p-components of the π_s -orbital (Figure 1.12). The face bearing the inward-tilted π_s -orbital was more repulsive to the filled π_s -orbital of the incoming dienophile. Thus, the dienophile preferentially attacked the face bearing the “outward-tilted” π_s -orbital. Subtle modifications to the parent molecule could cause “tilting” in the opposite direction, thus leading to a reversal of facial selectivity with some derivatives of isodicyclopentadiene.

A couple of years later, Brown and Houk²³ used an MM2 model to show that facial selectivity of isodicyclopentadiene and its derivatives was instead governed by torsional effects in the norbornane skeleton, which could be overcome by steric effects in substituted cases. In a later collaboration with Burnell and Valenta,²⁴ they used the same methodology to examine the facial selectivity of the Diels-Alder reaction of the two polycyclic dienes pictured in Figure 1.13 and $\text{Cp}(\text{CH}_3)_3\text{H}$. All facial selectivity could be rationalized on the basis of steric effects.



Figure 1.13 Dienes studied by Brown, Houk, Burnell and Valenta.

Coxon, Fong, McDonald and Steel²⁵ provided an example in which filled orbital repulsion could affect facial selectivity. Whereas MA predominantly attacked the *anti* face of the “caged ether” pictured in Figure 1.14, DMAD and PTAD both gave mostly *syn* addition products. Even though the *anti* face appeared to be the more sterically demanding side of the diene, the lone pairs on the ether oxygen repel the π -orbitals (perpendicular to the reactive π -orbitals) of DMAD and the lone pairs of PTAD.

In a 1987 paper, Kahn and Hehre²⁶ rationalized the facial selectivity of both dienes and dienophiles based on differences in electrophilicity and nucleophilicity. The more electrophilic face of the dienophile was predicted to react with the more nucleophilic face of the diene.

In the late eighties, Ishida, Aoyama, and Kato²⁷ suggested that there is a favourable backside interaction between the π -electrons of the developing norbornene bond and the polarized carbon-heteroatom bond in forming the TS structure (Figure 1.15). In a later paper with Inagaki,²⁸ these authors formulated an energetic criterion for facial selectivity based on Fukui’s “orbital mixing rule.” In their words, “nonequivalent extension of the π -orbitals of the plane-unsymmetric dienes is caused by mixing of the low-lying σ -orbitals of the carbon framework through the interaction with the high lying orbitals n of the 5-substituent.” They based facial selectivity on the relative energy of the π -HOMO (π_A), ϵ_σ , and the heteroatom’s n -orbital, ϵ_n , of the diene.

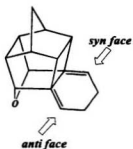


Figure 1.14 Caged ether studied by Coxon, Fong, McDonald and Steel.

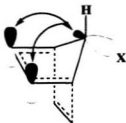


Figure 1.15 Backside interaction hypothesized by Ishida, Aoyama and Kato.

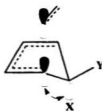


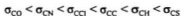
Figure 1.16 The "Cieplak effect" proposed by Macaulay and Fallis.

Three possible scenarios lead to three types of facial selectivity:

1. Group A: $\epsilon_x > \epsilon_n$ gave *syn* selectivity
2. Group B: $\epsilon_x = \epsilon_n$ gave no selectivity
3. Group C: $\epsilon_x < \epsilon_n$ gave *anti* selectivity

Their method predicted that cyclopentadienes substituted with NH_2 , OH , F , PH_2 , Cl , AsH_2 , Br and I all belong in Group A, while CpSH belonged in Group B, and SeH and TeH substituents belonged to Group C. They suggested that the incorrect prediction of facial selectivity for much of Group A was due to *anti*-driving steric hindrance, which is greater than the *syn*-driving effect of orbital mixing.

In a 1990 paper, Macaulay and Fallis¹⁶ adopted the "Cieplak effect" in their widely-accepted explanation of facial selectivity in the Diels-Alder reaction. In 1981, Cieplak²⁹ had rationalized the stereochemistry of the addition of nucleophiles to cyclohexanone and related systems based on hyperconjugation arguments. Cieplak suggested that the better σ -donor bond should lie antiperiplanar to the incipient bond, thus stabilizing the forming σ^* *anti*-bond. Macaulay and Fallis extended this concept to the Diels-Alder reaction, stating that the dienophile preferred to attack the face opposite the one bearing the better σ -donating substituent. According to Fallis and Macaulay, the order of increasing σ -donating ability is:



This explained why CpX and $\text{Cp}(\text{CH}_3)_2\text{X}$ substituted at C_5 with OR , NRR' or Cl gave predominantly *syn* addition products. Steric arguments were used to justify the fact that the

reaction of $\text{Cp}(\text{CH}_3)_3\text{H}$ and MA yielded only 21% *syn* addition product. Macaulay and Fallis attributed their order of σ -donor ability to a review by Epiotis, Cherry, Shaik, Yates and Bernardi.³⁰ The following is a reproduction of Table 36b of this review, which lists “the intrinsic donor ability of bonds”:

“ C-H > N-H > O-H > F-H
 H-I > H-Br > H-Cl > H-F
 H-S > H-O
 H-P > H-N
 N-Si > H-C
 C-I > C-Br > C-Cl > C-F
 C-Cl > C-C > C-H > C-F ”

Table 37a from the same review is presented below, which lists “the intrinsic acceptor ability of C-X sigma bonds”:

“ C-F > C-O > C-N > C-C
 C-I > C-Br > C-Cl > C-F
 C-S > C-O
 C-P > C-N
 C-Si > C-C ”

According to these tables, the C-C and the C-Cl bonds should be better σ -donors than C-H. Therefore, the Diels-Alder reactions of both CpCH_3 and CpCl should preferentially yield the product of *anti* addition. This is not the case for CpCl . Macaulay and Fallis also seem to have ordered the σ -donor ability of the C-O, C-N, and C-C bonds either by using the order of σ -donating ability of the corresponding H-X bonds, or by using the reverse order of σ -accepting ability of these C-X bonds. The latter case would be a groundless assumption, given that the opposite is true for carbon-halogen bonds. Finally, nowhere in the review by Epiotis *et al.* is it suggested that a C-S bond is a better σ -donor than a C-H or a C-C bond.

Thus, the basis used to support the “Cieplak effect” hypothesis is questionable.

In 1992, using both ultraviolet photoelectron spectroscopic studies and computational AM1 calculations, Werstiuk, Ma, Macaulay and Fallis found no significant evidence of Fukui's n - π orbital mixing in the π_A -HOMO.³¹ Ironically, two years later Werstiuk and Ma published another AM1 study in which they found no significant evidence of Fallis' “Cieplak effect” either.³² In this paper, Werstiuk and Ma concluded that facial selectivity in the Diels-Alder reaction of CpX-based dienes with MA was thermodynamically controlled. However, most Diels-Alder reactions are known to give kinetic products via early TS's.³³

The issue of facial selectivity in the Diels-Alder reaction of CpX has obviously not been settled. Facial selectivity of this reaction continues to be explained using the “Cieplak effect,”³⁴ Fukui's orbital mixing rules,³⁵ and orbital tilting arguments.³⁶ While these hypotheses have been used to rationalize observed facial selectivity, they have little predictive power. In the planning of a lengthy synthesis it would be more useful to be able to predict the stereochemistry of a reaction before it is attempted. The question remains, is there a single phenomenon or a combination of factors that control facial selectivity for all Diels-Alder reactions of CpX?

1.3 *Endo/exo* Stereoselectivity

A more widely known issue involving the Diels-Alder reaction is the question of *endo* versus *exo* stereoselectivity (Figure 1.17). With few notable exceptions, the kinetically controlled Diels-Alder reaction of most diene/dienophile combinations yields predominantly, and often exclusively, the product of *endo* addition. It can be argued that an explanation for this phenomenon is not necessary, given the predictability of the stereochemical outcome. However, there exist some dienophiles whose Diels-Alder reactions yield predominantly the product of *exo* addition. Furthermore, some dienophiles do not have a clear *endo* and *exo* designation (e.g. 1-chloro-1-cyanoethene). A general theory which addresses *endo* versus *exo* stereoselectivity for any dienophile is required.

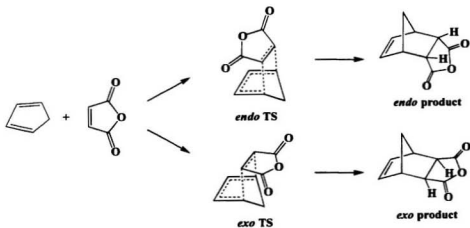


Figure 1.17 *Endo* versus *exo* stereoselectivity.

The first explanation for *endo* selectivity came from Alder and Stein²⁷ in 1937. Most reactive dienophiles have one or two carbonyls conjugated with the primary reactive centres. Alder and Stein attributed the preference for *endo* addition to a favourable “maximum accumulation of double bonds,” *i.e.*, the carbonyl of the dienophile prefers to subtend the diene π -system. In 1965 Woodward and Hoffman⁷ provided this “*endo* rule” with a quantum mechanical foundation using FMO theory. Whether the Diels-Alder reaction goes through a normal- or an inverse-electron-demand mechanism, p-orbitals on the atoms adjacent to the two reaction centres of the dienophile are “in phase” with the p-orbitals of middle carbons of the diene. Therefore, these orbitals can mix to give energetically favourable secondary orbital overlap (SOO) which stabilizes the *endo* TS, but SOO is not possible in the *exo* TS (Figure 1.18). This is still the most widely accepted explanation for *endo* selectivity.

Soon thereafter, other second-order orbital interactions (SOI's) were hypothesized. The terms SOO and SOI were often inappropriately used. In a review of SOI's published in

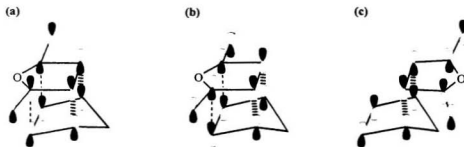


Figure 1.18 Secondary Orbital Overlap, (a) normal-electron-demand and (b) inverse-electron-demand possibilities for *endo* addition, and (c) *exo* addition for the Diels-Alder reaction of CpX with MA. Primary overlap is denoted by the heavy dashed lines, while secondary overlap is denoted by the thin broken line.

1983. Ginsburg³⁸ began by clearing up this ambiguity. He defined first-order orbital interactions to be,

“the in-phase and out-of-phase relationships between the atomic orbital coefficients at the pertinent reaction centres”

regardless of stereo- and regioselectivity. Secondly, he defined:

“Second-order orbital interactions are those which are determined by the magnitudes of the atomic orbital coefficients and/or the shape of the wavefunction (for example, the former determines regiospecificity, the latter, the efficacy of σ - π mixing). These include substituent effects which cause polarization of the π -systems and the σ - π mixing at the atoms where the new bonds are formed, polar group effects, and secondary orbital interactions between atoms which are not involved in bond formation or cleavage.”

Ginsberg cited a paper published earlier that year by Gleiter and Böhm,³⁹ who defined these terms in a similar fashion. Gleiter and Böhm distinguished between SOI's by dividing the diene and the dienophile into three regions: the active centres (AC), the active frame (AF), and the inactive frame (IF; Figure 1.19).

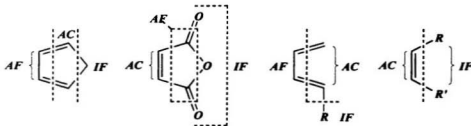


Figure 1.19 Examples of the subdivisions defined by Gleiter and Böhm.

Hence,

- first-order orbital interactions are in-phase relations between AO's of AC in an unperturbed frame
- second-order orbital interactions are subdivided into three types:
 1. secondary orbital effects: in-phase relation between AO's of AF
 2. substituent effects: a) polarization of π -systems, and b) σ/π mixing at AC
 3. polar group effects: interactions between AC and non-AC's, and between non-AC's.

Gleiter and Böhm's paper listed examples of how the three types of SOI's could be applied to explain *endo versus exo* stereoselectivity. Ginsburg provided situations from the literature where SOI's were invoked to explain observed stereoselectivities. He also reviewed the alternative rationalizations for *endo versus exo* stereoselectivity that had been proposed, including:

- van der Waals-type inductive forces which stabilize the *endo* TS
- charge transfer
- differences in the geometries of *endo versus exo* addition, resulting in differences in the primary orbital overlap of the reaction centre
- experimental parameters, including solvent effects and Lewis acid catalysis
- steric effects

Ginsburg concluded that SOI's were important in determining the course of various chemical reactions, but that sometimes SOI's were masked by other factors which could also influence

the reaction pathway.

The *endo* addition preferences of some dienophiles, such as cyclopentene and cyclopropene, cannot be rationalized based on SOO. However, it has been suggested that the sp^3 carbons of these dienophiles do have a p-component in a π -MO that can mix with the p-components of the middle carbons of the diene. Apeloig and Matzner⁴⁰ provided a systematic study of the role of SOI in determining the *endo/exo* product ratio of the Diels-Alder reaction of cyclopropene. They defined the stabilizing energy of the *endo* TS due to SOI as:

$$\Delta E(FMO) = \frac{(MOP)^2}{LUMO(diene) - HOMO(cyclopropene)}$$

where MOP is the calculated Mulliken overlap population between the methylene carbon of cyclopropene and the middle carbons of the diene. The inverse-electron-demand mechanism is selected because the LUMO (π_A^*) of cyclopropene has a node at the position of the methylene carbon, whereas the HOMO (π_s) does contain a p-component on the methylene carbon. $\Delta E(FMO)$ correlates well with the energy difference between the activation barriers for *endo* and *exo* addition reactions of a series of dienes with cyclopropene.

On the other hand, Jursic⁴¹ attributed the tendency for cyclopropene to give *endo* products as being due to a favourable SOI between the methylene hydrogen and the π -bond of the diene, which is not present in the *exo* (Figure 1.20). Jursic justified this hypothesis by citing the following evidence:

- the bond order calculated for the methylene hydrogen of cyclopropene with C_2 or C_3 of 1,3-butadiene was higher for the *endo* TS than the *exo* TS (0.02 and 0.002, respectively)
- the net atomic charge of the methylene hydrogen was higher in the *endo* TS than in the *exo* TS (0.21 and 0.20, respectively)
- the energy of the HOMO of the *endo* TS is lower than that of the *exo* TS

Dannenberg and co-workers⁴² also claimed that the dominant effect in determining the *endo* preference in the Diels-Alder reaction of cyclopropene was a $C-H\cdots\pi$ interaction. However, little evidence was presented to support this hypothesis or to reject the hypothesis of Apoleig and Matzner. The results of a kinetic isotope effect (KIE) study that Dannenberg's group presented in their paper did not support their argument. The only evidence they provided that supported the dominant role of a $C-H\cdots\pi$ interaction was a reference to a study of the T-shaped dimer of ethyne (available as supplementary material), which yielded a stabilization energy of $0.9 \text{ kcal}\cdot\text{mol}^{-1}$. Their main criticism of the work by Apoleig and Matzner was the neglect of the BSSE correction in the calculations. According

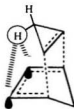


Figure 1.20 Jursic's SOI between the methylene hydrogen of cyclopropene and the π -system of the diene.

to the data presented by Dannenberg and co-workers, this correction should result in a change in the relative activation energies for *endo* versus *exo* addition of at most 0.5 kcal·mol⁻¹ (the difference in activation energy is about 2 kcal·mol⁻¹).

The problem with using SOI's to rationalize observed regio- and stereoselectivity is that they are neither directly observable experimentally nor are they uniquely determined computationally. The stabilizing effect of SOI's is difficult to quantify, and in turn the relative importance of other factors is problematic to determine. One such factor is the steric effect. Several authors have suggested that steric effects destabilize *exo* addition, thus making *endo* addition more favourable.⁴³

One paper which suggests that steric effects govern *endo/exo* stereoselectivity was by Fox, Cardona and Kiwiet.⁴⁴ They performed an MNDO and an AM1 study of the reaction paths of the retro-Diels-Alder reaction for several *endo* and *exo* addition products. This was accomplished by starting at the product geometries and elongating the incipient σ -bonds stepwise in a concerted, synchronous fashion. The geometry was then reoptimized while keeping the incipient σ -bonds fixed. For each evaluated structure the dihedral angle, which defined the angle of approach of the dienophile with respect to the diene, was determined. Fox *et al.* defined the difference between the product and TS values of this dihedral angle as Δ_d , and $\Delta(\Delta_d)$ to be the *endo/exo* difference in Δ_d values. They determined that there was an inverse correlation between $\Delta(\Delta_d)$ and $\Delta(\Delta H^\ddagger)$. Based on this evidence, Fox *et al.* suggested that steric effects were at least as important as SOI in controlling *endo* versus *exo* stereoselectivity.

Sodupe, Dannenberg, Oliva and Bertran⁴⁵ questioned the results of Fox *et al.* Dannenberg and co-workers claimed that the TS structures determined by Fox *et al.* were not fully optimized, and that two systems that were predicted to favour *endo* addition actually favoured *exo* addition. It should be noted that one of these systems was the dimerization of CpH, which is known to yield predominantly the product of *endo* addition. However, the paper by Dannenberg *et al.* is not flawless. For example, TS energies evaluated using MMX were presented. The MMX quadratic functions used to model bond energies are not accurate for bond lengths which are not close to ground state equilibrium lengths.

Section 4 of this thesis addresses both the question of *endo versus exo* stereoselectivity and the question of facial selectivity in the dienophile for the Diels-Alder reaction of 3-substituted-1,2-cyclopropenes (denoted CprX) and 1,3-butadiene (denoted Bdiene).

2. Facial Selectivity in the Diels-Alder Reactions of 5-Substituted-1,3-Cyclopentadienes

2.1 A Systematic Experimental and Theoretical Study

Section 1.2 introduced the topic of facial selectivity in the Diels-Alder reaction of CpX, and the dispute over its mechanism. An underlying problem with all of the hypotheses which attempted to rationalize the observed stereoselectivity was a combination of irregular experimental data and insufficient computational resources. To eliminate this deficiency a systematic study was required, involving both experimental and computational investigations of facial selectivity.

This effort involved the research groups directed by Dr. D. Jean Burnell and Dr. Raymond A. Poirier. The experimental study was primarily conducted by Lori Burry,⁴⁶ Jonathon Letourneau⁴⁷ and Mark Wellman,⁴⁸ while the computational investigation was carried out by Cory Pye⁴⁹ and myself. The two studies were complimentary and reciprocal. Observations from one study were used to confirm results and to stimulate investigations in the other. The experimental results are presented in Tables 2.1 through 2.3. The experimental facial selectivities are based upon NMR analysis of the total reaction mixture. In some cases, product ratios were also determined by X-ray crystallography.

Table 2.1 Experimental facial selectivities, expressed as percent *syn* addition to X, for the Diels-Alder reaction of CpX with NPM, PTAD and tetracyanoethene (TCNE).⁴⁸


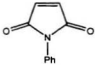
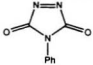
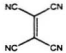
 X	 NPM	 PTAD	 TCNE
Cl	79	42	31
Br	15	0	0
I	0	0	0
CH ₃	40	79	0
Et	31	70	0
<i>n</i> -Bu	26	66	0
CH ₂ OCH ₃	84	84	0

Table 2.2 Experimental facial selectivities, expressed as percent *syn* addition to X, for the Diels-Alder reaction of CpCl_3X with the listed dienophiles.⁴⁶

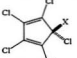
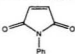
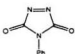
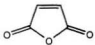

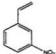
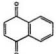

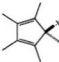
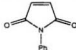
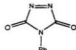
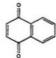
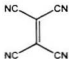

	X		
	H	CH_3	Br
	42	0	8
	78	81	18
	37	0	-
	67	25	6
	-	-	6
	-	-	11
	-	-	12

Table 2.3 Experimental facial selectivities, expressed as percent *syn* addition to X, for the Diels-Alder reaction of CpMe₃X with the listed dienophiles.⁴⁷

	X					
	H	Cl	Br	I	Et	CH ₂ OMe
	82	100	50	–	4	14
	75	0	0	0	5	26
	84	100	–	0	5	22
	97	100	5	0	3	7
	76	–	–	–	19	27

2.2 The *ab initio* Study

Facial selectivity in the Diels-Alder reaction of CpX might potentially be determined by a single factor or by a combination of factors. The hypotheses presented in Section 1.2.1 were a logical starting point for this investigation. These conjectures can be separated into two categories:

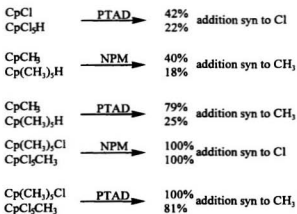
1. Phenomena which suggested that facial selectivity might be determined by factors which are present in the ground state (GS) diene:
 - substituent to π -HOMO orbital mixing
 - σ - π mixing of the carbon framework to give orbital tilting
 - facially different nucleophilicities or electrophilicities
2. Hypotheses which proposed that the factors controlling facial selectivity are not observable until the diene interacts with the dienophile:
 - lone pair of X with the LUMO of the dienophile mixing
 - backside interaction
 - torsional strain arguments
 - filled orbital repulsion
 - facially different van der Waals forces between diene and dienophile
 - hyperconjugation, including the "Cieplak effect"

There is also the question of whether facial selectivity is a thermodynamically controlled phenomenon. Therefore, a search for evidence of these effects required a study of both GS dienes and *syn* and *anti* TS structures, as well as *syn* and *anti* addition Diels-Alder products.

2.2.1 Facial Selectivity Model

A model which reproduced the trends in facial selectivity was required. The exact replication of experimental conditions using quantum chemical methods would involve the modelling of the unaltered addends and the inclusion of solvent effects. This accomplishment would be expensive computationally, and the number of degrees of freedom would be immense. The first approximation was to neglect solvent effects. The concerted and synchronous Diels-Alder reaction goes through a relatively nonpolar TS, thus solvent effects are relatively unimportant. It has been shown that solvent polarity affects the reaction rate of the Diels-Alder reaction by no more than a factor of ten,⁵⁰ and has a minor, unsystematic effect on facial selectivity.⁵¹

According to the data in Tables 2.1 to 2.3, substitution at C₁, C₂, C₃ and C₄ of CpX usually had a modest effect on facial selectivity. Below is a summary of comparable results:



Since differences of about 20% in facial selectivity amount to less than a 2 kJ·mol⁻¹ difference in activation energy, such substitution on the CpX ring usually has little effect on facial selectivity. The reactions presented in Figure 1.7 also support this conclusion. The reaction of CpCH₃ and Cp(CH₃)₃H with PTAD resulted in different facial preferences: 79% *versus* 25% addition *syn* to CH₃ (about a 6 kJ·mol⁻¹ difference in activation energy). Nevertheless, CpX was adopted as the model diene for this study.

Dienophiles whose two reactive centres are sp² carbons, such as NPM, MA and 1,4-naphthoquinone, usually give similar facial selectivities (Figure 1.7, Tables 2.2 and 2.3). Although ethene is a poor dienophile, it was hypothesized that it would serve as a good model, in terms of facial selectivity, for these dienophiles.

Based on all of these considerations, the primary model system for the computational study was the reaction of CpX and ethene. As a safeguard, some reactions of CpX and maleimide (Figure 2.1) were also studied. Reactions with ethyne were studied in place of dienophiles such as DMAD. Reactions of CpX's and PTAD often yielded facial selectivities that were different from reactions involving the same CpX's with other dienophiles (Figure 1.8, Tables 2.1, 2.2 and 2.3). To investigate this phenomenon, the reaction of CpX and 1,2,4-triazoline-3,5-dione (TAD) was studied.

For the primary study of the reaction of CpX and ethene, the set of X studied is comprised of the following main group hydrides and simple substituents:

X =	H	CH ₃	NH ₂	OH	F
	BH ₂	SiH ₃	PH ₂	SH	Cl
		GeH ₃	AsH ₂	SeH	Br
		SnH ₃	SbH ₂	TeH	I
	C≡CH	C≡N	CH=CH ₂	CF ₃	NO ₂

For this set of X, GS structures for CpX and *syn* and *anti* TS structures for the reaction with ethene were determined. Some *syn* and *anti* addition products were also determined. For the reaction of CpX with ethyne, maleimide and TAD, *syn* and *anti* (*endo*) TS structures were determined for the following set of X:

X =	H	CH ₃	NH ₂	OH	F
		SiH ₃	PH ₂	SH	Cl
	C≡CH	C≡N	Br	I	

Some *exo* TS structures and products were also determined.

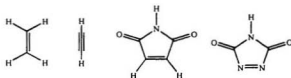


Figure 2.1 The four dienophiles: (from left to right) ethene, ethyne, maleimide and TAD.

2.2.2 Computational Methods

Molecular structures can be determined using empirical, semi-empirical or *ab initio* methods. Empirical methods, such as MMX, generally cannot be used to evaluate TS structures because they are designed using quadratic potentials for which only minima can be found. Semiempirical methods, such as AM1, have been shown to give good results in stereoselectivity studies.³² However, they are less reliable than *ab initio* calculations. For instance, it has been shown that AM1 gave the wrong *endo/exo* stereoselectivity for the reaction of CpH with cyclopropene.⁴² The parameterization schemes for semi-empirical methods are usually built to reproduce experimental results for GS molecules. TS species are not directly experimentally observable, and thus cannot be parameterized in this fashion. Therefore, *ab initio* methods were the most suitable for our study.

Ab initio methods have their own problems. Restricted Hartree-Fock (RHF) methods tend to overestimate the activation barrier, while MP2 calculations greatly underestimate the barrier.⁵² However, for the purposes of this study, absolute energies are not important; only relative energies are. For isodesmic processes, such as the energy difference between *syn* and *anti* TS's, HF methods can actually perform better than post-HF calculations.⁵³ The validity of the computational results can be best checked by comparing them to the experimentally determined facial selectivities.

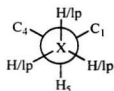
All of the calculations were performed using closed-shell RHF theory. The main assumption made by the closed-shell RHF wavefunction is that all MO's are either doubly-occupied or unoccupied. Pople's 6-31G(d) basis set⁵⁴ was used for all first, second, and third

period elements. Pople's 6-31G(d) basis sets have not been determined for fourth and fifth period elements, so Huzinaga's (43321/4321/41) and (433321/43321/431) split valence polarized basis sets⁵⁵ were used for these elements, respectively.

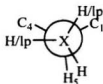
With few exceptions, all structures were optimized using MUNGAUSS.⁵⁶ When applicable, C_5 symmetry was enforced during optimization. GS minima for CpX and the evaluated products were optimized using Davidson's Optimally Conditioned (OC) method.⁵⁷ TS structures were obtained using a minimization of sum-of-squares method.⁵⁸ If any of these structures were incompletely converged, then the structures were optimized further using Pulay's DIIS method.⁵⁹ Gaussian 92 and 94⁶⁰ were used to evaluate most of the *syn* and *anti* TS structures for the reaction of CpX with maleimide and TAD, for X = CH₃, NH₂ and OH. Gaussian was also used to evaluate analytical force constants for all structures to ensure that the GS molecules had no imaginary frequencies, and that all TS's were first-order saddlepoints.

Where X was a non-linear, multi-atomic substituent, all probable rotational minima were optimized in order to determine the lowest energy minimum. Unless otherwise stated, only rotational global minima are reported here. The conformation names represent the arrangement of substituents about the atom of X which was directly attached to C₅ (denoted X^a), with respect to H₃ (Figure 2.2). The lowest energy conformations of X for GS CpX's are:

CH ₃	staggered	NH ₂	gauche	OH	staggered	BH ₂	gauche
SiH ₃	staggered	PH ₂	gauche	SH	staggered	CH=CH ₂	eclipsed
GeH ₃	staggered	AsH ₂	staggered	SeH	staggered	CF ₃	staggered
SnH ₃	staggered	SbH ₂	staggered	TeH	gauche	NO ₂	staggered



staggered (C_S)



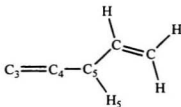
eclipsed (C_S)



gauche (C_1)



staggered NO₂ (C_S)



eclipsed CHCH₂ (C_S)



gauche BH₂ (C_1)

Figure 2.2 Newman projections and a side-on view of the conformation designations, including their respective symmetry point group (lp denotes lone pair). The relative position of the substituents on X^o with respect to C₁ and C₄ of the diene defined above is used consistently in this text.

2.3 Activation Barriers and Energies of Reaction

The factor that ultimately controls stereoselectivity in any reaction is energy. Tables 2.5 through 2.9 list the 6-31G(d)//6-31G(d) activation energies (denoted ΔE_{act}) for *syn* and *anti* addition in the Diels-Alder reactions of CpX with ethene, ethyne, maleimide (*endo* addition), TAD (*endo* addition), and maleimide and TAD (*exo* addition), respectively. Also listed is the conformation of X for each TS, the percentage of *syn* product predicted to be formed by a kinetically controlled reaction, and the most comparable experimental result. Percent *syn* addition is approximated using the equation:

$$\% \text{ syn} = \frac{100\%}{(1 + e^{\Delta\Delta E_{act}/RT})}$$

where $\Delta\Delta E_{act} = \Delta E_{act}(\text{syn}) - \Delta E_{act}(\text{anti})$, R is the gas constant, and T is temperature. This expression is derived from the Arrhenius equation, with the following two assumptions:

1. The Diels-Alder reaction obeys a second-order rate law
2. The Arrhenius pre-exponential factor is the same for both *syn* and *anti* addition for a given CpX.

Although the experimental facial selectivities were derived at various temperatures, the computational facial selectivities were determined at one temperature, 273.15K, to facilitate a comparison between the various computed results. Table 2.4 outlines the relationship between $|\Delta\Delta E_{act}|$ and facial selectivity.

Table 2.4 The relationship between $|\Delta\Delta E_{act}|$ (kJ·mol⁻¹) and facial selectivity

$ \Delta\Delta E_{act} $	ratio	$ \Delta\Delta E_{act} $	ratio	$ \Delta\Delta E_{act} $	ratio
0.0	50:50	5.0	10:90	10.0	1.2:98.8
1.0	39:61	6.0	7:93	11.0	0.8:99.2
2.0	29:71	7.0	4:96	12.0	0.5:99.5
3.0	21:79	8.0	3:97	15.7	0.1:99.9
4.0	15:85	9.0	2:98	20.9	0.01:99.99

Although zero point energy (ZPE) corrections were determined as a by-product of the computed frequencies, they have not been incorporated in the calculation of ΔE_{act} . For the reactions of CpF, CpCl, CpBr and CpI with ethene, $\Delta\Delta E_{act}$ would change by -0.3, -0.6, +0.8 and +1.0 kJ·mol⁻¹, respectively. These differences in $\Delta\Delta E_{act}$ would not translate to significant changes in the computed facial selectivities or in the analyses performed in this thesis. The ZPE corrections may even introduce other errors. For instance, the imaginary frequency, that corresponds to the “mode of vibration” about the reaction coordinate, is ignored in the calculation of the ZPE correction. As well, the evaluation of the ZPE correction for non-equilibrium structures is questionable, and thus applying the ZPE correction to the analysis that is presented in Section 2.6 would be problematic.

Table 2.5 TS conformation, activation energy (kJ·mol⁻¹) and calculated and experimental facial selectivity (% *syn* addition) for the reaction of CpX and ethene.

X	<i>syn</i>		<i>anti</i>		% <i>syn</i> addition	
	conform.	ΔE_{act}	conform.	ΔE_{act}	calc.	exp.(dienophile)
H		165.9				
BH ₂	staggered	181.9	gauche	168.6	0.3	
CH ₃	staggered	175.6	staggered	172.1	17.8	40 (NPM) ^a
NH ₂	gauche	162.4	gauche	169.6	95.9	100 (NPM) ¹⁶
OH	gauche	154.4	staggered	164.9	99.0	100 (NPM) ^{b,13,15}
F		138.7		163.9	100.0	100 (DMAD) ^{b,14}
SiH ₃	staggered	198.4	staggered	171.7	0.0	0 (Me acrylate) ^{c,12}
PH ₂	staggered	186.3	staggered	169.6	0.1	
SH	gauche	175.8	staggered	170.7	9.4	30 (NPM) ^a
Cl		163.5		165.7	72.5	79 (NPM) ^a
GeH ₃	staggered	199.3	staggered	171.3	0.0	
AsH ₂	staggered	191.7	staggered	168.2	0.0	
SeH	eclipsed	180.9	gauche	170.7	1.1	0 (MA) ^{c,11}
Br		171.7		165.2	5.4	15 (NPM) ^a
SnH ₃	staggered	209.9	staggered	171.6	0.0	
SbH ₂	staggered	204.0	staggered	168.5	0.0	
TeH	eclipsed	187.9	gauche	167.5	0.0	
I		182.9		164.9	0.0	0 (NPM) ^a
CH=CH ₂	eclipsed	175.0	eclipsed	167.9	4.3	
C≡CH		162.1		169.6	96.5	
C≡N		160.9		165.9	90.2	
CF ₃	staggered	182.7	staggered	174.0	2.2	
NO ₂	staggered	153.4	staggered	168.3	99.9	

^a Table 2.3. ^b Figure 1.7. ^c Figure 1.6.

Table 2.6 TS conformation, activation energy (kJ·mol⁻¹) and calculated and experimental facial selectivity (% *syn* addition) for the reaction of CpX and ethyne.

X	<i>syn</i>		<i>anti</i>		% <i>syn</i> addition	
	conform.	ΔE_{act}	conform.	ΔE_{act}	calc.	exp. (dienophile)
H		179.8				
CH ₃	staggered	187.9	staggered	185.7	27.4	24 (DMAD) ^a
NH ₂	gauche	169.5	gauche	181.7	99.5	100 (NPM) ^{b,c,16}
OH	staggered	156.0	staggered	176.1	100.0	100 (ethene) ^{b,13}
F		160.4		174.3	99.8	100 (DMAD) ^{b,14}
SiH ₃	eclipsed	204.8	staggered	186.9	0.0	0 (Me acrylate) ^{d,12}
PH ₂	gauche	195.4	staggered	184.4	0.8	
SH	eclipsed	186.4	staggered	183.5	21.5	40 (MA) ^{e,11}
Cl		182.5		177.9	11.6	40 (DMAD) ^{f,8}
Br		190.1		177.7	0.4	0 (DMAD) ^{d,8}
I		198.8		178.1	0.0	0 (PTAD) ^{d,9}
C≡CH		181.0		183.0	70.6	
C≡N		177.7		179.2	65.1	

^a Table 2.3. ^b Figure 1.7. ^c Cp(CH₃)₃NHAc. ^d Figure 1.6. ^e Figure 1.9. ^f Figure 1.8.

Table 2.7 TS conformation, activation energy ($\text{kJ}\cdot\text{mol}^{-1}$) and calculated and experimental facial selectivity (% *syn* addition) for *endo* addition of CpX to maleimide.

X	<i>syn</i>		<i>anti</i>		% <i>syn</i> addition	
	conform.	ΔE_{act}	conform.	ΔE_{act}	calc.	exp.(dienophile)
H		129.8				
CH ₃	staggered	140.4	staggered	135.7	11.1	40 (NPM) ^a
NH ₂	staggered	125.6	gauche	136.1	99.0	100 ^{b,16}
OH	gauche	118.7	staggered	136.0	100.0	100 ^{b,13,15}
F		108.5		137.5	100.0	100 (DMAD) ^{b,14}
SiH ₃	staggered	166.0	staggered	137.2	0.0	0 (Me acrylate) ^{c,12}
PH ₂	staggered	154.8	staggered	137.8	0.1	
SH	gauche	145.8	staggered	141.4	12.6	30 (NPM) ^a
Cl		136.5		141.3	89.3	79 (NPM) ^a
Br		145.5		143.7	31.7	15 (NPM) ^a
I		159.7		143.4	0.1	0 (NPM) ^a
C \equiv CH		129.8		139.1	98.4	
C=N		138.4		145.0	94.9	

^a Table 2.1. ^b Figure 1.7. ^c Figure 1.6.

Table 2.8 TS conformation, activation energy (kJ·mol⁻¹) and calculated and experimental facial selectivity (% *syn* addition) for *endo* addition of CpX to TAD.

X	<i>syn</i>		<i>anti</i>		% <i>syn</i> addition	
	conform.	ΔE_{act}	conform.	ΔE_{act}	calc.	exp.(dienophile)
H		95.0				
CH ₃	staggered	97.0	staggered	98.9	70.3	79 (PTAD) ^a
NH ₂	gauche	81.3	gauche	101.9	100.0	100 ^{b,16}
OH	staggered	73.1	staggered	106.6	100.0	100 ^{b,13,15}
F		96.3		107.6	99.3	100 (DMAD) ^{b,14}
SiH ₃	staggered	118.9	staggered	102.0	0.1	0 (Me acrylate) ^{c,12}
PH ₂	gauche	111.6	gauche	104.4	4.0	
SH	staggered	106.6	staggered	108.7	72.1	14 (PTAD) ^a
Cl		118.5		112.2	5.9	42 (PTAD) ^a
Br		127.0		115.2	0.5	0 (PTAD) ^a
I		134.3		115.8	0.0	0 (PTAD) ^a
C≡CH		108.6		105.3	19.0	
C≡N		119.4		116.3	20.2	

^a Table 2.1. ^b Figure 1.7. ^c Figure 1.6.

Table 2.9 Activation energy (kJ·mol⁻¹), calculated facial selectivity (% *syn* addition) and calculated total percent *exo* addition^a for the *exo* addition reaction of CpX to maleimide and TAD.

	maleimide				TAD			
X	ΔE_{act}		calc.	calc.	ΔE_{act}		calc.	calc.
	<i>syn</i>	<i>anti</i>	% <i>syn</i>	% <i>exo</i>	<i>syn</i>	<i>anti</i>	% <i>syn</i>	% <i>exo</i>
H	142.0			0.5	141.9			0.0
F	134.9	157.1	100.0	0.0	136.7	168.5	100.0	0.0
Cl	180.1	158.3	0.0	0.0	181.8	170.1	0.6	0.0
Br	224.6	188.9	0.0	0.0	221.3	195.8	0.0	0.0

^a Total percent *exo* addition is the combined percentage of *exo-syn* and *exo-anti* addition of all possible modes of addition. Percent addition of mode of addition *i* out of the possible four modes of addition (*j* = 1,4) is defined to be:

$$\% add.(i) = \frac{e^{-\Delta E_{act}(i)/RT}}{\sum_{j=1}^4 e^{-\Delta E_{act}(j)/RT}} \times 100\%$$

Thus, total percent *exo* addition is:

$$\%exo = \left(\frac{e^{-\Delta E_{act}(exo-syn)/RT} + e^{-\Delta E_{act}(exo-anti)/RT}}{e^{-\Delta E_{act}(endo-syn)/RT} + e^{-\Delta E_{act}(endo-anti)/RT}} \right) \times 100\%$$

$$+ \left(\frac{e^{-\Delta E_{act}(exo-syn)/RT} + e^{-\Delta E_{act}(exo-anti)/RT}}{e^{-\Delta E_{act}(endo-syn)/RT} + e^{-\Delta E_{act}(endo-anti)/RT}} \right) \times 100\%$$

The assumptions made on page 38 also apply here.

As can be seen in Tables 2.5 through 2.8, the calculated facial selectivities agree remarkably well with the experimental results in similar systems. This was amazing considering the approximations and assumptions that were made in the computational model. The one significant exception is the calculated facial selectivity for the reaction of CpSH and TAD (72.1% *syn* addition). The experimental result of 14% *syn* addition is for the reaction of CpSPH and PTAD. It is probable that in this case, using a hydrogen atom in place of a phenyl group in our computational model was not a good approximation. The agreement between facial selectivities derived by computation and by experiment is qualitative, since $\Delta\Delta E_{act}$'s have not been derived for the experimental results. 100% *syn* addition or 100% *anti* addition can correspond to absolute values of $\Delta\Delta E_{act}$ that can range from 12 kJ·mol⁻¹ to an infinite amount of energy. Nevertheless, qualitative or quantitative, the agreement with experiment provides a good level of trust in the computational model. The computed ΔE_{act} 's are at least 25% too high, in relation to experimental observation. However, the error in evaluating ΔE_{act} must be systematic and almost constant, given the good agreement with experimental facial selectivities.

The total amount of *exo* addition predicted for these reactions is negligible (Table 2.9). Therefore, the *endo* addition pathway was assumed unless otherwise specified in all further discussions.

The calculations predicted that Diels-Alder reactions involving CpX substituted with an electronegative substituent, such as F, OH and NH₂, yield very predominantly *syn* addition products. CpCH₃, CpSH and CpCl are predicted to be moderately facial selective, while

CpX's substituted with third and fourth row groups should produce primarily *anti* addition products. In addition, these calculations predicted that CpNO₂, CpC≡CH and CpC≡N would also react through a *syn* TS with most dienophiles, with the notable exception of TAD. Both experimentally and computationally, reactions with TAD can result in facial selectivities that are dramatically different from those resulting from the corresponding reactions with other dienophiles. Unlike reactions of ethene, ethyne and maleimide, reactions of TAD carbon-based CpC≡CH, CpC≡N, and CpCl were predicted to yield mostly *anti* products, while CpCH₃ and CpSH should prefer *syn* addition.

The good agreement between the calculated facial selectivities and experimental observation suggests that facial selectivity of these reactions is kinetically controlled. Table 2.10 lists the energy of reaction, ΔE_{rxn} , facial selectivity calculated based on the relative energies of the products, and experimentally observed facial selectivities for some *syn* and *anti* Diels-Alder additions. The exothermicity of these Diels-Alder reaction is too high to allow equilibration, and the wrong facial selectivity is predicted for the reaction of CpBr and CpI with ethene, and for the reaction of CpCl with TAD. Thus, facial selectivity cannot be a result of thermodynamic equilibrium in these reactions.

Table 2.10 Energies of reaction ($\text{kJ}\cdot\text{mol}^{-1}$) and calculated^a and experimental facial selectivities, for the given reactions.

reaction	<i>syn</i> ΔE_{rxn}	<i>anti</i> ΔE_{rxn}	calc. % <i>syn</i>	exp. % <i>syn</i> (dienophile)
CpH + ethene	-100.9			
CpF + ethene	-139.7	-125.2	99.8	100 (DMAD) ^{b,14}
CpCl + ethene	-121.0	-112.4	97.8	79 (NPM) ^c
CpBr + ethene	-114.0	-106.1	97.0	15 (NPM) ^c
CpI + ethene	-103.3	-98.8	88.2	0 (NPM) ^c
CpH + maleimide	-108.3			
CpCl + maleimide	-121.5	-110.6	99.2	79 (NPM) ^c
CpH + TAD	-129.4			
CpCl + TAD	-125.1	-121.7	81.7	42 (PTAD) ^c

^abased on relative product energies. ^b Figure 1.16. ^c Table 2.1.

The most important trend to note in Tables 2.5 through 2.8 is the range of ΔE_{act} for *syn* and *anti* addition. These ranges are summarized in Table 2.11. Regardless of dienophile, the *syn* ΔE_{act} 's vary over a broad range of values about the value for CpH. On the other hand, *anti* values do not vary much from the corresponding value for CpH. ΔE_{act} for the reaction of CpH with ethene and ethyne is within the range of the corresponding *anti* values. For the reaction of CpX with maleimide and TAD, all of the ΔE_{act} 's for *anti* addition are greater than the corresponding value for the reaction with CpH. These differences in the ranges suggest that there exists a phenomenon that affects *syn* significantly more than *anti* ΔE_{act} . Therefore, the factor which controls facial selectivity in these reactions affects the *syn* face more than the *anti* face of the diene, whether in the GS or in the TS. Thus, the answer to the facial selectivity paradox is unlikely to be found in the *anti* TS (*i.e.*, the "Cieplak effect" is not a significant factor).

Table 2.11 Ranges of ΔE_{act} (kJ·mol⁻¹) for *syn* and *anti* addition reactions.

Reaction	<i>syn</i> ΔE_{act} range	<i>anti</i> ΔE_{act} range
CpX + ethene	71.3	10.1
CpX + ethyne	42.7	12.5
CpX + maleimide	57.5	9.9
CpX + TAD	61.2	17.4

2.4 The Search for an Electronic Effect

Many of the hypotheses proposed to explain facial selectivity in the Diels-Alder reaction of CpX use as their basis orbital mixing arguments of some sort. Whether the orbital mixing is present in the diene or is manifested only in the TS, the assumption made for all of the hypotheses is that the primary favourable interaction between the diene and the dienophile in the TS is the mixing of the HOMO of the diene with the LUMO of the dienophile. No other favourable interaction between the two addends is considered important. Paquette and Gleiter²² even suggested that there is a repulsion between the filled π_s -MO of the diene and the π_s -MO of the dienophile.

The validity of MO arguments can be judged by looking at MO plots. MO plots are presented at the end of this section for a selection of GS CpX molecules and TS structures for the reaction of CpX with the four dienophiles studied. All plots were generated using Spartan 4.1,⁶¹ using wavefunctions evaluated using Gaussian 94. The default contour value of 0.032 was used for all MO plots.

CpH has three MO's with π -character: the HOMO (MO 18) is the predicted π_A -MO, while MO 12 and 17 form a bonding and antibonding mixing of the π_s -MO with the two C₃-H σ -MO's (Figure 2.3). This does not fit the simple FMO prediction in Figure 1.2.

The predicted π_A -HOMO exists for all CpX studied, and there are p_x -components on X^o for many CpX (Figure 2.4). These p_x -components are antibonding with respect to the π -lobes of the *syn* face. Where they exist, the size of the p_x -components on X^o increases as the period number of X^o increases. However, differences between the *syn* and *anti* faces for

most CpX, as were predicted by the Japanese research groups,^{21,28,35} do not appear to be present.

Both the HOMO and the π -HOMO of CpI, CpTeH and CpSeH have π_A -character (Figure 2.5). These MO's consist of an antibonding and a bonding addition of the *syn* face components of π_A and the p_x -components of X^o , respectively. In the π -HOMO, there is overlap between components on X^o and π_A . These are the only examples of mixing apparent between X and the π_A , but these were not the dienes that Fukui's group²¹ predicted to have such mixing.

There exists a π_5 -MO similar to MO 17 of CpH for all CpX. This MO exhibits one of three different types of σ - π mixing (Figure 2.6):

1. No significant overlap between the σ -orbitals and the π_5 orbital: CpH, CpCH₃, CpSH, CpBr, CpI, CpC \equiv CH, CpCH=CH₂, CpCF₃, CpNO₂.
2. Significant overlap between the C₅-X σ -bond and the π -lobe on the *anti* face: CpNH₂, CpOH, CpF, CpPH₂, CpCl, CpC \equiv N.
3. Significant overlap between the C₅-H σ -bond and the π -lobe on the *anti* face: CpBH₂, CpSiH₃, CpGeH₃, CpAsH₃, CpSeH, CpSnH₃, CpSbH₃, CpTeH.

All of the dienes listed in Case 2, except CpPH₂, have a tendency for *syn* addition, while all of the dienes in Case 3 favour *anti* addition. Facial selectivity for Case 1 ranges from 100% *anti* to 100% *syn* addition preference. While this π_5 -MO does exhibit characteristics that can be linked to facial selectivity, the connection is not perfect.

CpX with C₁ symmetry (*i.e.*, CpBH₂, CpNH₂, CpPH₂ and CpTeH) have remarkably

different MO structures, although π_A - and π_S -MO's can still be determined. Their complexity cannot be easily captured in a two-dimensional picture. Yet, while the MO's of corresponding C_5 and C_1 structures are significantly different, facial selectivity is rarely affected by the conformation of X. However, facial selectivity can be affected by the conformation of X for reactions with TAD (discussed later). In summary, there is no indication that there is a significant facial bias in the π_A -HOMO. However, the π_S -MO's of many CpX reveal a pattern which may be related to facial selectivity.

In general, FMO theory does not take into account the possibility that MO's other than the HOMO and LUMO of the reactants are interacting with each other in the TS. Other interactions do exist, and it would be unscientific to suggest that they have a negligible effect on the reaction. For the TS of the reaction of CpH and ethene, there are at least four occupied MO's that are important in describing the interaction between the addends. The HOMO (MO 26) was a surprise – it is the result of an antibonding addition of two occupied MO's: a π_S from CpH with the π_S of ethene (Figure 2.7a). MO 24 is the bonding counterpart of the HOMO (Figure 2.7b). MO 25 is the one predicted by FMO theory: the mixing of the π_A of CpH with the π_A^* of ethene (Figure 2.7c). MO 22 also exhibits visible overlap between the diene and the dienophile (Figure 2.7d). This MO is comprised of an unexpected mixing of σ -orbitals on CpH with σ -orbitals on ethene. All of these orbitals are “frontier molecular orbitals,” and all can significantly contribute to the kinetics of this reaction.

The TS's of all *syn* and *anti* additions of CpX and ethene possess similar diene/dienophile π_A/π_A^* , π_S/π_S bonding and π_S/π_S antibonding MO's. Similar σ/σ MO's are

present for many CpX and ethene TS's, as are other MO's which have significant mixing between the diene and the dienophile. For some TS's the π_A/π_A^* MO is the HOMO, for others it is the π_S/π_S^* , but there does not seem to be a clear pattern.

The FMO's of the TS structures for the reactions of CpH with ethyne and maleimide are very similar to those for the TS structures for the reaction of CpH and ethene. Figure 2.8 displays the π_A/π_A^* , π_S/π_S^* bonding and π_S/π_S^* antibonding MO's for the reaction of CpH with ethyne. For the *endo* and *exo* addition TS's for the reaction of CpX and maleimide, the π_A/π_A^* HOMO's are nearly identical for both TS's (Figures 2.9 and 2.10, respectively). As well, the *endo* and *exo* TS's each have three π_S/π_S^* -type MO's. There is significant overlap between components on the two addends in other MO's as well.

The MO's of the TS for the reaction of CpH and TAD are somewhat different from the other TS's involving CpH. The HOMO's for the *endo* and *exo* addition TS's are presented in Figure 2.11. For the corresponding TS's involving the other dienophiles, the components of the π_A/π_A^* -MO contributed by the dienophile are mostly centred on the reacting carbons. On the other hand, for both TS's involving TAD, the dienophile's contribution to the π_A/π_A^* -MO is not only on the reacting nitrogens, but encompasses part of the dienophile's ring. Both *endo* and *exo* TS's also have more high lying MO's, including the π_S/π_S^* -types observed in the other TS's, which have significant overlap between the diene and the dienophile. Figures 2.12 and 2.13 present some of the more interesting MO's of the *endo* and *exo* TS's for the reaction of CpH and TAD.

This brief overview of MO plots has led to a couple of conclusions. First, several

hypotheses could be conceived to explain facial selectivity by looking at individual MO's. However, there is no trend consistent for all cases. Second, there are so many MO's which describe the interaction between the diene and the dienophile, that one cannot reasonably consider one MO in isolation of the others.

We must not forget that an MO, ψ , is just one element of the mathematical solution to the Schrödinger equation. Furthermore, the canonical molecular orbitals (CMO's) are not a unique solution; the CMO's can be converted by unitary transformation to an infinite number of other bases. The significance of ψ , is more mathematical than physical in nature – it is not experimentally observable. What has physical significance is the “square” of the total wavefunction, $|\Psi(r)|^2$, i.e., electron density, and expectation values, i.e., $\langle \Psi | \hat{o} | \Psi \rangle$.

Atomic charges and bond orders also do not reveal any trends which can be linked to facial selectivity. Table 2.12 lists the Mulliken atomic charges⁶² for the four sp^2 carbons of CpX in the GS and in the *syn* and *anti* TS for the reaction with ethene, relative to the corresponding value for CpH. Table 2.13 lists relative bond orders according to Mayer⁶³ between X° and C_1 and C_4 for CpX and the corresponding *syn* and *anti* TS's. Also tabulated in Table 2.13 are bond orders for the incipient bond, and between X° and the carbons of ethene.

Table 2.12 Mulliken atomic charge on the sp^2 carbons of CpX in its GS and its *syn* and *anti* TS's for the reaction with ethene. Listed values are relative to the corresponding value for CpH.^a

X	relative atomic charge C_1, C_4			relative atomic charge C_2, C_3		
	GS	<i>syn</i>	<i>anti</i>	GS	<i>syn</i>	<i>anti</i>
H	0.000	0.000	0.000	0.000	0.000	0.000
BH ₂	-0.068 0.030	0.010	0.022 -0.039	0.031 -0.022	-0.003	-0.001 0.006
CH ₃	0.012	0.010	0.011	-0.005	-0.007	-0.001
NH ₂	-0.013 0.012	-0.011 0.013	-0.006 0.016	-0.002 -0.005	-0.008 -0.008	-0.010 -0.009
OH	-0.033	-0.036 -0.015	-0.015	0.000	-0.009 -0.009	-0.018
F	-0.041	-0.057	-0.041	0.004	-0.008	0.009
SiH ₃	-0.009	0.008	-0.002	0.000	-0.001	0.001
PH ₂	0.018 -0.009	0.004	-0.006	-0.004 0.007	-0.001	0.012
SH	0.019	0.011 0.015	0.019	0.001	-0.002 -0.003	-0.004
Cl	0.027	0.011	0.012	0.008	-0.003	0.015
GeH ₃	0.010	0.005	0.007	-0.004	-0.003	0.002
AsH ₂	-0.002	-0.005	-0.004	0.003	-0.002	0.007
SeH	0.011	0.004	0.016 -0.017	-0.003	-0.003	0.013 0.009
Br	0.012	-0.005	0.002	0.007	-0.004	0.013
SnH ₃	0.027	0.020	0.020	-0.004	-0.003	0.000
SbH ₂	0.015	0.011	0.008	0.000	-0.002	0.003
TeH	0.042 -0.001	0.020	0.030 -0.004	-0.004 0.012	-0.003	0.011 0.004
I	0.026	0.010	0.012	0.005	-0.004	0.013

^a Throughout the thesis, one value is tabulated for a pair of equivalent parameters for structures with C_s symmetry, whereas two values are given for structures with C_1 symmetry.

Table 2.13 Bond orders for CpX in the GS and the *syn* and *anti* TS's for the reaction with ethene. Listed values are relative to the corresponding value for CpH.

X	X ^o -C ₁ , X ^o -C ₄			X ^o -C ₆ , X ^o -C ₇	C ₁ -C ₆ , C ₄ -C ₇	
	GS	syn	anti	syn	syn	anti
H	0.000	0.000	0.000	0.000	0.000	0.000
BH ₂	0.088 0.030	0.007	0.034 0.075	0.010	-0.008	0.020 0.023
CH ₃	-0.005	-0.004	-0.001	-0.010	-0.012	0.003
NH ₂	-0.054 -0.044	0.006 -0.003	0.001 -0.008	-0.015 -0.015	-0.014 -0.012	-0.009 -0.005
OH	0.013	0.014 0.004	0.006	-0.024 -0.025	-0.015 -0.014	-0.014
F	0.002	0.021	0.012	-0.024	-0.009	-0.014
SiH ₃	0.032	0.014	0.033	0.001	-0.005	0.020
PH ₂	0.004 0.006	0.007	0.018	-0.007	-0.009	0.010
SH	-0.007	-0.002 0.000	-0.003	-0.016 -0.007	-0.009 -0.014	0.000
Cl	-0.013	-0.002	-0.010	-0.020	-0.014	-0.007
GeH ₃	0.036	0.016	0.036	-0.001	-0.007	0.020
AsH ₂	0.026	0.013	0.028	-0.005	-0.008	0.014
SeH	0.005	0.007	0.008 0.015	-0.009	-0.009	0.003 0.008
Br	-0.047	0.006	0.000	-0.019	-0.013	-0.003
SnH ₃	0.048	0.017	0.042	0.002	-0.005	0.025
SbH ₂	0.040	0.017	0.037	-0.002	-0.006	0.018
TeH	0.014 0.020	0.010	0.014 0.023	-0.006	-0.008	0.003 0.012
I	-0.042	0.010	0.006	-0.018	-0.012	-0.001

It should be noted that for all CpX, the incipient bonds have a lower bond order in the *syn* TS than in the corresponding *anti* TS. This is reflected in the geometry; the incipient bond is longer in the *syn* TS than it is in the *anti* TS (Section 2.5). While this is a distinguishing feature between *syn* and *anti* TS's, it does not result in facial selectivity.

Unfortunately, Mulliken atomic charges and Mayer's bond order are also based on a partitioning scheme that has a degree of arbitrariness. Both are constructed using the population matrix, which is the product \mathbf{PS} of the density matrix \mathbf{P} and the overlap matrix \mathbf{S} . The trace of \mathbf{PS} yields the total number of electrons. The Mulliken definition of the charge q_A on atom A is defined to be:

$$q_A = Z_A - \sum_{\mu \in A} (\mathbf{PS})_{\mu\mu}$$

where Z_A is the nuclear charge of atom A, and the sum is only over basis functions which are centred on atom A. The bond order according to Mayer, BO_{AB} , between atoms A and B is defined to be:

$$BO_{AB} = \sum_{\mu \in A} \sum_{\nu \in B} (\mathbf{PS})_{\mu\nu}$$

Mulliken atomic charges and Mayer's bond order do provide a qualitative picture of the electronic properties of molecular structures in many cases. However, they are known to fail to the point that currently they are rarely used in published theoretical analyses. Both of these methods ignore the fact that all basis functions contribute to the mapping of electron density about the whole molecular structure, not just for the atoms they are centred on.

A theoretically rigorous determination of atomic charge has been defined by Bader.⁶⁴ Bader defines the boundary of an atom as the surface about the atom where the Laplacian of the density, $\nabla^2\rho$, is equal to zero. All of the electron density that resides inside this surface “belongs” to the atom. Obtaining atomic charges using Bader’s definition would have been ideal, but the necessary code was unavailable. While Bader has defined an empirical measure of bond order for carbon-carbon bonds based on bond ellipticity, there is no theoretically rigorous derived formula for the general bond order between two non-bonded atoms.

Facial selectivity in the Diels-Alder reaction of CpX follows a periodic trend. Therefore, it is expected that electronegativity, which is a periodic property, should correlate with facial selectivity. Boyd and Edgecombe⁶⁵ calculated the electronegativity of groups, based on the relative position of the bond critical point defined by Bader. The calculated electronegativities were fitted to compare with the Pauling scale. Figure 2.14 presents a plot of ΔE_{act} versus group electronegativity of X for both *syn* and *anti* additions of CpX and ethene. Pauling electronegativity values (of X⁰) were used for X = H, SnH₃, SbH₂, TeH and I.^{66,a} There is a rough correlation between *syn* ΔE_{act} and group electronegativity ($r^2 = 0.82$ with CpH, $r^2 = 0.88$ without CpH). The narrow range of values for *anti* ΔE_{act} does not allow for a correlation with group electronegativity. Electronegativity is directly proportional to periodic trends such as ionization energy, electron affinity and atomic radius. Is it electronegativity, or another periodic trend that correlates with facial selectivity?

^a Boyd and Edgecombe group electronegativities and Pauling electronegativities are listed in Table A.42 of the appendix.

(a)



(b)



(c)

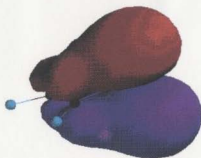
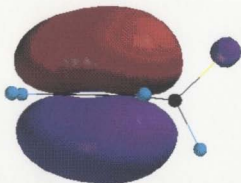
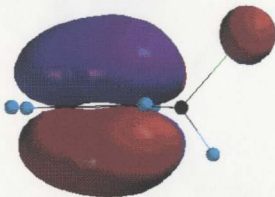


Figure 2.3 MO plots for CpH. (a) MO 18: a_2 (HOMO), (b) MO 17: b_1 , and (c) MO 12: b_1 .

(a)



(b)



(c)

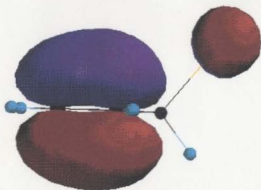
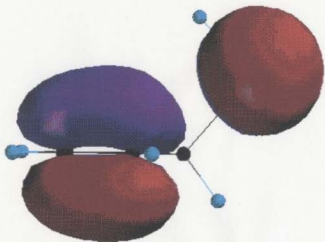


Figure 2.4 Plot of HOMO for (a) CpF, (b) CpCl and (c) CpBr. All HOMO's have a'' symmetry.

(a)



(b)

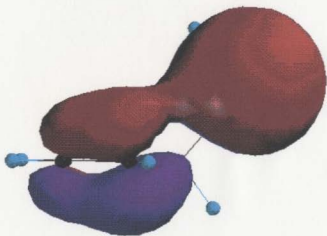
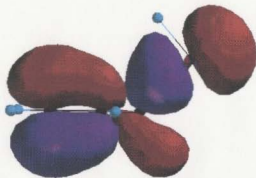
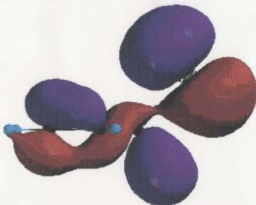


Figure 2.5 MO plots for CpSeH. (a) HOMO and (b) *n*-HOMO. Both MO's have a'' symmetry.

(a)



(b)



(c)

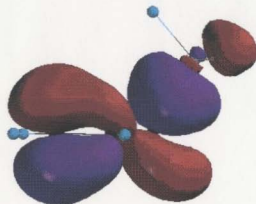


Figure 2.6 MO plots of the three types of π_g . (a) Case 1: MO 24 of CpSH, (b) Case 2: MO 25 of CpCl, and (c) Case 3: MO 25 of CpSiH₃. All MO's have d' symmetry.

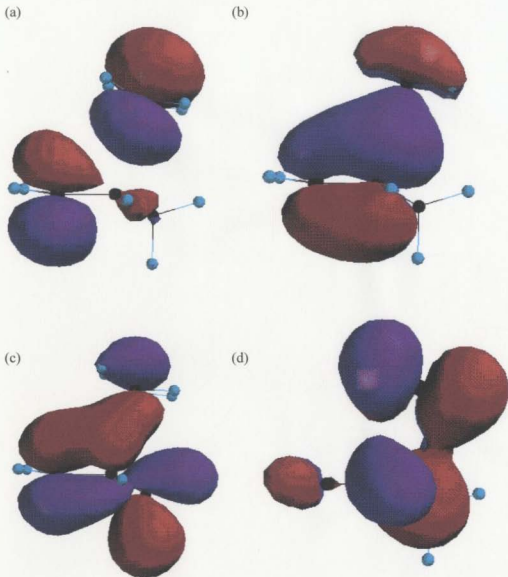
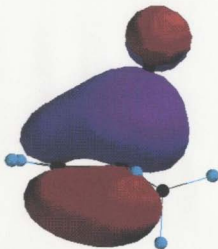
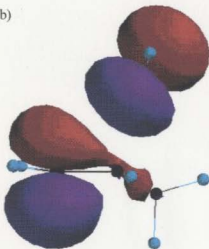


Figure 2.7 Plotted MO's for the TS for the reaction of CpH and ethene. (a) MO 26: d' (HOMO; π_s/π_s antibonding), (b) MO 25: d'' (π_A/π_A^*), (c) MO 24: d' (π_s/π_s bonding) and (d) MO 22: d' (σ/σ).

(a)



(b)



(c)

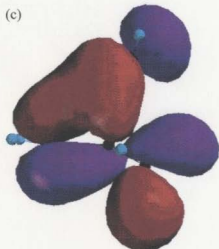


Figure 2.8 Plotted MO's for the TS for the reaction of CpH and ethyne. (a) MO 25: a'' (HOMO; π_A/π_A^*), (b) MO 24: a' (π_S/π_S antibonding) and (c) MO 22: a' (π_S/π_S bonding).

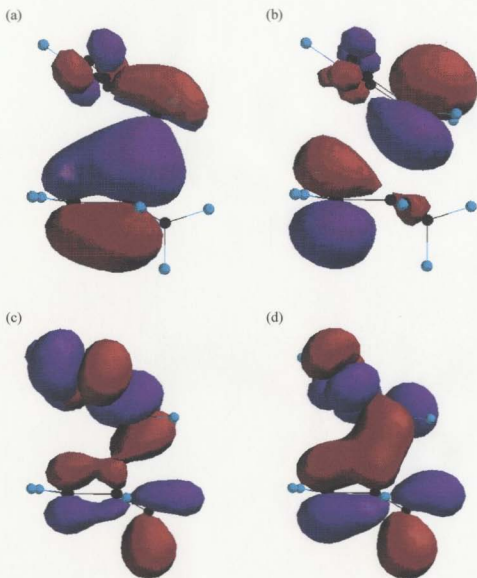


Figure 2.9 Plotted MO's for the *endo* addition TS of CpH and maleimide. (a) MO 43: a'' (HOMO), (b) MO 42: a' , (c) MO 39: a' and (d) MO 38: a' .

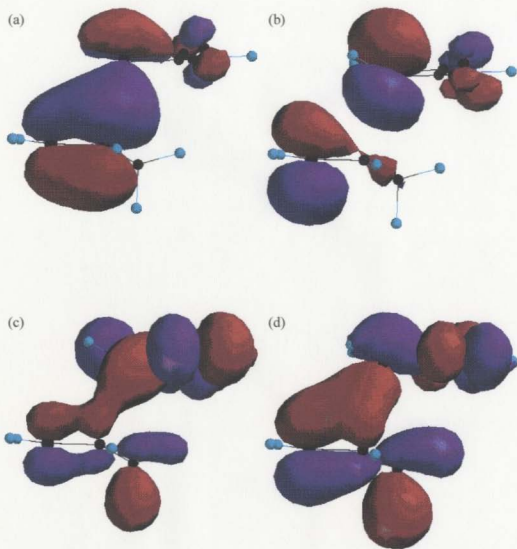
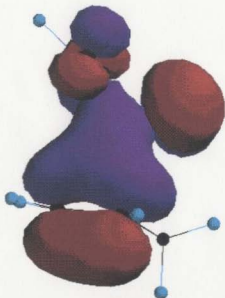


Figure 2.10 Plotted MO's for the *exo* addition TS of CpH and maleimide.

(a) MO 43: a'' (HOMO.), (b) MO 41: a' , (c) MO 39: a' and (d) MO 38: a' .

(a)



(b)

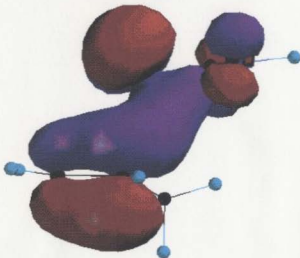


Figure 2.11 Plotted HOMO's (MO 43) for the TS for (a) *endo* and (b) *exo* addition of CpH and TAD (both have a'' symmetry).

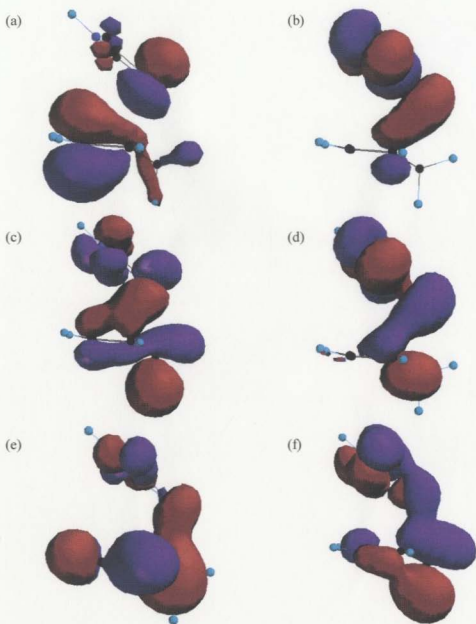


Figure 2.12 Plotted MO's for the TS for *endo* addition of CpH and TAD. (a) MO 42: d' , (b) MO 41: d'' , (c) MO 38: d' , (d) MO 37: d'' , (e) MO 35: d'' and (f) MO 30: d' .

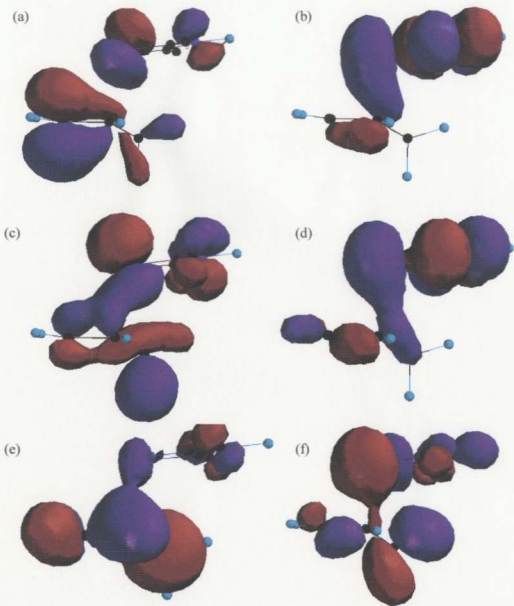


Figure 2.13 Plotted MO's for the TS for *exo* addition of CpH and TAD. (a) MO 42: d' , (b) MO 41: d'' , (c) MO 38: d' , (d) MO 37: d'' , (e) MO 36: d'' and (f) MO 35: d' .

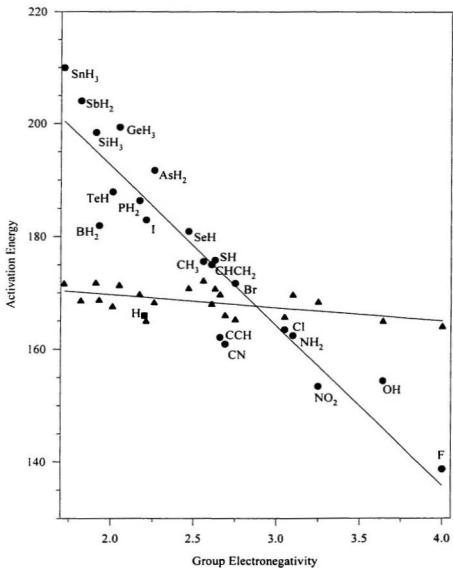


Figure 2.14 ΔE_{act} versus group electronegativity. ● = *syn*, ▲ = *anti*, ■ = C_{sp}H.

2.5 Geometry

Electronic modifications to the diene or the dienophile due to X should translate into geometric changes in the carbon framework of the diene and/or the dienophile, in the GS and/or the TS, depending on the phenomenon. Covalent bond lengths depend on the amount of electron density in the bond - the higher the electron density, the shorter the bond. Bond angles can reflect the hybridization of the central atom.

For GS CpX, the π -bonds $C_1=C_2$ and $C_3=C_4$ are of greatest interest. These bonds are shorter for CpX's that prefer *syn* addition, whereas the C_2-C_3 bonds are longer for these same CpX's. Figure 2.15 displays a graph of the C_2-C_3 bond length *versus* the average of the $C_1=C_2$ and $C_3=C_4$ bonds for a given CpX. Note that for all graphs, the scale of both axes is the same whenever two quantities have the same dimensions. There is excellent correlation between these two quantities ($r^2 = 0.96$). Moreover, the slope of -1.73 suggests that as the C_2-C_3 bond gets longer, the electron density is transferred largely to the two π -bonds. If π -donation from X to the ring were important, the C_2-C_3 bond would shorten with the increased π -donation due to conjugation. Instead, an inductive effect is probably the basis of these bond length trends. The electronegativity of X is playing a role here: as the electronegativity of X increases, the length of the two π -bonds decreases.

The length of these bonds is also related to facial selectivity. Figures 2.16 and 2.17 present plots of ΔE_{act} for the reaction of CpX and ethene *versus* the average $C_1=C_2/C_3=C_4$ bond and the C_2-C_3 bond in the corresponding GS CpX, respectively. *syn* ΔE_{act} is higher for CpX's that have longer π -bonds, while the reverse is true for the C_2-C_3 σ -bond.

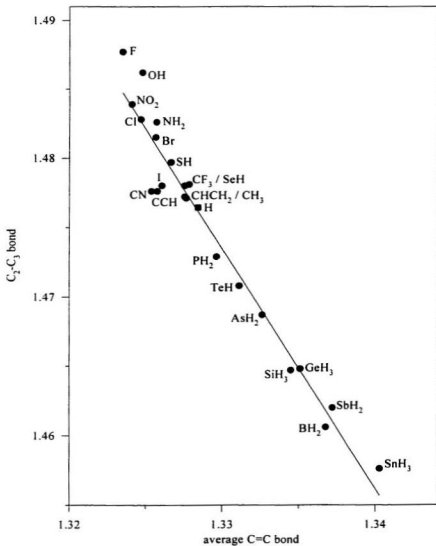


Figure 2.15 Graph of the C₂-C₃ bond length *versus* the average C=C bond length for ground state CpX's (Å).

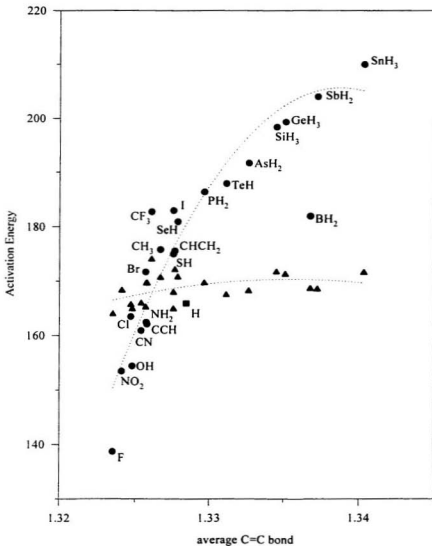


Figure 2.16 Graph of syn and anti ΔE_{act} ($\text{kJ}\cdot\text{mol}^{-1}$) versus average C=C bond length for ground state $\text{CpX}'\text{s}$ (Å). ● = syn, ▲ = anti, ■ = CpH.

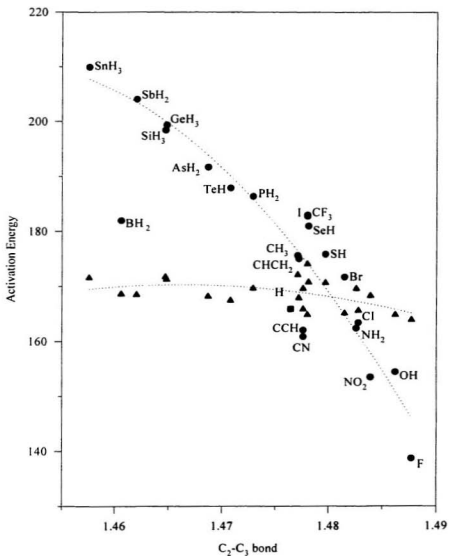


Figure 2.17 Graph of syn and anti ΔE_{ocr} ($\text{kJ}\cdot\text{mol}^{-1}$) versus $\text{C}_2\text{-C}_3$ bond length for GS CpX (Å). ● = syn, ▲ = anti, ■ = CpH.

A shorter π -bond should lead to a more reactive diene. However, if the effect is congruent for both the *syn* and *anti* face of CpX , this should not directly affect facial selectivity.

What is most interesting about the π -system in the TS is that the variation in geometry becomes even less than it was in the GS. In the TS for *syn* and *anti* addition of all CpX 's to ethene, the $\text{C}_1=\text{C}_2$, $\text{C}_3=\text{C}_4$ and C_2-C_3 bonds in the diene and the $\text{C}_6=\text{C}_7$ bond in the dienophile all fall in a range between 1.3772\AA and 1.4043\AA . This is a variance of less than 0.03\AA for four bonds which were dissimilar in the GS. Although the range of bond lengths is reduced in the TS, the relationships observed in Figures 2.15 through 2.17 are still maintained.

There are several consistent trends in these TS's. As was mentioned in the previous section, the incipient bond for *syn* addition is always longer than for *anti* addition in the TS. Other uniformities exist for all of the TS's, irrespective of the mode of addition, the dienophile or X. For example, the C_5 -substituent Y which faces the dienophile in the TS (Figure 2.18) is always almost coplanar with the four carbons of the diene. As well, the C_5-Y bond always becomes shorter in the TS than its corresponding value in GS CpX . Conversely, the C_5-Z bond, which lies antiperiplanar to the dienophile, always becomes longer than its GS value. is most interesting about these changes is that the C_5-Y and C_5-Z

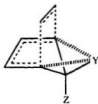


Figure 2.18 Definition of Y and Z; Y is nearly coplanar with the four carbons of the diene.

bonds return to their GS CpX value in the product. While it is difficult to associate this phenomenon with any one particular orbital mixing, we speculate that favourable mixing between the σ - or π -framework of the diene and the C₅-Y bond is enhanced in the TS, thus increasing the electron density in this bond, which leads to its shortening.

None of the trends in absolute geometry have addressed the problem of facial selectivity of CpX. However, the changes involved in transforming the GS diene to its TS geometry do provide more insight. Table 2.14 lists the ranges of these changes for the reaction of CpX and ethene. Whereas some of the individual changes are large, most of the geometric changes vary over a small range of values.

The exception lies in the group of angles about C₅. The range of these angle changes is about an order of magnitude greater than the range of any other angular change. As CpX is deformed into its *syn* TS geometry, the angles C₁-C₅-X and C₄-C₅-X widen, while the angles C₁-C₅-H₅ and C₄-C₅-H₅ compress by a similar amount. The angle X-C₅-H₅ experiences less change. The net effect is to tilt the X-C₅-H₅ triangle about the C₅ pivot, as illustrated in Figure 2.19.

Table 2.14 Maximum and minimum geometry changes (Δ_{\min} and Δ_{\max}) in transforming the GS reactants to their TS structures for the reaction of CpX and ethene.^a
 $\Delta\Delta = \Delta_{\max} - \Delta_{\min}$. Angle changes are in degrees, bond length changes are in Å.

parameter	<i>syn</i> TS - GS			<i>anti</i> TS - GS		
	Δ_{\min}	Δ_{\max}	$\Delta\Delta$	Δ_{\min}	Δ_{\max}	$\Delta\Delta$
C ₂ -C ₃	-0.1145	-0.0704	0.0441	-0.0885	-0.0781	0.0104
C ₁ -C ₂ , C ₃ -C ₄	0.0533	0.0635	0.0102	0.0543	0.0651	0.0108
C ₁ -C ₅ , C ₄ -C ₅	-0.0122	0.0296	0.0418	-0.0011	0.0143	0.0154
C ₃ -H ₅	0.0003	0.0179	0.0176	-0.0108	-0.0043	0.0065
C ₅ -X	-0.0269	0.0006	0.0275	-0.0010	0.0263	0.0273
C ₆ -C ₇	0.0602	0.0680	0.0078	0.0637	0.0708	0.0071
C ₁ -C ₂ -C ₃ , C ₂ -C ₃ -C ₄	-0.56	0.02	0.58	-0.61	-0.03	0.58
C ₅ -C ₁ -C ₂ , C ₅ -C ₄ -C ₃	-4.68	-2.20	2.48	-3.17	-2.01	1.16
C ₁ -C ₅ -C ₄	-4.43	-2.68	1.75	-3.76	-3.31	0.45
C ₁ -C ₅ -H ₅ , C ₄ -C ₅ -H ₅	-11.05	-1.64	9.40	-0.48	5.52	6.00
C ₁ -C ₅ -X, C ₄ -C ₅ -X	-0.28	23.15	23.43	-7.51	4.87	12.37
X-C ₅ -H ₅	-9.75	3.92	13.67	-1.98	3.14	5.12
C ₆ -C ₇ -H _{7a} , C ₇ -C ₆ -H _{6a}	-2.36	-1.31	1.05	-2.36	-1.94	0.43
C ₆ -C ₇ -H _{7b} , C ₇ -C ₆ -H _{6b}	-1.87	-1.46	0.41	-1.87	-1.55	0.32
H _{6a} -C ₆ -H _{6b} , H _{7a} -C ₇ -H _{7b}	-2.19	-0.60	1.58	-1.91	-1.48	0.43

^a The appendix contains tables of geometries for all structures studied in this thesis.

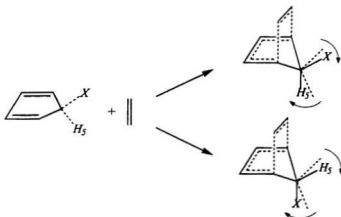


Figure 2.19 The tilting of X-C₅-H₅ triangle about the C₅ pivot in transforming CpX to its TS geometry. The dashed lines represent the GS position of the C₅-H₅ and the C₅-X bonds.

This same tilting occurs in the transformation of the GS CpX to its *anti* addition TS, albeit to a lesser degree.

The extent of the angular change about C₅ correlates well with facial selectivity. The mode of addition which experiences the lesser amount of angular change about C₅ is the preferred mode of attack. The total angular change, $\Delta\Theta_{\text{Total}}$, accounts for the change in all five angles:

$$\Delta\Theta_{\text{Total}} = |\Delta\Theta_{\text{C}_1-\text{C}_5-\text{X}}| + |\Delta\Theta_{\text{C}_4-\text{C}_5-\text{X}}| + |\Delta\Theta_{\text{C}_1-\text{C}_5-\text{H}_5}| + |\Delta\Theta_{\text{C}_4-\text{C}_5-\text{H}_5}| + |\Delta\Theta_{\text{X}-\text{C}_5-\text{H}_5}|$$

where $|\Delta\Theta_{\text{C}_1-\text{C}_5-\text{X}}|$ is the absolute value of the change in angle C₁-C₅-X from its GS to its TS value, and so forth. Table 2.15 lists the values of $\Delta\Theta_{\text{Total}}$ for the *syn* and *anti* addition of CpX and ethene, and Figure 2.20 contains the plot of ΔE_{act} versus $\Delta\Theta_{\text{Total}}$ for these reactions.

Table 2.15 $\Delta\Theta_{\text{Total}}$ (degrees) and facial selectivity for the reaction of CpX with ethene.

X	$\Delta\Theta_{\text{Total}}$ (<i>syn</i>)	$\Delta\Theta_{\text{Total}}$ (<i>anti</i>)	calc. % <i>syn</i>
H	17.0		
BH ₂	58.9	8.1	0.3
CH ₃	26.5	11.4	17.8
NH ₂	19.6	20.7	95.9
OH	14.4	16.2	99.0
F	9.7	18.4	100.0
SiH ₃	46.8	6.2	0.0
PH ₂	26.1	16.5	0.1
SH	20.4	10.9	9.4
Cl	21.3	14.0	72.5
GeH ₃	46.1	5.0	0.0
AsH ₂	38.5	3.9	0.0
SeH	23.0	16.4	1.1
Br	25.6	11.8	5.4
SnH ₃	54.8	6.1	0.0
SbH ₂	47.7	3.7	0.0
TeH	35.6	5.3	0.0
I	30.6	9.6	0.0
CH=CH ₂	27.1	11.7	4.3
C≡CH	18.5	14.5	96.5
C≡N	17.3	14.2	90.2
CF ₃	30.7	11.0	2.2
NO ₂	13.3	16.0	99.9

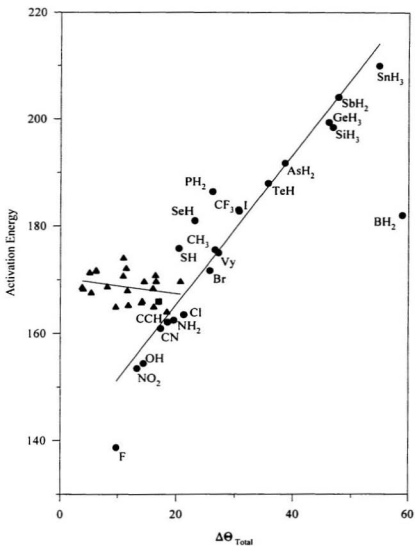


Figure 2.20 ΔE_{act} (kJ·mol⁻¹) versus $\Delta\Theta_{\text{Total}}$ (degrees) for the reaction of CpX and ethene, for CpH (■), and for *syn* (●) and *anti* (▲) addition. Vy denotes CH=CH₂.

Remarkably, $\Delta\Theta_{\text{Total}}$ accounts for facial selectivity in all cases, with the exception of CpNH_2 , CpCl , $\text{CpC}\equiv\text{N}$ and $\text{CpC}\equiv\text{CH}$ (all of which prefer *syn* addition). For *anti* addition, the value of $\Delta\Theta_{\text{Total}}$ is similar to that of CpH , while $\Delta\Theta_{\text{Total}}$ for *syn* addition is spread over a much wider range of values. Furthermore, for *syn* addition, with the exception of CpBH_2 , $\Delta\Theta_{\text{Total}}$ is linearly proportional to ΔE_{act} ($r^2 = 0.91$ for all CpX except CpBH_2 ; $r^2 = 0.75$ if CpBH_2 is included). This correlation suggests that angular deformation about C_3 for *syn* addition is an important factor in determining facial selectivity for CpX . However, $\Delta\Theta_{\text{Total}}$ does not correlate without exceptions with ΔE_{act} , and it fails to determine facial selectivity in some cases. This may be an indication that another factor important in controlling facial selectivity exists. On the other hand, it is more likely that the failures can be attributed to the fact that the energetic cost per unit of angular change cannot be the same for all of these angles in all of these dienes. A better comparison would be between ΔE_{act} and the energy required to change the angles about C_3 to their TS values.

2.6 Partitioning Activation Energy

Sections 2.4 and 2.5 highlighted the difficulty of assigning differences in electronic structure or geometry to their importance in controlling facial selectivity. It is the energetic consequences of such differences that determines the differences in ΔE_{act} that lead to facial selectivity. In Section 2.2, the various hypotheses proposed to explain facial selectivity were divided into two categories. Facial selectivity might be determined by factors which are either present in the GS CpX, or require an interaction between the diene and the dienophile to occur. The following partitioning scheme for ΔE_{act} allowed us to determine in which category each factor belongs.

The formation of a Diels-Alder TS can be imagined to occur in three distinct steps:

1. the diene is deformed into its TS structure (diene deformation)
2. the dienophile is deformed into its TS geometry (dienophile deformation)
3. the diene and dienophile are placed in their TS positions relative to each other (interaction)

The sum of the energies required to perform each of the above steps is ΔE_{act} for the reaction. Two more calculations are required: an SCF calculation on the diene and on the dienophile in their TS geometries. From these values the energy of the corresponding GS entities were subtracted, resulting in diene and dienophile deformation energies, ΔE_{diene}^{def} and $\Delta E_{dienophile}^{def}$, respectively. The energy of interaction, ΔE_{int} , was defined to be the remaining energy after subtracting the two deformation energies from ΔE_{act} . In summary,

$$\Delta E_{act} = \Delta E_{diene}^{def} + \Delta E_{dophile}^{def} + \Delta E_{int}$$

Figure 2.21 provides a pictorial representation of the different contributions to ΔE_{act} . Tables 2.16 through 2.19 list ΔE_{act} and its components for *syn* and *anti* additions of CpX to ethene, ethyne, maleimide and TAD, respectively.

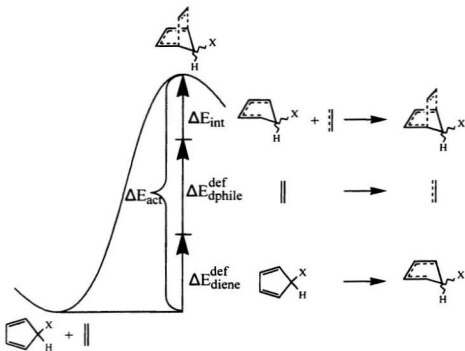


Figure 2.21 Pictorial definition of ΔE_{act} , ΔE_{diene}^{def} , $\Delta E_{dophile}^{def}$ and ΔE_{int} .

Table 2.16 ΔE_{act} , ΔE_{diene}^{def} , $\Delta E_{diphile}^{def}$ and ΔE_{int} (kJ·mol⁻¹) for *syn* and *anti* addition of CpX and ethene.

X	<i>syn</i>				<i>anti</i>			
	ΔE_{act}	ΔE_{diene}^{def}	$\Delta E_{diphile}^{def}$	ΔE_{int}	ΔE_{act}	ΔE_{diene}^{def}	$\Delta E_{diphile}^{def}$	ΔE_{int}
H	165.9	99.0	48.1	18.9				
BH ₂	181.9	112.2	52.1	17.7	168.6	94.8	51.8	22.1
CH ₃	175.6	107.9	46.0	21.6	172.1	99.9	48.4	23.7
NH ₂	162.4	98.8	45.2	18.4	169.6	100.6	46.3	22.6
OH	154.4	98.8	40.1	15.5	164.9	99.4	44.7	20.8
F	138.7	85.7	40.5	12.5	163.9	98.9	45.0	20.1
SiH ₃	198.4	127.7	50.3	20.4	171.7	97.4	52.6	21.8
PH ₂	186.3	119.9	47.4	19.0	169.6	96.1	50.0	23.5
SH	175.8	114.4	44.8	16.5	170.7	99.3	48.4	22.9
Cl	163.5	104.8	41.7	17.0	165.7	97.0	47.0	21.6
GeH ₃	199.3	128.3	49.5	21.5	171.3	96.8	53.0	21.4
AsH ₂	191.7	124.1	48.2	19.3	168.2	93.7	51.2	23.3
SeH	180.9	118.9	46.2	15.9	170.7	98.7	49.6	22.5
Br	171.7	111.9	42.1	17.6	165.2	95.3	48.2	21.7
SnH ₃	209.9	137.2	51.3	21.4	171.6	96.6	54.8	20.2
SbH ₂	204.0	133.4	50.1	20.5	168.5	93.1	53.0	22.4
TeH	187.9	123.0	47.8	17.1	167.5	94.4	50.7	22.5
I	182.9	120.5	43.4	19.1	164.9	93.5	49.3	22.1
CH=CH ₂	175.0	108.1	46.2	20.7	167.9	98.0	47.9	22.0
C≡CH	162.1	101.8	44.2	16.1	169.6	103.0	47.2	19.4
C≡N	160.9	102.7	45.4	12.7	165.9	102.3	46.5	17.1
CF ₃	182.7	119.4	44.7	18.5	174.0	102.0	48.5	23.5
NO ₂	153.4	99.4	44.2	9.8	168.3	103.5	46.0	18.8

Table 2.17 ΔE_{act} , ΔE_{diene}^{def} , $\Delta E_{diphile}^{def}$ and ΔE_{int} (kJ·mol⁻¹) for *syn* and *anti* addition of CpX and ethyne.

X	<i>syn</i>				<i>anti</i>			
	ΔE_{act}	ΔE_{diene}^{def}	$\Delta E_{diphile}^{def}$	ΔE_{int}	ΔE_{act}	ΔE_{diene}^{def}	$\Delta E_{diphile}^{def}$	ΔE_{int}
H	179.8	100.3	64.0	15.5				
CH ₃	187.9	108.3	61.6	17.9	185.7	101.6	64.1	19.9
NH ₂	169.5	97.1	61.4	11.1	181.7	101.1	61.1	19.5
OH	156.0	91.2	62.1	2.8	176.1	99.1	58.8	18.2
F	160.4	87.9	56.4	16.1	174.3	98.4	59.0	16.9
SiH ₃	204.8	127.5	66.0	11.3	186.9	100.0	68.8	18.1
PH ₂	195.4	118.8	63.7	12.9	184.4	98.5	65.9	19.9
SH	186.4	112.3	60.9	13.2	183.5	100.8	63.7	19.0
Cl	182.5	105.8	57.0	19.7	177.9	97.8	61.8	18.2
Br	190.1	112.3	57.3	20.5	177.7	96.3	63.3	18.1
I	198.8	120.0	58.5	20.2	178.1	94.8	64.7	18.6
C≡CH	181.0	102.5	59.9	18.6	183.0	104.2	62.4	16.4
C≡N	177.7	103.3	60.2	14.2	179.2	103.5	61.3	14.3

Table 2.18 ΔE_{act} , ΔE_{diene}^{def} , $\Delta E_{dophile}^{def}$ and ΔE_{int} (kJ·mol⁻¹) for *syn* and *anti* addition of CpX and maleimide.

X	<i>syn</i>				<i>anti</i>			
	ΔE_{act}	ΔE_{diene}^{def}	$\Delta E_{dophile}^{def}$	ΔE_{int}	ΔE_{act}	ΔE_{diene}^{def}	$\Delta E_{dophile}^{def}$	ΔE_{int}
H	129.8	93.9	54.3	-18.4				
CH ₃	140.4	103.5	51.9	-15.1	135.7	95.4	54.0	-13.7
NH ₂	125.6	101.7	46.9	-23.0	136.1	96.5	52.0	-12.4
OH	118.7	94.5	46.0	-21.8	136.0	95.2	49.6	-8.8
F	108.5	81.7	46.7	-19.9	137.5	95.9	49.8	-8.2
SiH ₃	166.0	123.9	57.6	-15.6	137.2	92.9	59.8	-15.4
PH ₂	154.8	117.0	55.2	-17.4	137.8	93.0	57.3	-12.5
SH	145.8	111.0	52.1	-17.4	141.4	96.7	55.1	-10.3
Cl	136.5	101.7	49.1	-14.4	141.3	95.2	53.1	-7.0
Br	145.5	108.9	49.9	-13.4	143.7	94.3	54.9	-5.4
I	159.7	117.8	51.4	-9.4	143.4	93.1	56.5	-6.2
C≡CH	129.8	97.6	50.5	-18.4	139.1	98.1	52.5	-11.5
C≡N	138.4	100.0	52.3	-13.9	145.0	98.2	52.2	-5.4

Table 2.19 ΔE_{act} , ΔE_{diene}^{def} , $\Delta E_{diphile}^{def}$ and ΔE_{int} (kJ·mol⁻¹) for *syn* and *anti* addition of CpX and TAD.

X	<i>syn</i>				<i>anti</i>			
	ΔE_{act}	ΔE_{diene}^{def}	$\Delta E_{diphile}^{def}$	ΔE_{int}	ΔE_{act}	ΔE_{diene}^{def}	$\Delta E_{diphile}^{def}$	ΔE_{int}
H	95.0	86.5	29.9	-21.4				
CH ₃	97.0	89.5	27.5	-20.0	98.9	87.5	29.9	-18.5
NH ₂	81.3	79.8	26.6	-25.2	101.9	89.0	28.3	-15.4
OH	73.1	75.6	26.2	-28.7	106.6	89.1	26.8	-9.4
F	96.3	77.4	24.6	-5.7	107.6	90.3	26.8	-9.5
SiH ₃	118.9	107.4	30.1	-18.6	102.0	86.8	33.3	-18.1
PH ₂	111.6	98.4	28.1	-15.0	104.4	89.1	31.9	-16.6
SH	106.6	92.7	26.8	-12.9	108.7	90.8	30.3	-12.3
Cl	118.5	92.5	24.8	1.2	112.2	90.8	29.1	-7.7
Br	127.0	98.6	25.1	3.3	115.2	91.2	30.6	-6.6
I	134.3	104.7	25.7	3.9	115.8	91.0	31.8	-7.0
C≡CH	108.6	88.9	26.6	-6.9	105.3	90.7	29.0	-14.4
C≡N	119.4	92.1	26.1	1.3	116.3	92.7	28.0	-4.3

A discussion of the data in Tables 2.16 through 2.19 is facilitated with plots. Figures 2.22 through 2.28 display plots of ΔE_{act} versus the components of ΔE_{act} for the various reactions with CpX. All axes corresponding to the same figure or reaction are drawn on the same scale.

Figure 2.22 displays a plot of ΔE_{act} versus ΔE_{dphile}^{def} and ΔE_{int} for the reaction of CpX and ethene. It is evident that both ΔE_{dphile}^{def} and ΔE_{int} , as well as ΔE_{act} for *anti* addition, vary over a proportionately narrow range of values compared to ΔE_{act} for *syn* addition. The reaction of CpX with the other three dienophiles exhibits similar behavior. Figure 2.23 contains a plot of ΔE_{act} versus ΔE_{dphile}^{def} and ΔE_{int} for the reaction of CpX with ethyne, maleimide and TAD.

The only notable correlation between ΔE_{act} and ΔE_{int} is for the reaction of CpX and TAD. Figure 2.24 focuses on this phenomenon. There is a very good linear dependence between ΔE_{act} and ΔE_{int} for *anti* addition ($r^2 = 0.91$, slope = 1.18). For *syn* addition, there are two distinct groups of dienes. One group consists of the halogen-substituted CpX, CpC≡CH and CpC≡N, while the other group consists of all of the other CpX (including CpH). These two groups will be referred to as the halo CpX and the non-halo CpX, respectively. Each group has a similar linear dependence between ΔE_{act} and ΔE_{int} ($r^2 = 0.81$ and 0.74, slope = 2.62 and 2.56, for halo and non-halo CpX, respectively). However, the halo CpX have a higher ΔE_{int} by about 12 kJ·mol⁻¹, which is also reflected in the higher values of ΔE_{act} . This phenomenon will be explored in greater depth later.

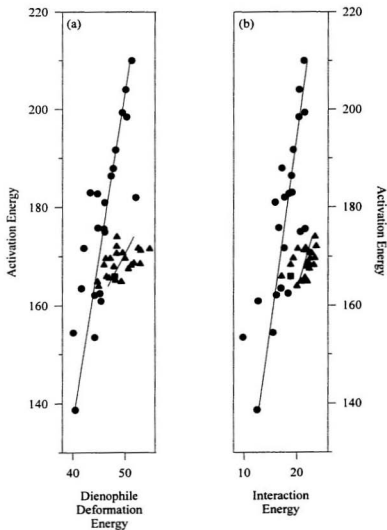


Figure 2.22 ΔE_{act} versus (a) ΔE_{dphile}^{def} and (b) ΔE_{int} (kJ·mol⁻¹) for the reaction of CpX and ethene, for CpH (■), *syn* addition (●) and *anti* addition (▲).

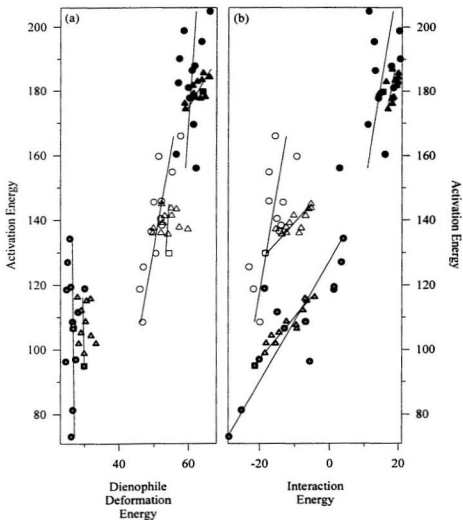


Figure 2.23 ΔE_{act} versus (a) $\Delta E_{def}^{dienophile}$ and (b) ΔE_{int} (kJ·mol⁻¹) for the reaction of CpX with ethyne (filled symbols), maleimide (empty symbols) and TAD (pluses in symbol), for CpH (square), *syn* addition (circles) and *anti* addition (triangles).

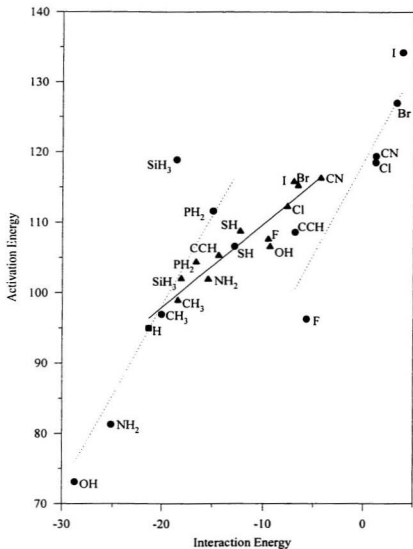


Figure 2.24 ΔE_{act} versus ΔE_{int} (kJ·mol⁻¹) for the reaction of CpX and TAD, for CpH (■), *syn* addition (●, dashed lines) and *anti* addition (▲, solid line).

Of greater importance to facial selectivity are the plots of ΔE_{act} versus ΔE_{diene}^{def} for all four dienophiles (Figures 2.25, 2.26 and 2.27). For the reaction of CpX with ethene, ethyne and maleimide, ΔE_{diene}^{def} correlates excellently with ΔE_{act} for *syn* addition ($r^2 = 0.96, 0.95, 0.93$, respectively; slope = 1.33, 1.20, 1.37, respectively). For *anti* addition, values of ΔE_{diene}^{def} , like ΔE_{act} , are similar to the corresponding value for CpH for these reactions. For a given value of ΔE_{diene}^{def} , ΔE_{act} is noticeably higher in energy for *anti* addition than for *syn* addition.

For the reaction of CpX with TAD (Figure 2.27), halo CpX and non-halo CpX again behave differently for *syn* addition. For each group, ΔE_{diene}^{def} correlates excellently with ΔE_{act} ($r^2 = 0.96, 0.97$; slope = 1.48, 1.44 for halo and non-halo CpX, respectively). However, ΔE_{act} is about 15 kJ·mol⁻¹ higher for the halo CpX. There is also a lesser correlation between ΔE_{act} and ΔE_{diene}^{def} for *anti* addition ($r^2 = 0.82$, slope = 3.23).

In all of these plots, we are comparing quantities (energies) which have the same units. Thus, both the range of energy values and the slopes obtained are physically meaningful in determining the relative importance of ΔE_{diene}^{def} , $\Delta E_{diphile}^{def}$ and ΔE_{int} to the differences in ΔE_{act} , and consequently, to facial selectivity. We have already concluded that the factor that controls facial selectivity is more prevalent for *syn* addition than it is for *anti* addition, due to the difference in the range of ΔE_{act} for all of the reactions studied.

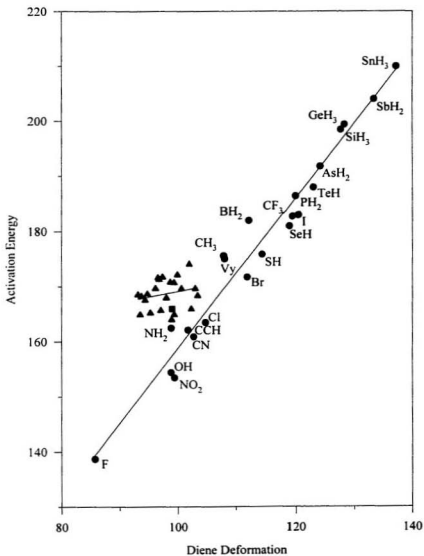


Figure 2.25 ΔE_{act} versus ΔE_{diene}^{def} (kJ·mol⁻¹) for the reaction of CpX and ethene, for CpH (■), syn addition (●) and anti addition (▲).

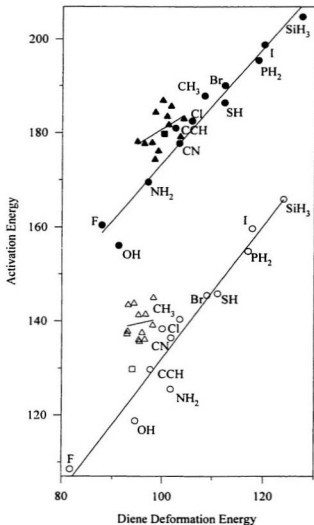


Figure 2.26 ΔE_{act} versus ΔE_{diene}^{def} ($\text{kJ}\cdot\text{mol}^{-1}$) for the reaction of CpX with ethyne (filled symbols) and maleimide (empty symbols), for CpH (square), *syn* addition (circles) and *anti* addition (triangles).

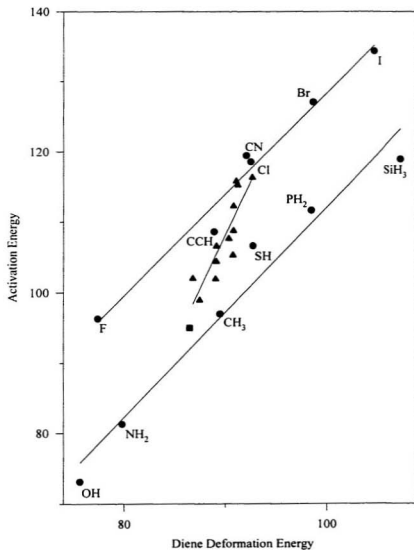


Figure 2.27 ΔE_{act} versus ΔE_{diene}^{def} (kJ·mol⁻¹) for the reaction of CpX and TAD, for CpH (■), *syn* addition (●) and *anti* addition (▲).

Now, due to the small range of values of $\Delta E_{dophile}^{def}$ and ΔE_{int} , and their lack of correlation with ΔE_{act} for the reaction of CpX with ethene, ethyne and maleimide, we can conclude that both dienophile deformation and the interaction between the two addends are also not important in determining facial selectivity in these reactions. *For the reaction of CpX with ethene, ethyne and maleimide, the primary factor which determines facial selectivity in these reactions is the energy required to deform the diene into its syn TS geometry.* This is supported by the wider range of both ΔE_{act} and ΔE_{diene}^{def} for *syn* addition. As well, the near unity slopes indicate the relationship between these two quantities is almost one-to-one.

For the reaction of CpX and TAD, the primary factor in determining facial selectivity is, again, the energy required to deform the diene into its *syn* TS geometry. This is supported by the wider range of ΔE_{act} and ΔE_{diene}^{def} for *syn* addition, and the near unity linear correlation between these quantities. However, there is an important secondary effect, which is near constant (near-parallel slopes for halo and non-halo CpX), that separates the CpX's into two groups. As well, there is a smaller, tertiary effect for *anti* addition, which leads to the observed correlations between ΔE_{act} and both ΔE_{diene}^{def} and ΔE_{int} . This is a minor effect, given the narrower range of these energy values.

The secondary effect is consistent with a closed-shell repulsion between the lone pairs on the reacting nitrogens of TAD with the lone pairs of CpF, CpCl, CpBr and CpI, and the π -bond of CpC \equiv N and CpC \equiv CH. This is similar to the arguments used by Coxon *et al.*, for facial selectivity in the Diels-Alder reaction of their caged ether (Figure 1.14). CpX's that have lone pairs, such as CpNH₂ and CpOH, prefer conformations in their *syn* addition TS's

where a hydrogen is pointing at the nitrogens of TAD. CpNH₂ in its staggered conformation and CpOH in its gauche conformation lead to second-order saddlepoints in the *syn* TS for their reaction with TAD. In these cases, both substituents have lone pairs pointing at TAD. For the other three dienophiles, these conformers give rise to first-order saddlepoints. The ΔE_{act} and ΔE_{diene}^{def} for the reaction of staggered CpNH₂ and gauche CpOH with TAD makes these dienes behave more like the halo CpX (Figure 2.28). This supports the closed-shell repulsion hypothesis.

We can conclude that facial selectivity is primarily determined by the energetic cost of deforming the diene into its TS geometry for all of these reactions. The secondary effect observed for the reaction of CpX with TAD also translates to an energetic cost in deforming the diene. Any factor involving an attractive interaction between the diene and the dienophile either does not significantly affect facial selectivity, or is translated into diene deformation in the TS. The latter possibility seems unlikely, and would be difficult to prove one way or another. Therefore, any of the hypotheses that suggested that facial selectivity is due to differences in the interactions between the diene and the dienophile is unlikely to be significant (*i.e.*, X and dienophile LUMO mixing, different van der Waals forces experienced by the two faces, and the “Cieplak effect”). There must be an interaction between the diene and the dienophile in order for diene deformation to occur. However, it is possible that the primary factor which controls facial selectivity in these reactions should be observable in the GS CpX.

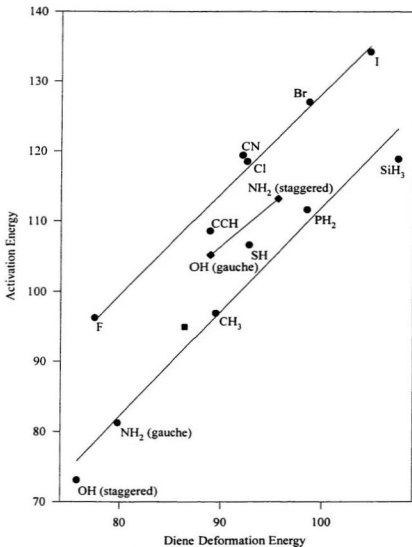


Figure 2.28 ΔE_{act} versus ΔE_{diene}^{def} (kJ·mol⁻¹) for the reaction of CpX and TAD, for CpH (■) and *syn* addition (●). Second order saddlepoints for the reaction of CpNH₂ and CpOH (◆) are included.

While ΔE_{diene}^{def} correlates with ΔE_{act} for *syn* addition, a straightforward comparison of ΔE_{diene}^{def} for *syn* and *anti* addition occasionally fails to predict facial selectivity. Although CpCl and CpC≡N both prefer *syn* addition to ethene, both have lower ΔE_{diene}^{def} for *anti* addition. Failures also exist for the reaction of CpCl with ethyne, for the reaction of CpNH₂, CpCl and CpC≡N with maleimide, and for the reaction of CpCH₃, CpSH, CpC≡CH and CpC≡N with TAD. Most of these reactions are less selective, and are thus more susceptible to minor effects and errors (*e.g.*, BSSE). Nevertheless, a comparison of ΔE_{diene}^{def} for *syn* and *anti* addition does successfully predict facial selectivity in most cases.

In the previous section, it was shown that $\Delta\Theta_{Total}$ for *syn* addition correlates well with facial selectivity. A comparison of Figures 2.20 and 2.25 reveals a striking resemblance between the behavior of $\Delta\Theta_{Total}$ and ΔE_{diene}^{def} for the reaction of CpX and ethene. ΔE_{diene}^{def} measures the energetic cost of angular deformation about C₅, as well as every other deformation in the diene. Given the consistency in all other geometric changes involved in transforming the GS diene into its TS shape (Table 2.15), it is probable that the variation in ΔE_{diene}^{def} is directly due to the variation in the angular deformation about C₅. Thus, ΔE_{diene}^{def} is a good approximation for the desired measure of the energetic cost of angular deformation about C₅, and it includes a constant factor for all of the other geometric changes required to transform the GS diene to its TS structure. ΔE_{diene}^{def} properly accounts for CpF and CpBH₂, whose value of $\Delta\Theta_{Total}$ would predict a higher value for *syn* ΔE_{act} .

What property of CpX determines the extent of angular change and consequently the amount of energy required to deform the diene into its *syn* TS? The differences in $\Delta\Theta_{Total}$ are

hinting at a steric hindrance factor which could determine facial selectivity in these reactions. The question is, what is the basis of such an argument? How can H be more sterically demanding than OH, NH₂, NO₂, C≡N, C≡CH, and Cl? Is the correlation between the electronegativity of X and facial selectivity due to an electronic effect or a periodic trend?

2.7 Size and Steric Hindrance

Steric hindrance can be thought of as molecular fragments “bumping” into each other. It is a function of the size and shape of the fragments, and their proximity to each other. An acetoxy group is usually considered to be more sterically demanding than a hydrogen atom. Is this always the case? How can one quantify the steric effect of an atom or a group?

Several empirical measures of size and steric hindrance have been derived. These include van der Waals radii and volumes,⁶⁷ Bragg-Slater radii,⁶⁸ A-values,⁶⁹ n-values,⁷⁰ P-values,⁷¹ molecular refractivity and Taft's E_s .⁷²

A rough measure of the size of a group is the atomic radius of its central atom. Van der Waals radii are determined by crystallography, and are defined to be the typical internuclear distances between nearest neighbour atoms in different molecules in condensed phases. Bragg-Slater radii were introduced by Bragg and later extended by Slater. They suggested that regardless of the bond type (*i.e.*, ionic, covalent or intermediate), good estimates of internuclear distances can be obtained by adding constant atomic radii. Figures 2.29 and 2.30 display plots of ΔE_{act} for *syn* addition of CpX and ethene, *versus* van der Waals and Bragg-Slater radius of X° , respectively. Both plots show that there is a correlation between *syn* ΔE_{act} and the radius of X° , for X° 's that belong to the same periodic group. In both cases ΔE_{act} also increases from right to left across a period. These correlations suggest that the size of X° must have some significance in determining facial selectivity.

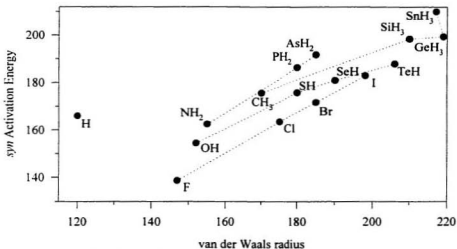


Figure 2.29 *syn* ΔE_{act} ($\text{kJ}\cdot\text{mol}^{-1}$) versus van der Waals radius of X^a (pm) for the reaction of CpX and ethene.

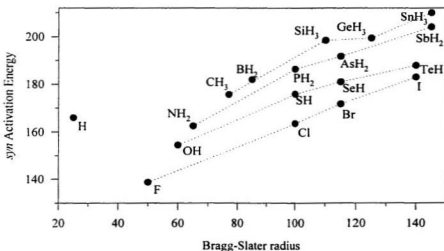


Figure 2.30 *syn* ΔE_{act} ($\text{kJ}\cdot\text{mol}^{-1}$) versus Bragg-Slater radius of X^a (pm) for the reaction of CpX and ethene.

One interpretation of these trends is that as the radius of an atom increases from period two through five of the periodic table, there is an increased amount of steric hindrance between the atom and the incoming dienophile. This results in a greater amount of angular deformation as X tries to get out of the way, which results in higher ΔE_{diene}^{def} , and consequently, higher ΔE_{act} . In going from right to left of a period, the number of hydrogens attached to X^0 increases. This increases steric hindrance between the dienophile and X, thus increasing angular deformation, ΔE_{diene}^{def} and ΔE_{act} . This is consistent with the periodic arrangement in Figures 2.29 and 2.30. A weakness in this argument is that neither the conformation of X for a periodic group, nor the length of the X^0 -H bond, is constant. For example, CpSeH and CpTeH both prefer the eclipsed conformation for *syn* addition to ethene, so these two dienes should behave like the halogen-substituted CpX. The arrangement of the points, especially for the plot of ΔE_{act} versus Bragg-Slater radius, is too good for such a variable effect. The major weakness in this analysis is that CpH does not fit this model. Both the van der Waals and the Bragg-Slater radius of hydrogen is predicted to be smaller than all other X^0 . Based on the small atomic radius of hydrogen, and its lack of substituents or lone pairs, every reaction of CpX should yield the product of *anti* addition.

The other empirical measures of steric hindrance take into account the full size of the X. Van der Waals volumes include the effective volume of the central atom and its attachments. P-values are defined to be ΔG^\ddagger for the rotational barrier of monosubstituted ethanes, relative to ethane itself. A-values are defined to be the logarithm of the equilibrium constant (*i.e.*, ΔG^0) for the *axial/equatorial* interconversion of monosubstituted

cyclohexanes. They have also been defined for 1-substituted-3,3-dimethylcyclohexanes. n -Values are based on the equilibrium pictured in Figure 2.31. ΔG° is determined for this equilibrium for various values of n and substituents X. For a given X, ΔG° is linearly dependent on the number of methylene groups, n . The n -value of X is defined to be the value of n obtained by interpolation which gives $\Delta G^\circ = 0$. Taft's E_s is a linear free energy relationship, based on the acidic hydrolysis of aliphatic esters of the type XCOOR. Its defining equation is $E_s = \log(k_X/k_0)$, where the reference system is the acidic hydrolysis of CH_3COOR . Molar refractivity is directly proportional to polarizability and is in units of volume.

Figures 2.32 through 2.36 present plots of $\text{syn } \Delta E_{\text{act}}$ for the reaction of CpX and ethene, *versus* A-value, Taft's E_s , molar refractivity, van der Waals volume and n -value, respectively. P-values are available only for the four halogens. A-values do not correlate with $\text{syn } \Delta E_{\text{act}}$. This is not surprising, given that Cl, Br, and I have similar A-values. A-values are a measure of the steric interaction between an axial substituent with the two axial hydrogens on the cyclohexane ring (Figure 2.37). Thus, although Br and I are arguably "bigger" than Cl, their longer bonds allow them to move away from the axial hydrogens.

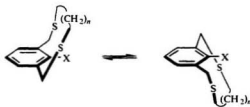


Figure 2.31 Equilibrium used to define n -values.

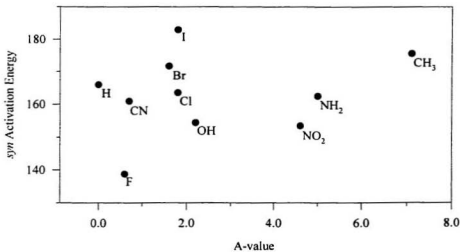


Figure 2.32 ΔE_{act} versus A-value of X (both in $\text{kJ}\cdot\text{mol}^{-1}$), for syn addition of CpX and ethene.

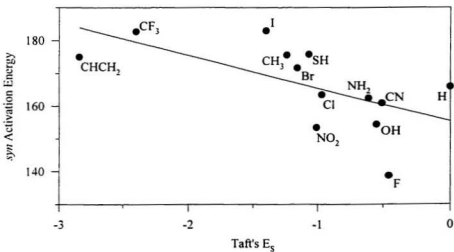


Figure 2.33 ΔE_{act} ($\text{kJ}\cdot\text{mol}^{-1}$) versus Taft's E_s for X, for syn addition of CpX and ethene.

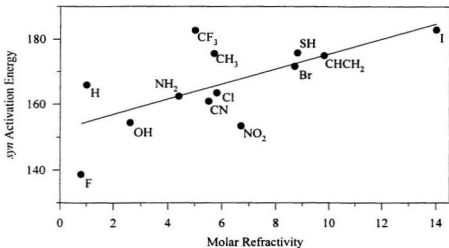


Figure 2.34 ΔE_{act} ($\text{kJ}\cdot\text{mol}^{-1}$) versus molar refractivity of X, for *syn* addition of CpX and ethene.

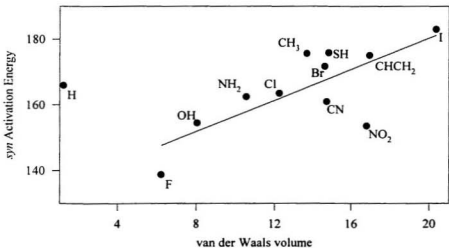


Figure 2.35 ΔE_{act} ($\text{kJ}\cdot\text{mol}^{-1}$) versus van der Waals volume of X, for *syn* addition of CpX and ethene.

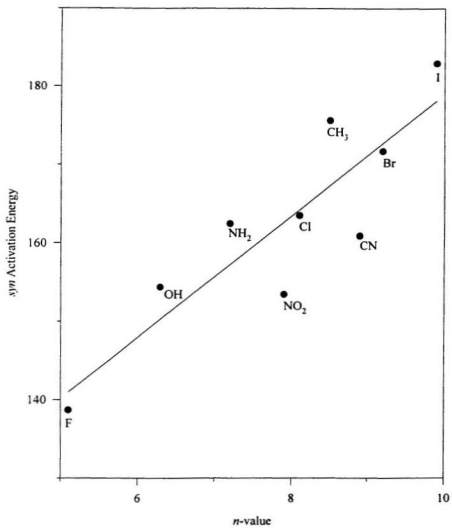


Figure 2.36 ΔE_{act} versus *n*-value of X (both in $\text{kJ}\cdot\text{mol}^{-1}$), for *syn* addition of CpX and ethene.

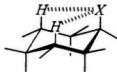


Figure 2.37 A-values measure the steric interaction between X in the *axial* position and the two *syn axial* hydrogens on the cyclohexane ring.

Taft's E_s also fails to give a good correlation with *syn* ΔE_{act} ($r^2 = 0.38$). Taft's E_s fails more for CpH, CpCH=CH₂ and CpCF₃; ignoring these CpX's leads to an improved correlation ($r^2 = 0.65$). Molar refractivity also gives a rough correlation with ΔE_{act} ($r^2 = 0.45$), however there is no CpX that can be singled out as being worse than the rest. There is a fairly good correlation between van der Waals volume and ΔE_{act} for all CpX, with the exception of CpH and CpNO₂ ($r^2 = 0.57$ and 0.81 for the inclusion and exclusion of these dienes, respectively). Finally, n -values give the best correlation with *syn* ΔE_{act} ($r^2 = 0.77$ and 0.93 for the inclusion and exclusion of CpC≡N and CpNO₂, respectively).

Thus, while A-values, molar refractivity and Taft's E_s values correlate poorly with *syn* ΔE_{act} , van der Waals volume and n -values do correlate. There are CpX's for which facial selectivity does not correlate with these parameters. Most notably, *the effect of hydrogen is consistently underestimated by all measures of the size and steric hindrance*. CpNO₂ and CpC≡N have lower *syn* ΔE_{act} than would be predicted based on their van der Waals volumes and n -values. Unlike the other X for which van der Waals volumes and n -values are known, NO₂ and C≡N contain more than one non-hydrogen atom (exception is the van der Waals volume of CH=CH₂). These parameters are probably overestimating the steric

hindrance due to the nitrogen of $\text{CpC}\equiv\text{N}$ and the oxygens of CpNO_2 . The underestimation of *syn* ΔE_{act} for CpF by its van der Waals volume is not as easily accounted for. Regardless of the few anomalies, these properties are all measures of steric hindrance, and therefore the correlations obtained indicate that steric interactions play a role in governing the facial selectivity in the Diels-Alder reactions of CpX 's.

There are clearly two main disadvantages in using empirical data for this investigation of steric hindrance. The amount of data available is limited, and these data sets are sometimes difficult to transfer to our system of study. Ideally, the best measure of size and steric hindrance would be one which can be defined for our system, and for all X studied.

There are a couple of ways to measure the size of an atom or group using quantum mechanical *ab initio* methods. An atomic radius can be derived using Bader analysis,⁶⁴ where the "boundaries" of an atom can be found using the density ρ and its gradient with respect to spacial coordinates, $\nabla\rho$. An atomic volume can be derived by integrating the space enclosed by the boundary of the atom. Similarly, the radius of a functional group or its volume can also be derived.

An alternative method for defining size was introduced by Robb, Haines and Csizmadia.⁷³ Unlike other measures of size that are defined with respect to a nuclear centre, they define a measure of the space occupied by an electron pair. Ideally, we would like to determine the space occupied by bond pairs and lone pairs. The CMO's obtained from an SCF calculation do not resemble the Lewis model of the molecule, which we need in order to define these electron pairs. However, CMO's are invariant to unitary transformation, and

thus can be converted to localized molecular orbitals (LMO's), which recapture the Lewis model. Robb *et al.* refer to two localization methods in their paper: Edmiston-Ruedenberg (ER) localization⁷⁴ and Boys localization.⁷⁵

ER localization involves the minimization of the sum of the exchange integrals, which arise due to the antisymmetry of the wavefunction. Thus, the resulting LMO's come as close as possible to interacting with each other only through their Coulombic repulsion. On the other hand, Boys' localization involves the minimization of the sum of the spherical quadratic moments for each LMO with the origin at the centroid of charge of the LMO. The centroid of charge is defined to be the expectation value of r for LMO α , $\langle \Psi_\alpha | r | \Psi_\alpha \rangle$. A consequence of this minimization is a maximization of the sum of the distances between the centroids of charge of the molecule.

Robb *et al.* stated a strong preference for the ER localization method because it is the more theoretically rigorous method; ER localization uses an energy criterion for convergence. As well, ER localization is more likely to give the better Lewis picture of a molecule; Boys' localization often yields LMO's with small "tails." However, ER localization requires an integral transformation of n^4 matrix elements, where n is the number of basis functions. On the other hand, the Boys' procedure requires the transformation of only $3n^3$ elements, making it more computationally practical and more popular. We used the Boys' localization method for this reason, and because this method yields the centroids of charge that we required.

Once LMO's are determined, the size of LMO α is defined to be the expectation value of r^2 , evaluated at the coordinates of its centroid of charge, R_α . It can be easily shown that this is equivalent to evaluating the expectation value of r^2 at the origin (denoted 0), then subtracting R_α . Thus,

$$S_\alpha = \langle \Psi_\alpha | r^2 | \Psi_\alpha \rangle_{R_\alpha} = \langle \Psi_\alpha | r^2 | \Psi_\alpha \rangle_0 - R_\alpha$$

where S_α is the size of LMO α . The evaluation of $\langle \Psi_\alpha | r^2 | \Psi_\alpha \rangle_{R_\alpha}$ yields a symmetrical 3×3 matrix with six unique components, which is then diagonalized to give the three components $\langle x^2 \rangle'_\alpha$, $\langle y^2 \rangle'_\alpha$ and $\langle z^2 \rangle'_\alpha$:

$$\begin{bmatrix} \langle x^2 \rangle_0 - \langle x \rangle \langle x \rangle & \langle xy \rangle_0 - \langle x \rangle \langle y \rangle & \langle xz \rangle_0 - \langle x \rangle \langle z \rangle \\ \langle xy \rangle_0 - \langle x \rangle \langle y \rangle & \langle y^2 \rangle_0 - \langle y \rangle \langle y \rangle & \langle yz \rangle_0 - \langle y \rangle \langle z \rangle \\ \langle xz \rangle_0 - \langle x \rangle \langle z \rangle & \langle yz \rangle_0 - \langle y \rangle \langle z \rangle & \langle z^2 \rangle_0 - \langle z \rangle \langle z \rangle \end{bmatrix} \xrightarrow{\text{diag}} \begin{bmatrix} \langle x^2 \rangle'_\alpha & 0 & 0 \\ 0 & \langle y^2 \rangle'_\alpha & 0 \\ 0 & 0 & \langle z^2 \rangle'_\alpha \end{bmatrix}$$

These three components are proportional to the magnitudes of an orthogonal set of vectors that define an ellipsoidal representation of the LMO. The size of LMO α , S_α , is defined to be the sum of these three components:

$$S_\alpha = \langle x^2 \rangle'_\alpha + \langle y^2 \rangle'_\alpha + \langle z^2 \rangle'_\alpha$$

Csizmadia^{73b} suggested that the size of a group can be defined as the summation of the sizes of all of the electron pairs of that group. This is probably an unreliable measure because the arrangement in space of the group is not taken into account. For example, an *n*-butyl, an *iso*-butyl and a *t*-butyl group would have approximately the same size using this definition, but each group would obviously be sterically different.

The electron pair which best represents the size of X is the C₅-X^o bond pair. Table 2.20 lists the values of the size of the C₅-X^o bond, S_{CX}, evaluated for all GS CpX studied. Figure 2.38 displays a plot of *syn* Δ*E*_{act} versus S_{CX} for the reaction of CpX and ethene. S_{CX} exhibits the same periodic relationship with *syn* Δ*E*_{act} as was observed with van der Waals and Bragg-Slater radii (Figures 2.29 and 2.30). S_{CX} correlates excellently with Bragg-Slater radius for all X except H (Figure 2.39; not including CpH, r² = 0.98, slope = 1.01).

The distinct difference between the empirical atomic radii and S_{CX} is the value for H. S_{CX} predicts that the C₅-H bond is larger than the C₅-F, C₅-OH, C₅-NH₂, C₅-NO₂, C₅-C≡N and C₅-C≡CH bonds. CpX substituted with these X yield primarily *syn* addition products. The C₅-CH=CH₂ and C₅-CF₃ are also smaller than the C₅-H bond, but CpCH=CH₂ and CpCF₃ yield primarily *anti* addition products. All of the other CpX's studied have bigger C₅-X bonds than CpH, and except for CpCl, all yield primarily *anti* addition products. Thus, in the Diels-Alder reaction of CpX, *the dienophile usually prefers to approach the face of CpX bearing the smaller C₅-X^o bond*. Eighteen out of twenty-one CpX's studied conform with this conclusion for the reaction of CpX with ethene, ethyne and maleimide.

Table 2.20 Values of S_{CX} , R_{CX} and Ξ_{CX} derived for GS CpX.

X	S_{CX}	R_{CX}	Ξ_{CX}
H	0.73	0.73	1.01
BH ₂	0.88	0.64	1.36
CH ₃	0.75	0.75	1.00
NH ₂	0.63	0.82	0.78
OH	0.53	0.86	0.62
F	0.43	0.91	0.48
SiH ₃	1.04	0.68	1.53
PH ₂	1.00	0.78	1.28
SH	0.94	0.88	1.08
Cl	0.88	0.98	0.90
GeH ₃	1.17	0.73	1.60
AsH ₂	1.17	0.81	1.43
SeH	1.12	0.91	1.22
Br	1.08	1.02	1.05
SnH ₃	1.38	0.72	1.93
SbH ₂	1.38	0.79	1.73
TeH	1.35	0.90	1.49
I	1.34	1.03	1.30
CH=CH ₂	0.70	0.74	0.95
C≡CH	0.65	0.75	0.86
C≡N	0.64	0.77	0.83
CF ₃	0.62	0.75	0.83
NO ₂	0.56	0.86	0.65

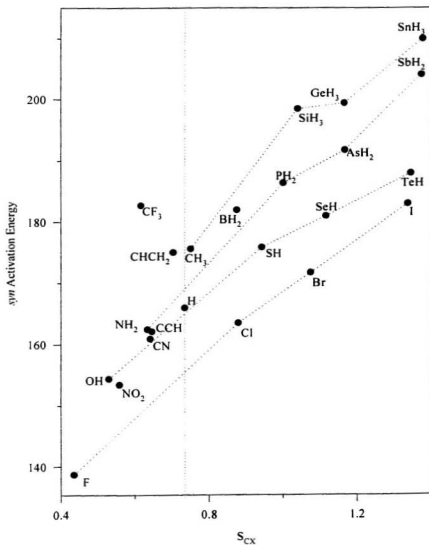


Figure 2.38 ΔE_{act} (kJ·mol⁻¹) versus S_{CX} (eÅ²), for *syn* addition of CpX and ethene. The vertical dotted line intercepts the value of S_{CX} for CpH.

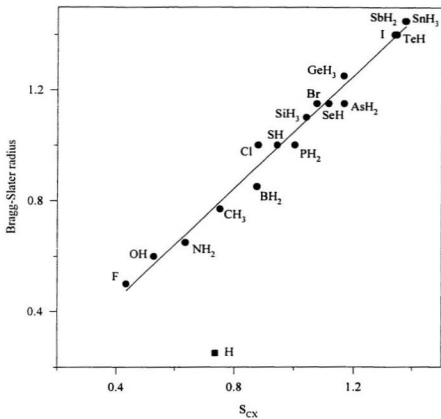


Figure 2.39 Bragg-Slater radius (Å) versus S_{CX} ($e\text{\AA}^2$). Axes have the same scale.

This strongly supports the argument that steric hindrance is responsible for facial selectivity in these reactions. Preferential *anti* addition of CpCH=CH_2 and CpCF_3 is probably due to the additional steric hindrance of the atoms attached to X^0 for these dienes. Only the preferential *syn* addition of these dienophiles to CpCl cannot be rationalized in this fashion, as well as the preferential *syn* addition of TAD to CpCH_3 and CpSH . These dienes give facial selectivities which are marginal, thus are more susceptible to minor effects. It is not too surprising that bonds between carbon and F, OH, NH_2 , NO_2 , $\text{C}\equiv\text{N}$, $\text{C}\equiv\text{CH}$, CH=CH_2 and CF_3 are smaller than a C-H bond. All of these X are more electronegative than carbon. Thus, electron density in these bonds should be held "tighter" than for bonds between carbon and X which have similar or lower electronegativities than carbon. A "tighter" bond should be less sterically demanding than a "looser" bond. This is consistent with the relationship between facial selectivity and electronegativity (Figure 2.14).

S_{CX} satisfactorily explains facial selectivity in the Diels-Alder reaction of most CpX . However, the question remains of why *syn* ΔE_{act} increases from right to left across a period. It was argued earlier that an increased number of hydrogens on X^0 could lead to an increase in steric hindrance, and consequently, an increase in ΔE_{act} . The counter-argument was that neither the variability in the conformation of X, nor the variability in the X-H bond length supported this theory.

The similarity of the A-values for chlorine, bromine and iodine discussed earlier reinforced the fact that steric hindrance depends on not only the size of a substituent, but also on its proximity to other parts of the molecule. The position of the centroid of charge is a

measure of the polarization of the C_5-X° bond. It is thus related to the position of the centre of the bulk of the electron density in the C_5-X° bond. R_{CX} is defined to be the distance between C_5 and the centroid of charge of the C_5-X° bond. Although the length of the C_5-X° bond increases as the atomic number of X° increases for a given group, R_{CX} remains approximately constant for the group (Table 2.20). As well, R_{CX} increases as the atomic number of X° increases for a given period. Steric hindrance of X should increase as S_{CX} increases, but decrease as R_{CX} increases. Therefore, it is intuitive that a steric factor which incorporates both S_{CX} and R_{CX} should have the form:

$$\Xi_{CX} = \frac{S_{CX}}{R_{CX}}$$

where Ξ_{CX} is the steric factor defined for the C_5-X° bond in the GS. Table 2.20 lists values of Ξ_{CX} for all of the dienes studied. Figure 2.40, 2.41 and 2.42 provide plots of *syn* ΔE_{act} versus Ξ_{CX} for the reaction of CpX with ethene, for the reactions of CpX with ethyne and maleimide, and for the reaction of CpX with TAD. In all cases, *syn* ΔE_{act} correlates very well with Ξ_{CX} : $r^2 = 0.90, 0.91, 0.93, 0.90, 0.95$ for the reaction of CpX with ethene, ethyne, maleimide, TAD (for halo CpX) and TAD (for non-halo CpX), respectively.

For reactions not involving TAD, all dienes that prefer *syn* addition have a smaller value of Ξ_{CX} than CpH (*i.e.*, for $X = NH_2, OH, F, Cl, C=CH, C=N$ and NO_2). Unlike all other measures of steric hindrance, Ξ_{CX} predicts that the C_5-Cl bond is “smaller” than the C_5-H bond, in accordance with both experimental and calculated facial selectivities.

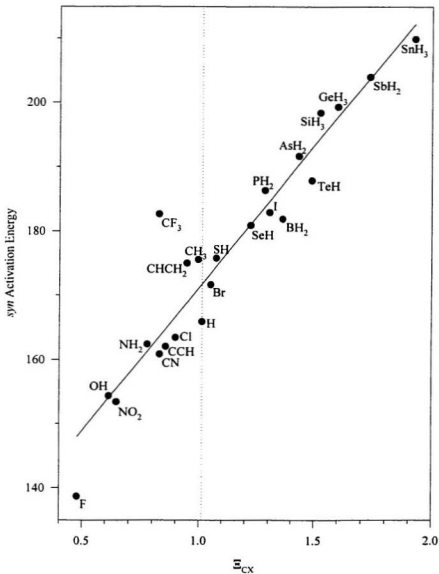


Figure 2.40 ΔE_{act} versus Ξ_{CX} for syn of CpX and ethene.

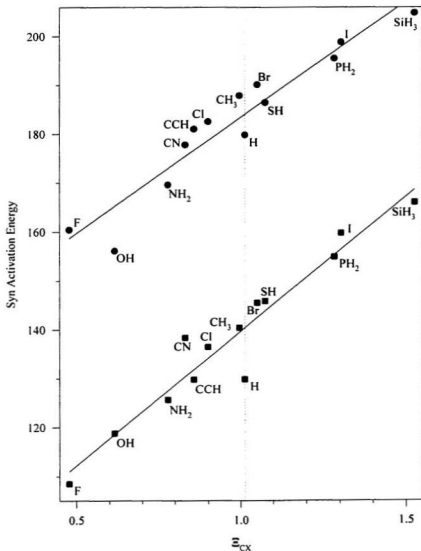


Figure 2.41 Plot of syn ΔE_{act} versus Ξ_{CX} for the reaction of CpX with ethyne (●) and maleimide (■).

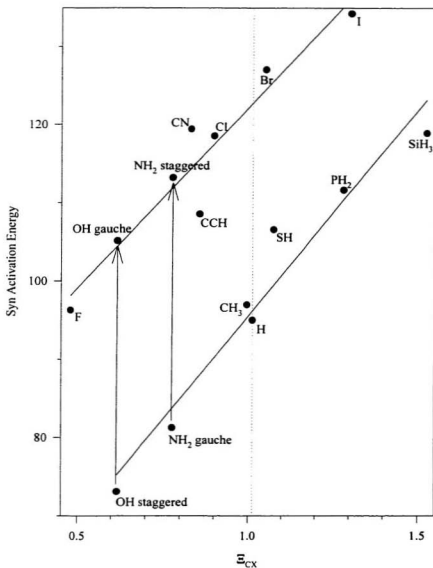


Figure 2.42 Plot of syn ΔE_{act} versus Σ_{CX} for the reaction of CpX and TAD.

The correlation is good, regardless of the fact that whatever is attached to X^o is only indirectly included in the evaluation of Ξ_{CX} . However, this is not the case for $CpCH=CH_2$ and $CpCF_3$. Both C_5-C bonds are predicted to be smaller than the C_5-H bond, however the reaction of $CpCH=CH_2$ and $CpCF_3$ with ethene yields over 95% *anti* addition in both cases. Non-hydrogen atoms attached to X^o may exert additional steric hindrance in some cases, but not all; Ξ_{CX} predicts facial selectivity well for $CpNO_2$, $CpC\equiv CH$ and $CpC\equiv N$. The value of Ξ_{CX} for $CpCH_3$ is also smaller than the value for CpH , but barely so. This is consistent with the fact that addition to $CpCH_3$ is not very stereoselective. Nevertheless, within a small margin of error, Ξ_{CX} correctly predicts all available experimental facial selectivities for the reaction of CpX with non-TAD dienophiles.

Once again, the reaction of CpX with TAD gives some unique results. As was the case for plot of ΔE_{act} versus ΔE_{diene}^{def} and ΔE_{int} for *syn* addition to TAD, the halo and non-halo CpX yield separate, but good correlations between ΔE_{act} and Ξ_{CX} . The halo CpX have ΔE_{act} 's which are about 25 $\text{kJ}\cdot\text{mol}^{-1}$ higher than those for the non-halo CpX . As was done in Figure 2.28, staggered $CpNH_2$ and the gauche conformer of $CpOH$ are included in the plot of Ξ_{CX} versus *syn* ΔE_{act} (Figure 2.42). Unlike the lowest energy rotamers, these conformers of $CpNH_2$ and $CpOH$ behave exactly like the halo CpX . This provides even stronger support for the existence of an additional steric interaction involving the closed-shell repulsion between the lone pairs on the halogens and the π -bonds of $C\equiv CH$ and $C\equiv N$ with the lone pairs on the nitrogens of TAD. Ξ_{CX} does not predict the calculated preferred *syn* addition for the reaction of $CpSH$ with TAD. Like $CpCH_3$, the value of Ξ_{CX} for $CpSH$ is only slightly

higher than that of CpH. The reaction of CpSH with TAD is not very stereoselective, thus is more susceptible to minor effects.

In conclusion, the good correlation between Ξ_{CX} and *syn* ΔE_{act} suggests that, with some minor exceptions, that Ξ_{CX} accounts for facial selectivity in the Diels-Alder reaction of CpX. For the reaction of CpX with TAD, an additional steric interaction exists between the lone pairs on a halogen or the π -bond of $\text{C}\equiv\text{CH}$ and $\text{C}\equiv\text{N}$ and the lone pairs on the nitrogens of TAD. Thus, facial selectivity in the Diels-Alder reaction of CpX can be fully explained using steric arguments. The main question remaining is why does the defined steric factor Ξ_{CX} work so well?

2.8 What is Ξ_{CX} Measuring?

The correlations between $\text{syn } \Delta E_{\text{act}}$ and $\Delta\Theta_{\text{Total}}$, $\Delta E_{\text{diene}}^{\text{def}}$, n -values, S_{CX} and Ξ_{CX} all suggest that steric hindrance is playing a dominant role in determining facial selectivity in the Diels-Alder reaction of CpX. If this is the case, then what parts of CpX and/or the dienophile are “bumping” into each other?

Intuitively, the interaction should be between X and the dienophile. There is no question that diene deformation requires the presence of the dienophile. But does this imply that the extent of diene deformation is determined by this interaction? Ξ_{CX} is composed of S_{CX} and R_{CX} . What converts the periodic trend observed in the plot of $\text{syn } \Delta E_{\text{act}}$ versus S_{CX} to the linear correlation in the plot of $\text{syn } \Delta E_{\text{act}}$ versus Ξ_{CX} (Figures 2.38 and 2.40) is division by R_{CX} . R_{CX} changes by less than 0.1 Å for X^o belonging to adjacent groups in the periodic table. According to Figure 2.38, this small difference leads to a significant energy difference between the groups. The distance between any point on the dienophile in the TS and the centroid of charge of the C₃-X^o bond in the diene is more than 2 Å. A shift of less than 0.1 Å in the position of the centroid of charge cannot have such a significant effect. Moreover, the variation in the incipient bond length has a similar magnitude. Therefore, while diene deformation requires an interaction between CpX and the dienophile in order to occur, it is unlikely that the interaction between the two addends results in facially different diene deformations.

An alternative explanation is based on VSEPR theory.⁷⁶ For the Lewis model of a molecular species, the bond angles about a central atom are determined by a minimization of

the Coulombic repulsion between the valence electron pairs about the central atom. In the case of CpX° 's, the geometry about C_3 is based on the balance of interaction between the $\text{C}_1\text{-C}_3$, $\text{C}_4\text{-C}_3$, $\text{C}_3\text{-H}_3$ and $\text{C}_3\text{-X}^{\circ}$ bond-pair electrons. When the dienophile approaches the diene, there is a significant amount of redistribution of the electron density about both reactants, *i.e.*, rehybridization. The equilibrium geometry of both addends must necessarily deform to accommodate the new interactions and electron density redistribution. Consequently, the balance in the equilibrium geometry about C_3 is disrupted. As C_3 is forced away from the plane of the diene due to the rehybridization of C_1 and C_4 , the steric interaction between the $\text{C}_1\text{-C}_3$ and $\text{C}_4\text{-C}_3$ bonds and the $\text{C}_3\text{-Y}$ bond (Figure 2.18) increases. The extent of this interaction would be directly proportional to the size for the $\text{C}_3\text{-Y}$ bond, and would be related to the distribution of electron density in this bond. The higher the concentration of electron density close to C_3 , the more sterically demanding the $\text{C}_3\text{-Y}$ bond. Thus, the energetic cost of diene deformation would be directly related to S_{CX} , and inversely related to R_{CX} . This explains why Ξ_{CX} correlates so well with facial selectivity.

The question that remains is why there is an increase in the steric interaction between the $\text{C}_1\text{-C}_3$ and $\text{C}_4\text{-C}_3$ bonds and the $\text{C}_3\text{-Y}$ bond. This could be related to the shortening of the $\text{C}_3\text{-Y}$ bond in the transformation of the diene to its TS geometry. This indicates an increase of electron density in this bond, and therefore an increase in steric hindrance between the $\text{C}_3\text{-Y}$ bond and the $\text{C}_1\text{-C}_3$ and $\text{C}_4\text{-C}_3$ bonds. However, it is not clear why the $\text{C}_3\text{-Y}$ is shorter and the $\text{C}_3\text{-Z}$ bond is longer in the TS than the corresponding bond lengths in both CpX and the Diels-Alder product.

It is possible that Ξ_{CX} is not measuring steric hindrance. Ξ_{CX} correlates well with group electronegativity (Figure 2.43; $r^2 = 0.87$). Electronegativity is related to atomic size and to the polarization of a bond. The steric arguments just presented used both the size and bond polarity components of Ξ_{CX} to rationalize why it works so well in determining facial selectivity. Thus, whether or not Ξ_{CX} is measuring steric hindrance, it should still correlate with electronegativity. There is the possibility that Ξ_{CX} is measuring an inductive effect that has not yet been determined. If so, it would be difficult to distinguish between the two effects.

The electronegativity of an atom is dependent on its position on the periodic table, as well as the oxidation state of the atom and what it is attached to. While the Pauling electronegativity scale is useful, it is static. It is hypothesized that Ξ_{CX} can be used as a dynamic measure of electronegativity. While Ξ_{CX} is a measure of the electronegativity of X attached to a carbon atom, Ξ_{YX} can be defined to measure electronegativity of X when it is attached to atom Y. Thus, electronegativity of an atom could be determined regardless of its chemical environment. Ξ_{CX} itself should remain constant for X attached to any sp^3 carbon centre.

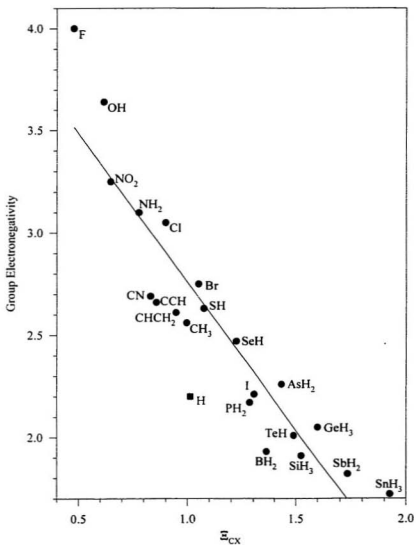


Figure 2.43 Group electronegativity *versus* Ξ_{CX} ($\text{e}\text{\AA}^3$).

3. Facial Selectivity of Protonated and Deprotonated 5-Substituted-1,3-Cyclopentadienes

3.1 Computational Method

We have concluded that facial selectivity in the Diels-Alder reaction of CpX can be rationalized on the basis of steric hindrance arguments. If there exists an electronic factor that plays a minor role in controlling facial selectivity, then this factor should be accentuated if CpX is ionized. Moreover, it is possible to design experiments where CpX or similar dienes are protonated or deprotonated, using acidic or basic media. Therefore, a study of the Diels-Alder reaction of protonated and deprotonated CpX was undertaken. The protonated and deprotonated species will be referred to as CpX^+ and CpX^- , respectively, while the corresponding parent diene will be referred to as CpX^0 . CpX denotes all 5-substituted-1,3-cyclopentadienes.

The Diels-Alder reaction of CpX and ethene was studied for the following neutral, protonated and deprotonated X:

X	=	H	NH ₂	OH	PH ₂	SH
		F	NH ⁺	O ⁻	PH ⁺	S ⁻
		Cl	NH ₃ ⁺	OH ₂ ⁺	PH ₃ ⁺	SH ₂ ⁺

It is well known that diffuse functions are necessary to describe properly negative ions using *ab initio* HF methods.⁵³ In order to have a fully comparable set of data, all GS CpX structures, ethene, and *syn* and *anti* TS's were determined at 6-31++G(d)//6-31++G(d),⁷⁷ using

the methodology outlined in Section 2.2.2. Listed below are the lowest-energy conformations of X for the dienes:

NH ₂	gauche	OH	staggered	PH ₂	gauche	SH	staggered
NH ₂ ⁺	staggered	OH ₂ ⁺	gauche	PH ₂ ⁺	staggered	SH ₂ ⁺	gauche
NH ⁺	staggered			PH ⁺	staggered		

Unexpectedly, a TS for the *anti* addition of CpOH₂⁺ and ethene does not exist at this level of theory. All attempts to optimize this structure led to the breaking of the C₃-O bond. To verify this, the *anti* TS was optimized while keeping the C₃-O bond fixed. A series of SCF and gradient calculations were performed on this TS for a range of C₃-O bond lengths. No energy minimum was found, and the gradient for the C₃-O bond remained negative for all evaluated points. A negative parameter gradient indicates that the parameter value must increase in order to reach an energy minimum. While it would have been interesting to continue the optimization to see what sort of TS or complex is formed, it would have had no value for this study. At least we have shown that water can be as good a leaving group computationally as it is experimentally.

3.2 Activation Energy and its Components

In Section 2.6 we showed that an examination of the components of ΔE_{act} , i.e., ΔE_{diene}^{def} , $\Delta E_{diphile}^{def}$ and ΔE_{int} , allowed us to identify the possible factors which could significantly affect facial selectivity. Table 3.2 lists ΔE_{act} , ΔE_{diene}^{def} , $\Delta E_{diphile}^{def}$ and ΔE_{int} for neutral and ionic CpX, as well as their conformations of X at the TS, and facial selectivities evaluated at 273.15K.

A comparison between ΔE_{act} evaluated at 6-31G(d)//6-31G(d) and at 6-31++G(d)//6-31++G(d) for the same reactions (Tables 2.5 and 3.2) demonstrates that the addition of diffuse functions increased ΔE_{act} , and increased the proportion of *syn* addition. Nevertheless, the change in ΔE_{act} is systematic; Figure 3.1 illustrates the excellent linear relationship between ΔE_{act} evaluated using the two basis sets ($r^2 = 0.99$, slope = 0.93). The increase in the predicted proportion of *syn* addition with an increase in the number of basis functions is a noteworthy phenomenon. Table 3.1 demonstrates this trend for the reaction for CpCl with ethene. While this is a general trend for all CpX, the only dramatic change in facial selectivity occurs for CpCl and CpC≡N.

Table 3.1 A comparison of facial selectivity and level of theory for the reaction of CpCl and ethene. Calculated % *syn* is evaluated at 273.15K.

Level of theory	ΔE_{act} (<i>syn</i>)	ΔE_{act} (<i>anti</i>)	calc. % <i>syn</i>
STO-3G//STO-3G	151.2	143.8	3.7
3-21G//3-21G	125.7	118.4	3.9
3-21G(d)//3-21G(d)	122.4	121.7	42.5
6-31G(d)//6-31G(d)	163.5	165.6	72.5
6-31++G(d)//6-31++G(d)	170.4	175.0	88.3

Table 3.2 Energies (kJ·mol⁻¹) for the Diels-Alder reaction of CpX and ethene, evaluated at 6-31++G(d)//6-31++G(d).

X	syn					anti					%syn ^a
	conform.	ΔE_{ext}	$\Delta E_{\text{dione}}^{\text{def}}$	$\Delta E_{\text{qibale}}^{\text{def}}$	ΔE_{int}	conform.	ΔE_{ext}	$\Delta E_{\text{dione}}^{\text{def}}$	$\Delta E_{\text{qibale}}^{\text{def}}$	ΔE_{int}	
H		173.6	98.3	47.6	27.6						
NH	staggered	161.0	92.9	41.2	27.0	staggered	180.6	97.6	49.8	33.3	100.0
NH ₂	gauche	170.3	98.0	44.7	27.6	gauche	178.6	100.7	45.8	32.2	97.5
NH ₃	staggered	170.3	108.9	49.8	11.7	staggered	153.4	99.2	42.8	11.3	0.1
O		138.9	80.6	38.1	20.3		182.1	102.4	46.8	32.8	100.0
OH	gauche	162.3	97.8	39.6	24.8	staggered	173.7	99.5	44.1	30.0	99.4
OH ₂	gauche	162.9	106.5	49.4	7.0						
F		150.2	86.7	39.8	23.8		172.6	98.2	44.3	30.1	100.0
PH	staggered	192.7	117.1	44.6	31.0	staggered	187.7	98.4	57.2	32.2	10.2
PH ₂	staggered	193.8	119.0	46.9	27.8	staggered	179.8	97.3	49.4	33.1	0.2
PH ₃	staggered	193.3	126.0	51.6	15.7	staggered	156.8	98.9	45.5	12.5	0.0
S		173.6	106.1	41.0	26.5		186.1	98.9	53.6	33.6	99.6
SH	gauche	182.7	113.5	44.3	24.8	staggered	179.5	99.5	47.7	32.2	19.4
SH ₂	staggered	178.7	119.7	48.1	11.0	staggered	148.8	94.1	44.7	10.0	0.0
Cl		170.4	103.7	41.1	25.6		175.0	97.3	46.1	31.6	88.3

^a evaluated at 273.15K

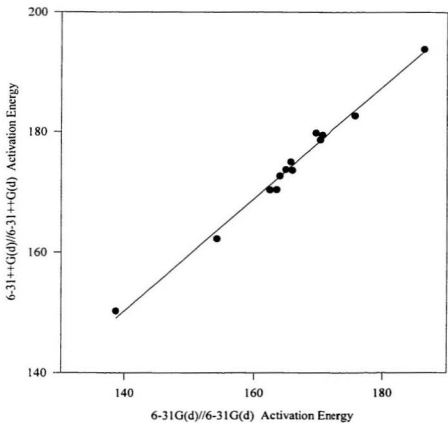


Figure 3.1 ΔE_{act} evaluated at 6-31++G(d)//6-31++G(d) versus ΔE_{act} evaluated at 6-31G(d)//6-31G(d) (kJ·mol⁻¹) for all available reactions of CpX and ethene.

For *syn* addition, the value of ΔE_{act} for all $\text{CpX}^{\cdot\cdot}$ s, except CpSH_2^+ , is less than a $\text{kJ}\cdot\text{mol}^{-1}$ different from the corresponding value for CpX^0 , while ΔE_{act} for the corresponding CpX^- is lower in energy. For *anti* addition, ΔE_{act} increases for CpX^- with respect to the parent CpX^0 , while ΔE_{act} decreases to a greater extent for the corresponding CpX^+ . This is consistent with the energies of reaction, $\Delta E_{isodesmic}$, for the isodesmic process pictured in Figure 3.2 (Table 3.3). Isodesmic reactions give reliable energies at the HF level. A negative value of $\Delta E_{isodesmic}$ indicates a stabilization of the Diels-Alder TS by the charged species, with respect to the TS involving the corresponding CpX^0 . The opposite is true for positive $\Delta E_{isodesmic}$. Deprotonation stabilizes the *syn* TS and destabilizes the *anti* TS. Protonation has little effect on the *syn* TS, while it has a strong stabilizing effect on the *anti* TS. The net effect is that protonation increases the preference for *anti* addition, while deprotonation increases the preference for *syn* addition.

Table 3.4 lists the ranges of ΔE_{act} for *syn* and *anti* addition for all CpX , and for CpX^+ , CpX^0 and CpX^- separately. The range of *anti* ΔE_{act} values for all CpX is proportionately high with respect to the range of ΔE_{act} for *syn* addition. However, a comparison of the relative range of ΔE_{act} for each type of CpX is closer to the proportions observed in Table 2.11. Once again, there exists a factor that affects ΔE_{act} for *syn* addition much more than for *anti* addition.

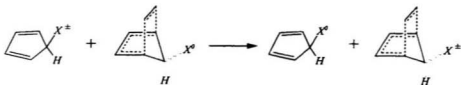


Figure 3.2 Isodesmic reaction used to illustrate the effect of ionization on the stability of the Diels-Alder TS, where X^\pm denotes the protonated or deprotonated substituent.

Table 3.3 $\Delta E_{\text{isodesmic}}$ ($\text{kJ}\cdot\text{mol}^{-1}$) for the reaction pictured in Figure 3.2, evaluated at 6-31++G(d)//6-31++G(d).

X	$\Delta E_{\text{isodesmic}}$ (syn)	$\Delta E_{\text{isodesmic}}$ (anti)
NH ⁺	-9.3	2
NH ₃ ⁺	0	-25.2
O ⁺	-23.3	8.4
OH ₂ ⁺	0.7	
PH ⁺	-1.1	7.9
PH ₃ ⁺	-0.4	-23
S ⁺	-9.1	6.6
SH ₂ ⁺	-3.9	30.7

Table 3.4 Ranges of ΔE_{act} ($\text{kJ}\cdot\text{mol}^{-1}$) for the reaction of CpX and ethene, evaluated at 6-31++G(d)//6-31++G(d).

reaction	range syn ΔE_{act}	range anti ΔE_{act}	(anti range/syn range)×100%
CpX + ethene	54.9	38.9	70.9
CpX ⁺ + ethene	53.8	7.1	13.2
CpX ⁰ + ethene	43.6	7.2	16.5
CpX ⁻ + ethene	30.4	8	26.3

It was demonstrated in Section 2.6 that the component of ΔE_{act} that had the most significant effect on facial selectivity for neutral CpX was ΔE_{diene}^{def} (Figures 2.25 to 2.27). Figure 3.3 contains the plot of ΔE_{act} versus ΔE_{diene}^{def} for the reactions studied in this section. There is a good correlation between ΔE_{act} and ΔE_{diene}^{def} for *syn* addition ($r^2 = 0.85$, slope = 1.12), regardless of the charge on CpX. ΔE_{diene}^{def} for *anti* addition is almost constant for all CpX. In this regard, the ionic CpX⁺s and the neutral CpX have the same characteristics.

However, the CpX⁺s can be grouped in a different way. When *syn* additions to CpX⁰ and to CpX⁺ are considered separately, the correlation is better ($r^2 = 0.95$, slope = 1.33). Moreover, there is an excellent correlation for *syn* and *anti* addition of CpX⁺ ($r^2 = 0.98$, slope = 1.33). Amazingly, these two linear regressions, as well as the corresponding linear regression in Figure 2.25 have the same slope, to three significant figures. This suggests that this regrouping has a physical significance. One interpretation is that there exists a factor that affects the *syn* and the *anti* face of CpX⁺ equally, with a net effect of reducing ΔE_{act} with respect to the value that would be predicted based on ΔE_{diene}^{def} alone for these dienes.

This conjecture is supported by the plot of ΔE_{act} versus ΔE_{int} (Figure 3.4). It is evident that for *syn* and *anti* addition of CpX⁺, ΔE_{int} is almost constant, but about 10 kJ·mol⁻¹ lower in energy than the corresponding values for CpX⁰ and CpX⁻. This is consistent with a phenomenon that affects both faces of the diene. The plot of ΔE_{act} versus $\Delta E_{diphole}^{def}$ provides no other facially selective trend.

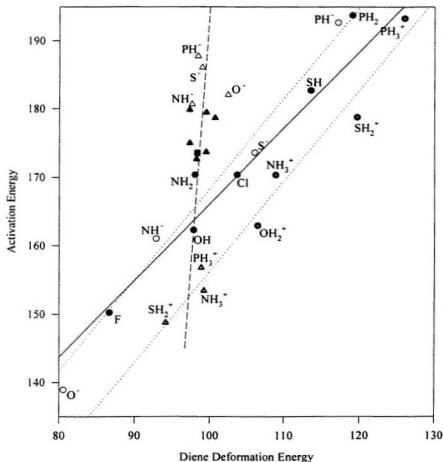


Figure 3.3 ΔE_{act} versus ΔE_{diene}^{def} ($\text{kJ}\cdot\text{mol}^{-1}$) for the reaction of CpX and ethene, for *syn* (circle) and *anti* (triangle) addition of CpX^0 (filled), CpX^- (unfilled), CpX^+ (pluses) and CpH (■) with ethene. The linear regressions are for all *syn* additions (solid), all *anti* additions (dashed), *syn* addition for CpX^0 and CpX^- (upper dotted) and for *syn* and *anti* additions of CpX^- (lower dotted).

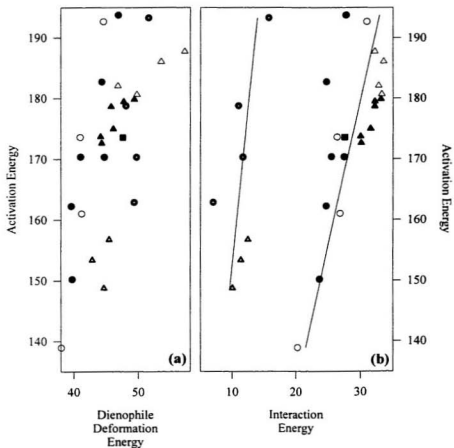


Figure 3.4 ΔE_{act} versus (a) ΔE_{dphile}^{def} and (b) ΔE_{int} (kJ·mol⁻¹) for the reaction of CpX and ethene, for *syn* (circle) and *anti* (triangle) addition of CpX⁻ (unfilled), CpX⁰ (filled), CpX⁺ (pluses) and CpH (■) with ethene.

The method of evaluation of ΔE_{diene}^{def} , $\Delta E_{diphile}^{def}$ and ΔE_{int} employed does not take into account the effect of charge transfer between the diene and the dienophile in the TS. A significant charge transfer between the two addends might skew all three components of ΔE_{act} . A rough measure of charge transfer would be to sum the Mulliken net atomic charges on the dienophile in the TS (Table 3.5). The charge on the dienophile is usually within ± 0.1 for TS's involving CpX^- and CpX^0 , while it is greater than -0.2 for all of the TS structures for the reaction of CpX^- and ethene. While the correlations between ΔE_{act} and ΔE_{diene}^{def} are too good to be coincidental, the partitioning scheme for ΔE_{act} may be less reliable for ionic species. To determine what factors govern facial selectivity for ionic CpX , other properties of the dienes and their TS's will have to be studied.

Table 3.5 Sums of the Mulliken net atomic charges resident on the dienophile in the TS.

X	charge (<i>syn</i>)	charge (<i>anti</i>)
H	-0.08	
NH [·]	-0.32	-0.25
NH ₂	-0.14	-0.09
NH ₃ [·]	-0.01	0.07
O [·]	-0.20	-0.22
OH	-0.02	-0.06
OH ₂ [·]	-0.02	
F	-0.04	-0.05
PH [·]	-0.22	-0.23
PH ₂	-0.05	-0.06
PH ₃ [·]	-0.01	0.09
S [·]	-0.18	-0.19
SH	-0.06	-0.05
SH ₂ [·]	0.03	0.13
Cl	-0.07	-0.02

3.3 Geometry and Electronic Structure

In most respects, the geometry and electronic structure of the protonated and deprotonated CpX and their Diels-Alder TS's with ethene are very similar to those of the parent diene. Moreover, no new geometric or electronic parameter has been found that correlates with facial selectivity.

Tables 3.6 and 3.7 contain bond lengths and angles for the dienes studied in this section. In the gas phase, a charged molecule is expected to delocalize its charge as much as possible over the molecule. Accordingly, the C_3-X^\ominus bond length decreases considerably for CpO^- and $CpNH^-$, and increases considerably for all of the $CpX^{+\cdot}$'s, with respect to the length of the C_3-X^\ominus bond in the corresponding CpX^\ominus . However, there is no evidence of any delocalization of electron density to any other bond in the diene. In fact, in most cases the opposite is true. The C_1-C_2 , C_3-C_4 , C_1-C_5 , C_4-C_5 and the C_3-H_3 bonds are usually longer for CpX^\cdot and are usually shorter for CpX^- than are the same bond lengths in the corresponding CpX^\ominus . This suggests that the electron density in CpX^\cdot is polarized towards the negatively charged substituent, while the electron density in CpX^+ is polarized away from the positively charged substituent. All angles involving C_3 as a central point or as a terminus change significantly for charged species, with respect to the same angles in the corresponding CpX^\ominus . The observed differences are consistent with VSEPR theory.

Table 3.6 Bond lengths (Å) for CpX,^a evaluated at 6-31++G(d)//6-31++G(d).

X	C ₂ -C ₃	C ₁ -C ₂ C ₃ -C ₄	C ₁ -C ₅ C ₄ -C ₅	C ₅ -H ₅	C ₅ -X
H	1.4760	1.3320	1.5064	1.0889	1.0889
NH ⁺	1.4827	1.3343	1.5303	1.1012	1.4331
NH ₂	1.4824	1.3291 1.3289	1.5188 1.5121	1.0896	1.4547
NH ₃ ⁺	1.4861	1.3273	1.5102	1.0833	1.5197
O ⁺	1.4829	1.3333	1.5364	1.1289	1.3255
OH	1.4861	1.3280	1.5157	1.0861	1.4015
OH ₂ ⁺	1.4955	1.3264 1.3262	1.5023 1.5016	1.0782	1.5575
F	1.4881	1.3263	1.5095	1.0856	1.3739
PH ⁺	1.4722	1.3387	1.4988	1.0910	1.9316
PH ₂	1.4728	1.3330 1.3329	1.5034 1.5071	1.0893	1.8774
PH ₃ ⁺	1.4731	1.3322	1.5132	1.0868	1.8218
S ⁺	1.4764	1.3350	1.5055	1.0912	1.8445
SH	1.4795	1.3299	1.5082	1.0870	1.8281
SH ₂ ⁺	1.4829	1.3288 1.3285	1.5064 1.5115	1.0840	1.8642
Cl	1.4827	1.3276	1.5066	1.0822	1.8010

^a For structures with C_s symmetry, one value is tabulated for a pair of equivalent parameters, whereas two values are given for structures with C_i symmetry.

Table 3.7 Angles (degrees) for CpX, evaluated at 6-31++G(d)//6-31++G(d).

X	C ₁ -C ₂ -C ₃ C ₂ -C ₃ -C ₄	C ₂ -C ₁ -C ₅ C ₃ -C ₄ -C ₅	C ₁ -C ₃ -C ₄	C ₁ -C ₅ -H ₅ C ₄ -C ₅ -H ₅	C ₁ -C ₅ -X C ₄ -C ₅ -X	H ₅ -C ₅ -X
H	109.15	109.60	102.51	111.90	111.90	106.85
NH ⁺	108.65	111.60	99.50	105.12	119.15	107.27
NH ₂	109.09 109.17	109.83 110.00	101.87	108.53 108.34	117.95 112.68	107.10
NH ₃ ⁺	109.60	108.47	103.78	113.09	110.49	105.98
O ⁺	108.82	111.40	99.40	102.00	118.69	113.35
OH	109.22	109.57	102.29	109.19	115.43	105.21
OH ₂ ⁺	109.66 109.69	107.55 107.57	105.34	116.59 115.78	110.77 107.07	100.94
F	109.32	108.95	103.17	110.51	113.12	106.49
PH ⁺	108.57	110.56	101.71	110.48	116.10	102.18
PH ₂	109.05 109.18	109.79 109.60	102.37	111.33 110.93	115.62 111.10	105.61
PH ₃ ⁺	109.74	108.61	103.29	114.09	108.31	108.45
S ⁺	108.63	110.68	101.37	108.55	115.16	107.71
SH	109.22	109.44	102.67	110.50	114.83	103.69
SH ₂ ⁺	109.75 109.76	108.21 108.07	104.18	114.78 114.16	112.46 107.53	103.75
Cl	109.33	109.02	103.20	111.41	112.90	105.22

The differences in geometry between the charged and neutral GS species are maintained in their TS's. This is evident in the small ranges of bond length changes between the GS addends and their TS's (Table 3.8). As was the case in Section 2.5, the only significant variation in geometric difference occurs in the angles about C₅. Table 3.9 lists the values of $\Delta\Theta_{\text{Total}}$ evaluated for the reactions studied in this section. Figure 3.5 presents a plot of ΔE_{act} versus $\Delta\Theta_{\text{Total}}$. There is fair correlation between ΔE_{act} and $\Delta\Theta_{\text{Total}}$ for *syn* addition for all CpX ($r^2 = 0.76$). The correlation is improved when CpX⁻'s, CpX⁰'s and CpX⁺'s are considered separately ($r^2 = 1.00, 0.86$ and 0.85 , respectively). This suggests that *syn* diene deformation is an important factor in determining facial selectivity for charged CpX. There is another factor which decreases ΔE_{act} for *syn* addition of CpX⁻ and *anti* addition of CpX⁺, and increases ΔE_{act} for *anti* addition of CpX⁻. This latter factor is probably electronic in nature.

If an electronic factor were to involve a flow of electron density to or from the ionic substituent in the TS, then the atomic charge on X⁰ in the TS should be considerably different from the corresponding value in the GS. However, this is not the case. Table 3.10 lists the Mulliken net atomic charges on X⁰ for CpX in the GS, and in the *syn* and *anti* TS for the reaction with ethene. Except for *syn* addition of ethene to CpSH₂⁺, there is a negligible difference between the charge on CpX in the GS and in the corresponding two TS's. Keeping in mind the limitations of the Mulliken definition of atomic charge (Section 2.4), this is modest evidence against the notion that the protonated, deprotonated or neutral substituent is involved in electron donation in the TS.

Table 3.8 Maximum and minimum geometry changes in transforming the GS reactants to their TS structures for the reaction of neutral, protonated and deprotonated CpX and ethene, evaluated at 6-31++G(d)//6-31++G(d). Angle changes are measured in degrees, bond length changes in Å.

parameter	<i>syn</i> TS - GS			<i>anti</i> TS - GS		
	Δ_{\min}	Δ_{\max}	$\Delta\Delta$	Δ_{\min}	Δ_{\max}	$\Delta\Delta$
C ₂ -C ₃	-0.0972	-0.0805	0.0167	-0.0889	-0.0801	0.0088
C ₁ -C ₂ , C ₃ -C ₄	0.0580	0.0631	0.0051	0.0499	0.0630	0.0131
C ₁ -C ₃ , C ₄ -C ₅	-0.0114	0.0163	0.0277	-0.0066	0.0170	0.0236
C ₅ -H ₅	-0.0074	0.0063	0.0137	-0.0274	0.0028	0.0302
C ₅ -X	-0.0381	-0.0039	0.0342	-0.0083	0.0461	0.0544
C ₆ -C ₇	0.0602	0.0666	0.0064	0.0629	0.0756	0.0127
C ₁ -C ₂ -C ₃ , C ₂ -C ₃ -C ₄	-0.25	0.05	0.30	-0.46	0.13	0.59
C ₅ -C ₁ -C ₂ , C ₅ -C ₄ -C ₃	-5.43	-3.04	2.40	-3.20	-2.01	1.19
C ₁ -C ₅ -C ₄	-4.05	-2.71	1.34	-4.39	-3.19	1.20
C ₁ -C ₅ -H ₅ , C ₄ -C ₅ -H ₅	-7.69	-1.05	6.64	-3.52	6.39	9.91
C ₁ -C ₅ -X, C ₄ -C ₅ -X	-0.28	10.26	10.53	-6.83	4.04	10.87
X-C ₅ -H ₅	-4.93	3.96	8.89	-1.88	2.91	4.78
C ₆ -C ₇ -H _{7n} , C ₇ -C ₆ -H _{6n}	-1.78	-1.39	0.39	-1.91	-1.46	0.44
C ₆ -C ₇ -H _{7x} , C ₇ -C ₆ -H _{6x}	-3.12	-0.80	2.32	-2.22	-1.83	0.39
H _{6n} -C ₆ -H _{6x} , H _{7n} -C ₇ -H _{7x}	-3.32	0.40	3.72	-2.21	-1.40	0.81

Table 3.9 $\Delta\Theta_{\text{Total}}$ evaluated for the reaction of neutral and ionic CpX with ethene, evaluated at 6-31++G(d)//6-31++G(d).

X	$\Delta\Theta_{\text{Total}} (\text{syn})$	$\Delta\Theta_{\text{Total}} (\text{anti})$
H	16.65	
NH ⁺	18.60	14.91
NH ₂	18.26	14.95
NH ₃ ⁺	21.51	13.47
O ⁺	7.12	21.59
OH	13.74	16.10
OH ₂ ⁺	17.06	
F	10.66	17.58
PH ⁺	34.26	5.88
PH ₂	25.34	16.09
PH ₃ ⁺	38.21	7.46
S ⁺	25.82	11.14
SH	19.33	11.21
SH ₂ ⁺	20.40	19.33
Cl	20.41	14.21

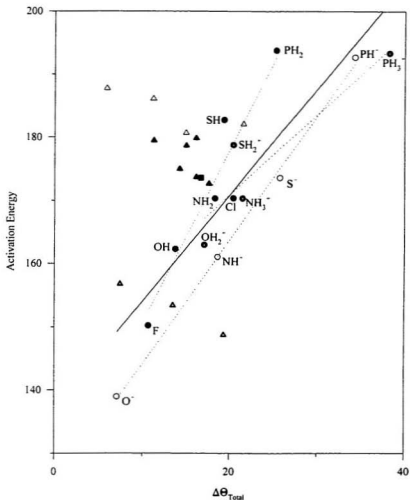


Figure 3.5 ΔE_{act} ($\text{kJ}\cdot\text{mol}^{-1}$) versus $\Delta\Theta_{\text{Total}}$ (degrees) for *syn* (circle) and *anti* (triangle) addition of CpX^- (unfilled), CpX^0 (filled) and CpX^+ (pluses), and CpH (square) with ethene. Linear regressions are for all *syn* additions (solid) and for the *syn* additions of CpX^- , CpX^0 and CpX^+ (dotted) separately.

Table 3.10 Mulikan net atomic charge on X^o in CpX and in the *syn* and *anti* TS's for the reaction of CpX and ethene, evaluated at 6-31++G(d)/6-31++G(d).

X	atomic charge on X ^o		
	GS	<i>syn</i> TS	<i>anti</i> TS
H	0.19	0.2	0.22
NH ⁻	-0.93	-0.89	-0.84
NH ₂	-0.77	-0.74	-0.73
NH ₃ ⁺	-0.92	-0.96	-0.96
O ⁻	-0.84	-0.83	-0.83
OH	-0.61	-0.72	-0.62
OH ₂ ⁺	-0.70	-0.74	-0.74
F	-0.37	-0.39	-0.40
PH ⁻	-0.73	-0.70	-0.76
PH ₂	0.23	0.13	0.17
PH ₃ ⁺	0.7	0.63	0.62
S ⁻	-0.89	-0.92	-0.94
SH	-0.08	-0.09	-0.17
SH ₂ ⁺	0.43	0.01	0.32
Cl	-0.10	-0.14	-0.16

The *anti* effect, which decreases ΔE_{act} for *anti* addition of CpX^+ and increases ΔE_{act} for *anti* addition of CpX^- , could be a dipolar effect. The dipole moment of the *anti* TS would be directed towards the dienophile for CpX^+ , whereas the dipole moment would be in the opposite direction for CpX^- (Figure 3.6). The normal-electron-demand Diels-Alder reaction should involve a flow of electron density from the diene to the dienophile, so a dipole moment directed towards the dienophile should have a stabilizing effect. A dipole moment in the opposite direction would have a destabilizing effect. An investigation of this phenomenon is hampered by the fact that the dipole moment of a charged species because it cannot be computed uniquely. The dipole moment of a charged species depends on the choice of the origin of the coordinate system. Further work is required to determine more clearly the nature of this effect, and the nature of the *syn* effect.

As a final note, the MO's for the protonated and deprotonated CpX 's and their *syn* and *anti* addition TS's for their reaction with ethene are similar to the MO's for the neutral CpX and their TS's.

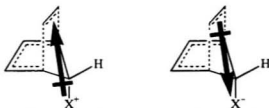


Figure 3.6 Hypothesized direction of the dipole moment of the *anti* addition TS of CpX^+ and CpX^- with ethene.

3.4 Steric Hindrance

The correlations between ΔE_{act} and ΔE_{diene}^{def} and between ΔE_{act} and $\Delta\Theta_{Total}$ for the reaction of protonated and deprotonated CpX suggest that the steric hindrance of X is an important factor in determining facial selectivity for these reactions. The steric factor Ξ_{CX} could not be evaluated at 6-31++G(d)//6-31++G(d) because Boys localization failed to converge for all CpX at this level of theory. Instead, 6-31G(d)//6-31++G(d) localized orbitals were obtained, from which R_{CX} , S_{CX} and Ξ_{CX} were determined (Table 3.11). A comparison with Table 2.20 shows that the difference between Ξ_{CX} evaluated at 6-31G(d)//6-31G(d) and at 6-31G(d)//6-31++G(d) is negligible; differences occur at the fourth significant figure.

S_{CX} does not change systematically with charge. R_{CX} is shorter for CpX^- and longer for CpX^+ , with respect to the corresponding value for CpX^0 . This is consistent with the differences in the C_3-X^0 bond length between the three species. Conversely, the value of Ξ_{CX} is larger for CpX^- and smaller for CpX^+ , with respect to the corresponding value for CpX^0 . Figure 3.7 presents the plot of *syn* ΔE_{act} versus Ξ_{CX} for the reaction of the CpX with ethene.

Values of *syn* ΔE_{act} are separated by an almost constant amount of energy for the three groups of dienes ($r^2 = 0.97, 0.95$ and 0.95 , slope = 58.6, 49.0 and 47.1, for CpX^- , CpX^0 and CpX^+ , respectively). The good correlations for a group indicates that steric hindrance in the *syn* TS is one factor controlling facial selectivity. The CpX^- 's have higher ΔE_{act} 's than would be predicted on the basis of steric hindrance alone. On the other hand, the CpX^+ 's have lower ΔE_{act} 's than would be predicted on the basis of steric hindrance alone.

Table 3.11 S_{CX} (eÅ²), R_{CX} (Å), and Ξ_{CX} (eÅ), evaluated at 6-31G(d)//6-31++G(d).

X	S_{CX}	R_{CX}	Ξ_{CX}
H	0.7348	0.7250	1.0134
NH ⁺	0.6870	0.7305	0.9405
NH ₂	0.6325	0.8150	0.7761
NH ₃ ⁺	0.6324	0.9386	0.6737
O ⁺	0.5321	0.7521	0.7075
OH	0.5298	0.8615	0.6150
OH ₂ ⁺	0.5425	1.0870	0.4991
F	0.4369	0.9119	0.4791
PH ⁺	1.1187	0.7100	1.5755
PH ₂	1.0009	0.7803	1.2827
PH ₃ ⁺	0.9275	0.8409	1.1029
S ⁺	1.0017	0.7890	1.2695
SH	0.9400	0.8754	1.0737
SH ₂ ⁺	0.9449	1.0032	0.9419
Cl	0.8770	0.9762	0.8983

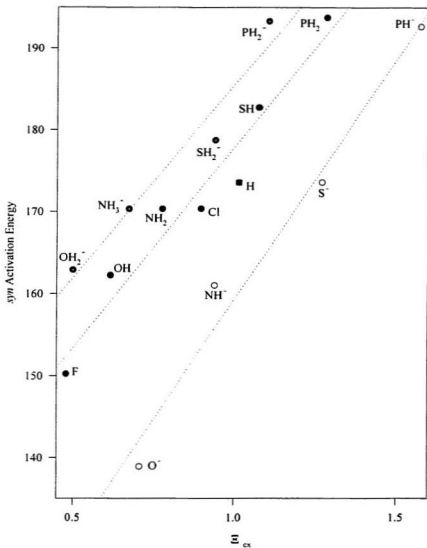


Figure 3.7 $\text{syn} \Delta E_{\text{act}}$ ($\text{kJ} \cdot \text{mol}^{-1}$) versus Ξ_{cx} ($\text{e}\text{\AA}^2$) for *syn* addition of ethene to CpX^- (\circ), CpX^0 (\bullet) and CpX^+ (plus in circle), and CpH (\blacksquare).

The destabilization effect of CpX^- and the stabilization effect of CpX^+ on the *syn* TS could be due to TS antiaromaticity and aromaticity, respectively. While this rationale would explain the observed trends in *syn* ΔE_{act} , no evidence of these effects has been found, and further investigation into this effect is required.

In conclusion, facial selectivity in the Diels-Alder reaction of protonated and deprotonated CpX is controlled by up to three factors. As was the case for neutral CpX, steric hindrance between the $\text{C}_3\text{-X}^0$ bond and the diene resulted in variable amounts of angular deformation about C_3 leading to the *syn* TS. This resulted in a larger variation for *syn* ΔE_{diene}^{def} , and consequently for *syn* ΔE_{act} , than for the corresponding *anti* values. There are probably two separate electronic factors. One factor leads to a destabilization of the *anti* TS for CpX^- and a stabilization of the *anti* TS by CpX^+ . The other factor has a reverse effect in the *syn* TS. The nature of these factors has not been clearly determined, although two hypotheses have been proposed. Unlike the Diels-Alder reactions involving conventional dienes, it is probable that polar and protic solvents will have a significant effect on reaction rates and facial selectivities for the Diels-Alder reactions involving ionic dienes.

In spite of the shortcomings in the theories we have proposed to explain the changes in facial selectivity upon protonation and deprotonation of CpX, what is qualitatively indisputable is that large changes in facial selectivity are predicted. This might have considerable importance in organic synthesis as the change from a neutral to a strongly acidic or basic medium might effectively reverse the facial selectivity of a reaction.

4. Stereoselectivity in the Diels-Alder Reaction of 1,3-Butadiene and 3-Substituted Cyclopropene

4.1 Computational Method

A study of the Diels-Alder reaction of 1,3-butadiene (Bdiene) with 3-substituted cyclopropenes (CprX) was designed to accomplish two objectives. The first aim was to focus on facial selectivity with a plane-nonsymmetric dienophile (Figure 4.1). CprX is the simplest substituted cyclic dienophile. Additionally, the debate in the literature over the mechanism for *endo* versus *exo* stereoselectivity with CprH (Section 1.4) prompted a study of this phenomenon. Although there have been many experimental⁷⁸ and computational^{40,41,42} examinations of *endo* versus *exo* stereoselectivity for the Diels-Alder reaction of CprH, there do not appear to be any studies of facial selectivity involving CprX. Thus, the study of stereoselectivity of these reactions could yield new information that could be used in the planning of syntheses involving CprX.

GS CprX and *cisoid*-Bdiene, and TS structures for *endo-anti*, *endo-syn*, *exo-anti* and *exo-syn* additions were determined at 6-31++G(d)//6-31++G(d) using MUNGAUSS, following the procedures outlined in Section 2.2.2. Although *trans*-Bdiene ($C_4-C_5-C_6-C_7$ torsion = 180.0°) is lower in energy than *cisoid*-Bdiene ($C_4-C_5-C_6-C_7$ torsion = 39.4°), the *cisoid*-Bdiene is the lowest energy conformer of Bdiene that has the potential of reacting in a Diels-Alder reaction (*cis*-Bdiene with the $C_4-C_5-C_6-C_7$ torsion = 0.0° is a first-order saddlepoint). The following is the list of C_3 -substituents (X) employed in this study along with the conformations of X (Figure 2.2) for the lowest energy rotamers of CprX:

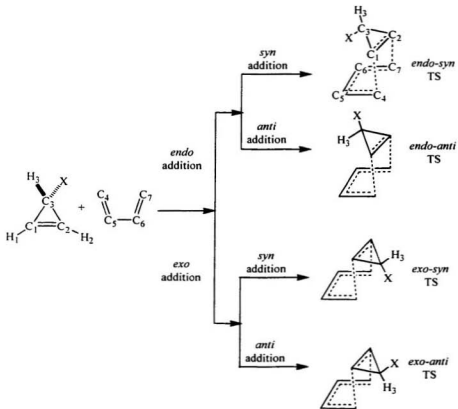


Figure 4.1 The four modes of addition for the reaction of CprX and Bdiene.

X =	H		BH ₂	eclipsed			
	CH ₃	staggered	NH ₂	gauche	OH	gauche	F
	SiH ₃	staggered	PH ₂	staggered	SH	gauche	Cl

The 6-31++G* basis set was chosen for two reasons. First, diffuse functions could be necessary to describe properly the hypothesized interaction between H₃ of CprH and Bdiene in the *endo-anti* TS that was suggested by Jursic⁴¹ and Dannenberg's group.⁴² Additionally, post-HF energies for these structures were desired, and 6-31++G* would have been the minimum acceptable HF basis upon which to perform CI. However, even the lowest level CI which is size-consistent, QCISD(T), was too computationally expensive for this study. Nevertheless, Dannenberg's group showed that while HF wavefunctions overestimate ΔE_{act} for the reaction of Bdiene and CprH, the *endo/exo* difference, $\Delta \Delta E_{act}$, derived at HF was comparable with higher level calculations and, more importantly, with experiment.

4.2 Activation Energy and its Components

Stereoselectivity for a mode of addition (*i*) of the four possible modes of addition for the reaction of CprX and Bdiene is defined as:

$$\% (i) = \frac{e^{-\Delta E_{act}(i)/RT}}{\sum_{j=1}^4 e^{-\Delta E_{act}(j)/RT}} \times 100\%$$

Table 4.1 lists predicted product distribution, evaluated at 273.15K, for *endo-syn* and *endo-anti* addition of CprX and Bdiene, and Table 4.2 lists the same for *exo-syn* and *exo-anti* addition. Listed are the corresponding values of ΔE_{act} , ΔE_{diene}^{def} , ΔE_{dphile}^{def} and ΔE_{int} for each mode of addition, and the corresponding conformation of X for each TS structure.

Endo-anti is in most cases predicted to be the preferred mode of addition, while *exo-anti* addition is predicted to yield the second most abundant product. The exceptions are the reactions of CprOH and CprF with Bdiene, for which it is predicted that *exo-anti* addition is barely preferred over *endo-anti* addition. Moreover, the reaction of CprF and Bdiene is predicted to yield a significant amount of *exo-syn* addition. *Syn* addition is always predicted to be less favourable than *anti* addition, especially *endo-syn* addition, which is predicted to yield no measurable amount of product. Table 4.3 lists the values for relative energies to the corresponding values for *endo-anti* addition (*i.e.*, $\Delta \Delta E_{act}(i) = \Delta E_{act}(i) - \Delta E_{act}(endo-anti)$, and so forth).

Table 4.1 Energy data (kJ·mol⁻¹) and percent (i) (273.15K) for *endo* additions of CprX and Bdiene.

X	conform.	ΔE_{oct}	ΔE_{diene}^{def}	ΔE_{diene}^{def}	ΔE_{int}	% (i)
H		136.8	74.7	50.2	11.9	96.5
<i>endo-anti</i>						
BH ₂	staggered	134.9	72.5	53.0	9.4	99.1
CH ₃	staggered	137.6	75.0	49.8	12.9	94.2
NH ₂	staggered	143.0	78.6	49.1	15.3	69.0
OH	staggered	148.8	81.3	52.0	15.5	47.8
F		154.6	85.2	55.9	13.6	32.5
SiH ₃	staggered	128.4	70.8	49.7	7.9	99.3
PH ₂	staggered	133.6	73.4	51.3	8.9	98.3
SH	gauche	137.8	76.5	51.3	10.0	92.0
Cl		143.9	80.9	53.5	9.5	72.3
<i>endo-syn</i>						
BH ₂	eclipsed	165.1	68.1	79.7	17.3	0.0
CH ₃	staggered	175.0	82.9	68.0	24.1	0.0
NH ₂	gauche	173.7	82.0	70.0	21.6	0.0
OH	gauche	173.3	87.8	66.7	18.7	0.0
F		173.7	86.6	72.8	14.3	0.0
SiH ₃	staggered	167.4	75.4	71.0	21.0	0.0
PH ₂	staggered	168.1	79.6	68.6	20.0	0.0
SH	gauche	171.5	81.0	73.8	16.7	0.0
Cl		174.0	83.0	79.2	11.7	0.0

Table 4.2 Energy data (kJ·mol⁻¹) and percent (i) (273.15K) for *exo* additions of CprX and Bdiene.

X	conform.	ΔE_{act}	ΔE_{def}^{def} <i>diene</i>	ΔE_{def}^{def} <i>diolate</i>	ΔE_{int}	% (i)
H		144.3	72.0	53.4	18.8	3.5
<i>exo-anti</i>						
BH ₂	eclipsed	145.5	71.7	56.4	17.4	0.9
CH ₃	staggered	143.9	71.6	52.6	19.6	5.8
NH ₂	staggered	145.1	73.2	52.0	20.0	27.7
OH	gauche	148.8	75.4	55.9	17.5	48.1
F		153.5	78.2	59.1	16.3	52.0
SiH ₃	staggered	139.8	69.7	53.2	16.9	0.7
PH ₂	staggered	142.8	71.1	54.7	16.9	1.7
SH	gauche	143.3	72.5	55.0	15.8	7.9
Cl		146.1	75.3	57.1	13.8	27.6
<i>exo-syn</i>						
BH ₂	eclipsed	158.9	71.4	66.5	21.0	0.0
CH ₃	staggered	164.8	72.8	66.0	26.0	0.0
NH ₂	gauche	150.0	71.5	65.4	13.1	3.3
OH	staggered	154.4	74.3	67.8	12.3	4.1
F		156.3	77.7	69.9	8.7	15.5
SiH ₃	staggered	159.1	70.7	65.9	22.5	0.0
PH ₂	staggered	156.5	72.5	66.6	17.4	0.0
SH	staggered	156.7	72.8	70.6	13.4	0.0
Cl		159.3	75.4	76.0	8.0	0.1

Table 4.3 Energies ($\text{kJ}\cdot\text{mol}^{-1}$) relative to the corresponding value for *endo-anti* addition.

X	$\Delta\Delta E_{\text{act}}$	$\Delta\Delta E_{\text{diene}}^{\text{def}}$	$\Delta\Delta E_{\text{diolate}}^{\text{def}}$	$\Delta\Delta E_{\text{int}}$
<i>exo - endo</i>				
H	7.5	-2.6	3.2	6.9
<i>(endo-syn) - (endo-anti)</i>				
BH ₂	30.1	-4.4	26.7	7.8
CH ₃	37.4	8.0	18.3	11.2
NH ₂	30.6	3.4	20.9	6.3
OH	24.4	6.5	14.7	3.2
F	19.1	1.4	16.9	0.8
SiH ₃	38.9	4.5	21.3	13.1
PH ₂	34.5	6.2	17.3	11.1
SH	33.8	4.5	22.5	6.8
Cl	30.0	2.0	25.8	2.2
<i>(exo-anti) - (endo-anti)</i>				
BH ₂	10.6	-0.8	3.5	8.0
CH ₃	6.3	-3.3	2.9	6.7
NH ₂	2.1	-5.5	2.9	4.7
OH	0.0	-5.9	3.9	2.0
F	-1.1	-7.0	3.2	2.7
SiH ₃	11.3	-1.2	3.5	9.0
PH ₂	9.2	-2.2	3.4	8.0
SH	5.6	-4.0	3.7	5.8
Cl	2.2	-5.6	3.6	4.2
<i>(exo-syn) - (endo-anti)</i>				
BH ₂	24.0	-1.1	13.5	11.6
CH ₃	27.2	-2.1	16.2	13.1
NH ₂	6.9	-7.2	16.3	-2.2
OH	5.6	-7.0	15.7	-3.2
F	1.7	-7.5	14.0	-4.9
SiH ₃	30.7	-0.2	16.2	14.7
PH ₂	22.9	-0.9	15.3	8.5
SH	19.0	-3.8	19.3	3.4
Cl	15.4	-5.6	22.5	-1.5

Figures 4.2 through 4.4 display plots of ΔE_{act} versus ΔE_{diene}^{def} , $\Delta E_{diphile}^{def}$ and ΔE_{int} , respectively, for *endo-syn* and *endo-anti* addition of CprX to Bdiene, and Figures 4.5a, 4.6 and 4.5b display the same for *exo-syn* and *exo-anti* addition. The energy scales for the axes of all of these graphs are the same. These plots accentuate the difference in ΔE_{act} for *syn* and *anti* addition. While for most cases ΔE_{act} is lowest for *endo-anti* addition, the range of values of ΔE_{act} for this mode of addition is significantly greater than the ranges of ΔE_{act} for the other three modes of addition (26.2 kJ·mol⁻¹ for *endo-anti* addition, versus 9.9, 13.7 and 14.8 kJ·mol⁻¹ for *endo-syn*, *exo-anti* and *exo-syn* additions, respectively).

As was the case for the Diels-Alder reaction of CpX, the best correlations are between ΔE_{act} and ΔE_{diene}^{def} . For *endo-anti* addition, the correlation is excellent ($r^2 = 0.96$, slope = 1.67), and for *exo-anti* addition, the correlation is good ($r^2 = 0.89$, slope = 1.39). *endo-syn* addition gives a rough correlation ($r^2 = 0.77$, slope = 0.52), and *exo-syn* addition gives no correlation. The near one-to-one correlations and the good linear dependence between ΔE_{act} and ΔE_{diene}^{def} for *endo-anti* and *exo-anti* additions indicate that ΔE_{diene}^{def} is an important factor in determining stereoselectivity in these reactions.

There is no correlation between ΔE_{act} and ΔE_{int} for these reactions (Figure 4.4 and 4.5b). ΔE_{int} is lowest for *endo-anti* addition for most CprX. The exceptions are the CprX's which bear electronegative X, i.e., for X = NH₂, OH, F and Cl. For these dienophiles, ΔE_{int} is lowest for *exo-syn* addition. Also related to electronegativity is the trend in $\Delta\Delta E_{int}$ (Table 4.3). $\Delta\Delta E_{int}$ is lower for CprX's which bear an electronegative X.

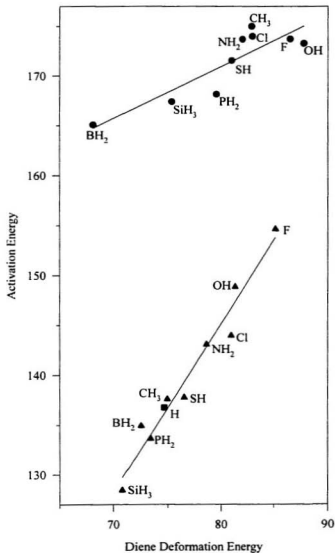


Figure 4.2 ΔE_{act} versus ΔE_{diene}^{def} (kJ·mol⁻¹) for *endo-syn* (●) and *endo-anti* (▲) addition of CprX and Bdiene, and *endo* addition (■) of CprH and Bdiene.

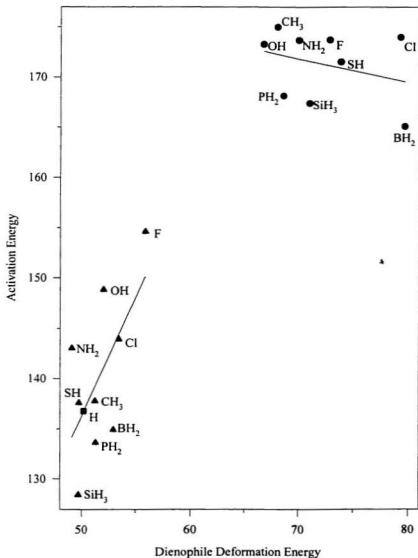


Figure 4.3 ΔE_{act} versus ΔE_{dphile}^{def} (kJ·mol⁻¹) for *endo-syn* (●) and *endo-anti* (▲) addition of CprX and Bdiene, and *endo* addition (■) of CprH and Bdiene.

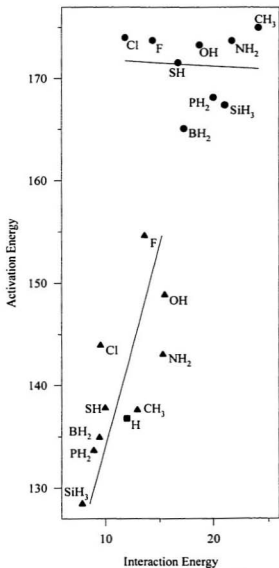


Figure 4.4 ΔE_{act} versus ΔE_{int} (kJ·mol⁻¹) for *endo-syn* (●) and *endo-anti* (▲) addition of CprX and Bdiene, and *endo* addition (■) of CprH and Bdiene.

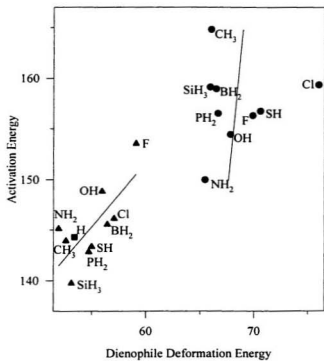


Figure 4.6 ΔE_{acr} versus ΔE_{dphile}^{def} (kJ·mol⁻¹) for *exo-syn* (●) and *exo-anti* (▲) addition of CprX and Bdiene, and *exo* addition (■) of CprH and Bdiene.

There is also no correlation between ΔE_{act} and $\Delta E_{diphile}^{def}$ for these reactions (Figures 4.3 and 4.5a). However, a survey of the relative energy data in Table 4.3 reveals that $\Delta E_{diphile}^{def}$ is the primary factor that leads to the relatively high ΔE_{act} for the two *syn* additions. $\Delta E_{diphile}^{def}$ is between 13.5 and 26.7 kJ·mol⁻¹ greater for *endo-syn* and *exo-syn* additions than it is for *endo-anti* addition. Except for CprOH, $\Delta E_{diphile}^{def}$ is highest for *endo-syn* addition. The values of $\Delta\Delta E_{diene}^{def}$ and $\Delta\Delta E_{int}$ are all smaller in magnitude. Only a few values of $\Delta\Delta E_{int}$ for *exo-syn* addition come close to the magnitude of the corresponding value for $\Delta\Delta E_{diphile}^{def}$. Therefore, for the reaction of CprX and Bdiene, *syn/anti facial selectivity is primarily determined by the amount of energy required to transform the dienophile from its GS geometry to its TS structure.*

All three components of ΔE_{act} for *exo-syn* addition are usually less than the corresponding value for *endo-syn* addition. The exceptions are ΔE_{int} for CprX bearing BH₂, SiH₃ or PH₂ (the most electropositive X), and ΔE_{diene}^{def} for CprBH₂. For the most part, *exo-syn* addition is preferred to *endo-syn* addition due to the lower energy required to deform both addends, and the lower energy required to place them in their TS structures.

ΔE_{diene}^{def} is always lower for *exo-anti* addition than for *endo-anti* addition, while $\Delta E_{diphile}^{def}$ is always lower for *endo-anti* addition than for *exo-anti* addition (Table 4.3). Interestingly, ΔE_{diene}^{def} is lower for *exo-anti* addition than it is for *endo-anti* addition, while $\Delta E_{diphile}^{def}$ is lower by a similar amount energy for *endo-anti* addition. Thus, the differences in ΔE_{diene}^{def} and $\Delta E_{diphile}^{def}$ for *endo-anti* and *exo-anti* additions nearly cancel for all CprX except CprF. Thus, $\Delta\Delta E_{act}$ is close to the value of $\Delta\Delta E_{int}$ for the *anti* additions. Therefore, *the difference*

in the energy of interaction between the two addends in their TS structures is the primary factor which determines the relative ΔE_{act} of *endo-anti* versus *exo-anti* addition in the reaction of *CprX* and *Bdiene*.

The energies, $\Delta E_{isodesmic}$, for the isodesmic reactions pictured in Figure 4.7 provide information about the effect of X, relative to H, on the TS's. A negative value of $\Delta E_{isodesmic}$ indicates that X stabilizes the TS with respect to the corresponding addition of *CprH*, while a positive value indicates that X destabilizes the TS. Table 4.4 lists values of $\Delta E_{isodesmic}$ for the four modes of addition.

X is more destabilizing than H for all *syn* additions. This is consistent with the relatively high values of ΔE_{dphile}^{def} observed earlier for these additions. For *endo-anti* addition, the TS is significantly destabilized by electronegative X, and stabilized by electropositive X. This effect is more moderate for *exo-anti* addition. This is consistent with an electronic effect. The electronegativity of X has been cited several times so far as the basis of a number of trends in energy. The only good correlation found so far in this study has been between ΔE_{act} and ΔE_{diene}^{def} for *endo-anti* and *exo-anti* addition. Is there a connection between this correlation and the electronegativity of X?

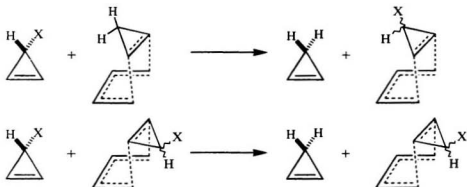


Figure 4.7 Isodesmic reactions defined for *endo* and *exo* addition of CprX and Bdiene.

Table 4.4 $\Delta E_{\text{isodesmic}}$ (kJ·mol⁻¹) for the isodesmic reactions defined in Figure 4.7.

X	$\Delta E_{\text{isodesmic}}$			
	<i>endo-anti</i>	<i>endo-syn</i>	<i>exo-anti</i>	<i>exo-syn</i>
BH ₂	-1.8	28.3	1.3	14.6
CH ₃	0.8	38.2	-0.4	20.5
NH ₂	6.3	36.9	0.8	5.7
OH	12.1	36.5	4.6	10.1
F	17.8	36.9	9.3	12.0
SiH ₃	-8.3	30.6	-4.5	14.8
PH ₂	-3.1	31.4	-1.5	12.2
SH	1.0	34.8	-0.9	12.5
Cl	7.2	37.2	1.8	15.1

4.3 The Destabilization of the *endo-syn* and *exo-syn* Transition States

In Section 2.5, it was shown that facial selectivity in the Diels-Alder reaction of CpX could be explained by focussing on the ranges in geometric differences between the diene in its GS and in its corresponding *syn* and *anti* TS's. Tables 4.5 (*endo-anti* and *endo-syn* additions) and 4.6 (*exo-anti* and *exo-syn* additions) list the ranges in geometric differences between GS CprX and its four possible TS's. Ranges in the incipient bond lengths and geometries of the Bdiene portion of the TS are also listed.

It is evident that the angular changes about C₃ vary over a wider range of values for *endo-syn* addition, followed by *exo-syn* addition. Unlike CpX, there is a significant opening of the H₃-C₃-X angle in the transformation to these TS's. Analogous to the original definition of $\Delta\Theta_{\text{Total}}$ in Section 2.5, $\Delta\Theta_{\text{Total}}$ can be redefined for the reaction of CprX and Bdiene:

$$\Delta\Theta_{\text{total}} = |\Delta\Theta_{\text{C}_1-\text{C}_3-\text{X}}| + |\Delta\Theta_{\text{C}_2-\text{C}_3-\text{X}}| + |\Delta\Theta_{\text{C}_1-\text{C}_3-\text{H}_3}| + |\Delta\Theta_{\text{C}_2-\text{C}_3-\text{H}_3}| + |\Delta\Theta_{\text{X}-\text{C}_3-\text{H}_3}|$$

Table 4.7 contains values of $\Delta\Theta_{\text{Total}}$ for the four modes of addition. $\Delta\Theta_{\text{Total}}$ is usually highest for *endo-syn* addition, followed by *exo-syn* addition. However, some values of $\Delta\Theta_{\text{Total}}$ for the other two modes of addition are almost as high as the two *syn* values. In the case of CprOH, $\Delta\Theta_{\text{Total}}$ is highest for *endo-anti* addition. There is no correlation between $\Delta\Theta_{\text{Total}}$ and ΔE_{act} or $\Delta E_{\text{diphile}}^{\text{def}}$ for any mode of addition. Facial selectivity cannot be determined solely based on the changes in the angles about C₃ in the transformation of CprX to its TS structure, although these angular changes are greater in most cases for the *syn* additions.

Table 4.5 Maximum and minimum changes in geometry between *endo-anti* and *endo-syn* TS structures and the corresponding value in CprX, and minimum and maximum values of other TS parameters. Bond lengths are in Å, angles are in degrees.

	<i>endo-anti</i> TS - GS			<i>endo-syn</i> TS - GS		
	Δ_{\min}	Δ_{\max}	$\Delta\Delta$	Δ_{\min}	Δ_{\max}	$\Delta\Delta$
C ₁ =C ₂	0.0565	0.0625	0.0060	0.0555	0.0711	0.0156
C ₁ -C ₃ , C ₂ -C ₃	-0.0245	0.0004	0.0249	-0.0473	0.0088	0.0561
C ₁ -H ₁ , C ₂ -H ₂	-0.0010	0.0007	0.0017	0.0000	0.0020	0.0020
C ₃ -H ₃	0.0027	0.0072	0.0045	0.0018	0.0150	0.0132
C ₃ -X	-0.0189	0.0039	0.0228	-0.0078	0.0287	0.0365
C ₁ -C ₂ -C ₃ , C ₂ -C ₁ -C ₃	-2.64	-0.43	2.21	-2.35	-0.59	1.76
C ₁ -C ₃ -C ₂	2.73	3.33	0.60	2.34	4.69	2.35
C ₁ -C ₃ -H ₃ , C ₂ -C ₃ -H ₃	-3.43	-1.51	1.91	-3.19	0.63	3.82
C ₁ -C ₃ -X, C ₂ -C ₃ -X	-3.77	1.04	4.81	-2.24	8.82	11.06
H ₃ -C ₃ -X	-0.19	5.80	5.99	-12.65	3.76	16.41
	<i>endo-anti</i> TS			<i>endo-syn</i> TS		
	min	max	Δ	min	max	Δ
C ₁ -C ₄ , C ₂ -C ₇	2.2184	2.2702	0.0518	2.2184	2.2895	0.0711
C ₄ =C ₅ , C ₆ =C ₇	1.3674	1.3734	0.0060	1.3669	1.3739	0.0070
C ₅ -C ₆	1.4034	1.4108	0.0074	1.4001	1.4139	0.0138
C ₄ -C ₅ -C ₆ , C ₅ -C ₆ -C ₇	122.28	122.49	0.21	122.44	122.76	0.32

Table 4.6 Maximum and minimum changes in geometry between *exo-anti* and *exo-syn* TS structures and the corresponding value in CprX, and minimum and maximum values of other TS parameters. Bond lengths are in Å, angles are in degrees.

	<i>exo-anti</i> TS - GS			<i>exo-syn</i> TS - GS		
	Δ_{\min}	Δ_{\max}	$\Delta\Delta$	Δ_{\min}	Δ_{\max}	$\Delta\Delta$
C ₁ =C ₂	0.0552	0.0654	0.0102	0.0522	0.0619	0.0097
C ₁ -C ₃ , C ₂ -C ₃	-0.0129	0.0065	0.0194	-0.0044	0.0110	0.0154
C ₁ -H ₁ , C ₂ -H ₂	-0.0004	0.0012	0.0016	-0.0011	0.0007	0.0018
C ₃ -H ₃	0.0018	0.0032	0.0014	0.0018	0.0071	0.0053
C ₃ -X	-0.0093	0.0061	0.0154	-0.0006	0.0117	0.0123
C ₁ -C ₂ -C ₃ , C ₂ -C ₁ -C ₃	-1.62	-1.21	0.41	-1.64	-0.47	1.17
C ₁ -C ₃ -C ₂	2.42	3.10	0.68	2.11	2.62	0.51
C ₁ -C ₃ -H ₃ , C ₂ -C ₃ -H ₃	-1.70	-0.04	1.67	-1.59	-0.60	1.00
C ₁ -C ₃ -X, C ₂ -C ₃ -X	0.33	3.93	3.59	-3.66	4.97	8.63
H ₃ -C ₃ -X	-3.95	0.32	4.27	-5.65	3.70	9.35
	<i>exo-anti</i> TS			<i>exo-syn</i> TS		
	min	max	Δ	min	max	Δ
C ₁ -C ₄ , C ₂ -C ₇	2.2305	2.2686	0.0381	2.2293	2.2809	0.0516
C ₄ =C ₅ , C ₆ =C ₇	1.3675	1.3713	0.0038	1.3687	1.3729	0.0042
C ₅ -C ₆	1.4036	1.4096	0.0060	1.4036	1.4085	0.0049
C ₄ -C ₅ -C ₆ , C ₅ -C ₆ -C ₇	122.46	122.53	0.07	122.36	122.77	0.42

Table 4.7 $\Delta\Theta_{\text{Total}}$ (degrees) evaluated for the reaction of CprX and Bdiene.				
X	$\Delta\Theta_{\text{Total}}$			
	<i>endo-anti</i>	<i>endo-syn</i>	<i>exo-anti</i>	<i>exo-syn</i>
H		7.0		5.1
BH ₂	4.9	31.6	4.4	9.5
CH ₃	7.2	14.0	4.0	10.3
NH ₂	8.1	12.9	3.8	11.1
OH	17.4	10.8	4.7	10.8
F	9.2	10.6	5.1	4.0
SiH ₃	5.9	24.9	4.2	17.5
PH ₂	6.0	17.6	3.5	8.5
SH	6.3	15.8	10.2	9.1
Cl	8.6	17.7	3.6	11.2

For these TS's, the range of bond lengths changes may also contribute to facial selectivity. Every range involving bond lengths in Tables 4.5 and 4.6 is widest for *endo-syn* addition. The ranges of changes in the cyclopropene ring angles are also greater for *endo-syn* addition. Thus, more geometric change is required to form the *endo-syn* TS than to form the other three TS's. This translates to the higher ΔE_{act} for this mode of addition. Many of the geometric ranges are also high for *exo-syn* addition. While there is no very strong evidence to support any explanation, it is hypothesized that for the *syn* additions steric hindrance between X and the diene leads to the observed differences in facial selectivity. Given the higher $\Delta E_{diphile}^{def}$ for *endo-syn* and *exo-syn* additions, steric hindrance should translate to more energetically costly dienophile deformations. If this conjecture is correct, then the effects of steric hindrance must be delocalized in CprX in the *syn* TS's.

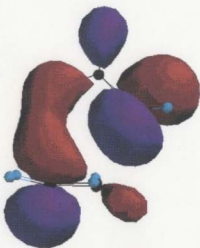
Exo-syn addition is disfavoured for most reactions of CprX and Bdiene. However, due to the low ΔE_{int} for the reactions of CprNH₂, CprOH, CprF and CprCl (Table 4.2), a detectable amount of *exo-syn* product is predicted to form in each case. A favourable hydrogen-bonding interaction is possible between the electronegative X's and the hydrogen atoms on C₄ and C₇ of Bdiene. However, all bond orders between X and the atoms in Bdiene are less than 0.01, and most are negative (*i.e.*, repulsive). In fact, an electropositive X tends to have less unfavourable, albeit weak, bond orders with the atoms of Bdiene than does an electronegative X in the *exo-syn* TS. It is uncertain whether Mayer's bond orders are providing a good qualitative picture in this case. If they are, then the nature of the significant lowering of ΔE_{int} for CprX bearing electronegative X for *exo-syn* addition is uncertain.

4.4 *Endo-anti* versus *exo-anti* Stereoselectivity

Whatever factor controls *endo/exo* stereoselectivity in the Diels-Alder reaction of CprH should also be the factor that determines *endo-anti* versus *exo-anti* stereoselectivity in the reaction of CprX and Bdiene. It was shown in Section 4.2 that the difference in ΔE_{int} between these two modes of addition is the primary factor which determines this stereoselectivity. This is consistent with the proposed hypotheses involving SOI's between CprH and the diene (Section 1.3). Figures 4.8 and 4.9 display MO 26 (HOMO), MO 25 and MO 23 for the *endo* and *exo* TS's, respectively, for the reaction of CprH and Bdiene. There is a significant contribution of the methylene hydrogen in the π_5 -MO of Bdiene in the HOMO of the *endo-anti* TS. A similar orbital mixing is not present in the *exo-anti* TS. This is the π_5 -MO/ H_3 orbital mixing that Dannenberg and his group⁴² and Jursic⁴¹ hypothesized was the factor that decided the *endo/exo* stereoselectivity of the reaction of CprH and Bdiene.

Assuming that the primary orbital interaction is similar for *endo* and *exo* addition, and that the only energetically significant SOI between the diene and the dienophile is the π_5 -MO/ H_3 orbital mixing in the *endo-anti* TS, then an approximation for the energy of this interaction is $\Delta\Delta E_{int}((exo-anti) - (endo-anti))$ (Table 4.3). $\Delta\Delta E_{int}$ is smaller for electronegative X, and larger for electropositive X.

(a)



(b)



(c)

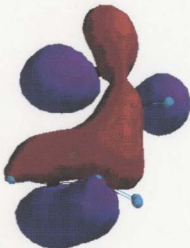


Figure 4.8 Plotted MO's for the *endo* addition TS for the reaction of CprH and Bdiene.
(a) MO 26: a' (HOMO), (b) MO 25: a'' and (c) MO 23: a' .

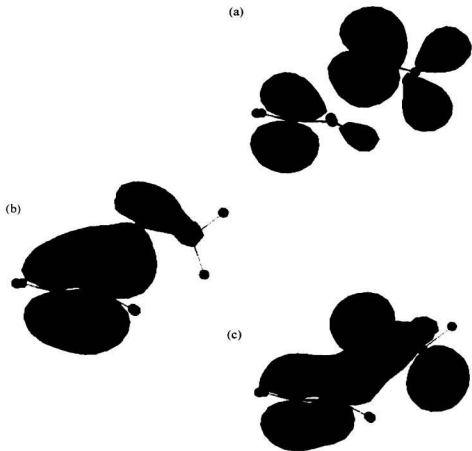


Figure 4.9 Plotted MO's for the *exo* addition TS for the reaction of CprH and Bdiene. (a) MO 26: a' (HOMO), (b) MO 25: a'' and (c) MO 23: a' .

The π_5 -MO/ H_3 orbital mixing should be more favourable for more positively charged H_3 . A more reliable measure of charge on H_3 than Mulliken atomic charge is the C_3 - H_3 bond length. The longer the C_3 - H_3 bond is, the less electron density is in the bond, hence H_3 should be more positively charged. Figure 4.10 displays a plot of $\Delta\Delta E_{int}$ versus C_3 - H_3 bond length in the GS CprX. There is a rough correlation between the two quantities (Figure 4.10; $r^2 = 0.78$). Thus, as H_3 becomes more positive, the π_5 -MO/ H_3 interaction becomes more favourable. This is consistent with the SOI hypothesis. Thus, *endo/exo stereoselectivity in the Diels-Alder reaction of CprH and Bdiene is largely due to a favourable interaction between the π_5 -MO of Bdiene and the methylene hydrogen of CprH that faces the diene. CprX's which bear an electronegative X destabilize this SOI, while an electropositive X will enhance this SOI.*

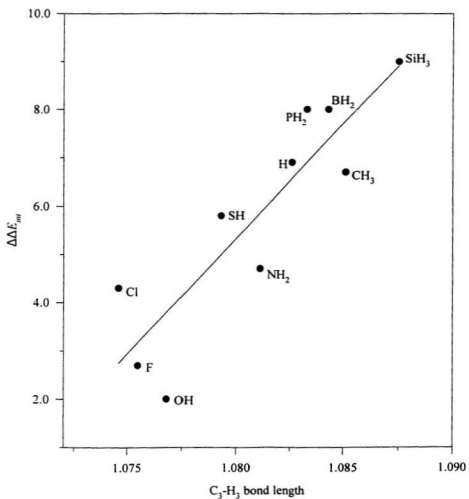


Figure 4.10 $\Delta\Delta E_{int}$ (kJ·mol⁻¹) versus C₃-H₃ bond length (Å) in GS CprX.

4.5 Reactivity of 3-Substituted-1,2-Cyclopropenes

This section probes the properties of CprX. The geometry of CprX's is highly dependent on the electronegativity of X. It was shown in Section 2.8 that Ξ_{CX} correlates well with electronegativity (Figure 2.43). If Ξ_{CX} is to be used as a measure of electronegativity, then it should be transferable from system to system. Table 4.8 lists values of S_{CX} , R_{CX} and Ξ_{CX} evaluated for CprX at 6-31G(d)//6-31++G(d) (see Section 3.4 for justification), and Ξ_{CX} evaluated for CpX (evaluated at 6-31G(d)//6-31G(d)). Figure 4.11 displays a plot of Ξ_{CX} evaluated for CpX *versus* Ξ_{CX} evaluated for CprX. There is a good correlation between the two evaluated Ξ_{CX} 's ($r^2 = 0.90$, slope = 1.12). Thus, Ξ_{CX} evaluated for CpX is transferable, and will be used in the study of CprX and its Diels-Alder reaction with Bdiene.

Table 4.8 Values of S_{CX} , R_{CX} and Ξ_{CX} evaluated for CprX, and Ξ_{CX} evaluated for CpX.

X	S_{CX} (CprX)	R_{CX} (CprX)	Ξ_{CX} (CprX)	Ξ_{CX} (CpX)
H	0.66	0.75	0.88	1.01
BH ₂	0.90	0.65	1.40	1.36
CH ₃	0.68	0.77	0.88	1.00
NH ₂	0.59	0.83	0.72	0.78
OH	0.50	0.87	0.58	0.62
F	0.42	0.93	0.46	0.48
SiH ₃	0.86	0.73	1.18	1.53
PH ₂	0.87	0.81	1.08	1.28
SH	0.87	0.90	0.96	1.08
Cl	0.85	1.02	0.83	0.90

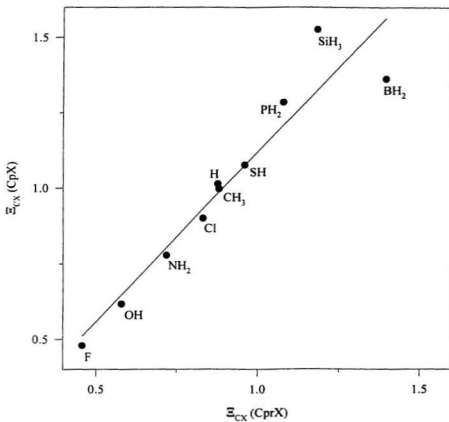


Figure 4.11 Ξ_{CX} evaluated at 6-31G(d)//6-31G(d) for CpX *versus* Ξ_{CX} evaluated at 6-31G(d)//6-31++G(d) for CprX.

Ξ_{CX} correlates well with the bonds and angles of CprX. Figure 4.12 displays a plot of $\text{C}_1=\text{C}_2$ bond length and the average of the C_1-C_3 and C_2-C_3 bond lengths, *versus* Ξ_{CX} . Figure 4.13 displays a plot of the C_3-H_3 bond length and the average of the C_1-H_1 and C_2-H_2 bond lengths, *versus* Ξ_{CX} . There is a rough correlation in all cases ($r^2 = 0.83, 0.74, 0.64$ and 0.51 , respectively, for the bond lengths as listed). In general, the C_1-C_3 , C_2-C_3 and C_3-H_3 bond lengths increase as Ξ_{CX} increases, while the $\text{C}_1=\text{C}_2$, C_1-H_1 and C_2-H_2 bond lengths decrease as Ξ_{CX} increases. Figures 4.14 and 4.15 display plots of the angles of CprX *versus* Ξ_{CX} . For the plots of the $\text{C}_1-\text{C}_3-\text{C}_2$ angle, the average of the $\text{C}_1=\text{C}_2-\text{C}_3$ and $\text{C}_2=\text{C}_1-\text{C}_3$ angles, the average of the $\text{C}_1-\text{C}_3-\text{H}_3$ and $\text{C}_2-\text{C}_3-\text{H}_3$ angles, the average of the $\text{C}_1-\text{C}_3-\text{X}$ and $\text{C}_2-\text{C}_3-\text{X}$ angles, and the $\text{X}-\text{C}_3-\text{H}_3$ angles, *versus* Ξ_{CX} , $r^2 = 0.80, 0.80, 0.71, 0.71, 0.07$ and 0.72 , respectively. The only geometric parameter with which Ξ_{CX} does not correlate is the average of the $\text{C}_1-\text{C}_3-\text{X}$ and $\text{C}_2-\text{C}_3-\text{X}$ angles. Nevertheless, the rough correlations between Ξ_{CX} and most of the geometry of CprX indicates that X has a large impact on the total geometry of CprX.

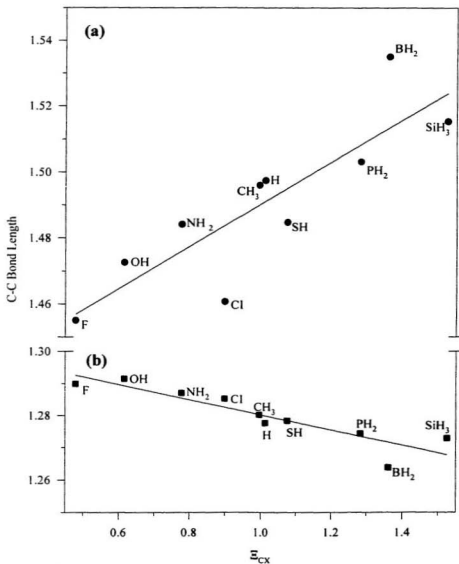


Figure 4.12 (a) The average of the C_1-C_2 and the C_2-C_3 bond lengths (●) and (b) the $C_1=C_2$ bond length (■) of CprX (Å) versus Ξ_{CX} .

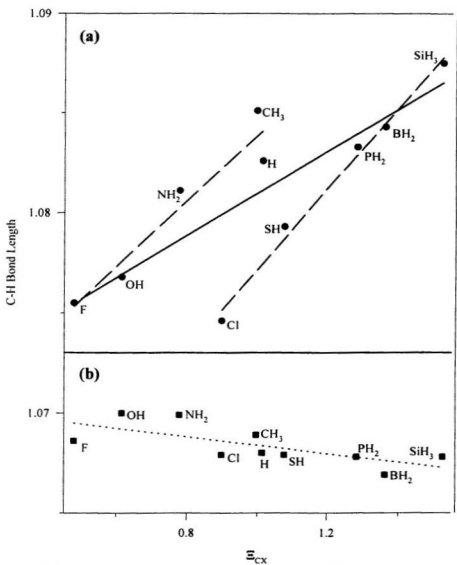


Figure 4.13 (a) The C₃-H₃ bond length (●) and (b) the average of the C₁-H₁ and the C₂-H₂ bond lengths (■) of CprX (Å) versus Ξ_{CX} .

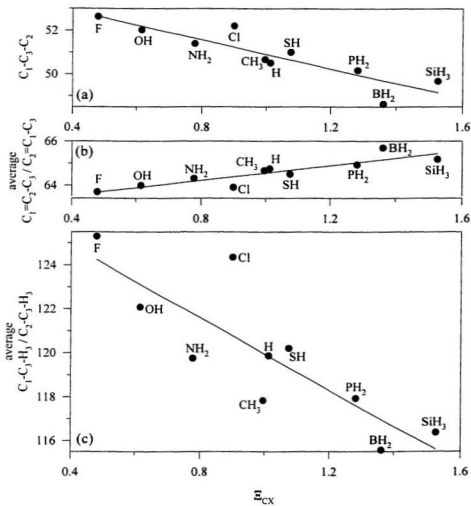


Figure 4.14 (a) The $C_1-C_2-C_3$ angle, (b) the average of the $C_1-C_2-C_3$ and $C_2-C_1-C_3$ angles, and (c) the average of the $C_1-C_2-H_3$ and $C_2-C_3-H_1$ angles of $CprX$ (degrees), versus χ_{CX} .

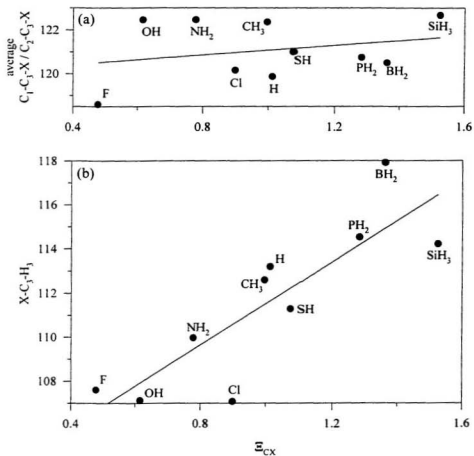


Figure 4.15 (a) The average of the C_1-C_3-X and C_2-C_3-X angles, and (b) the H_3-C_3-X angle of $CprX$ (degrees), versus χ_{CX} .

In terms of reactivity, the $C_1=C_2$ bond is the most important geometric parameter. As Ξ_{CX} decreases, *i.e.*, as X increases in electronegativity, the $C_1=C_2$ bond length increases, and thus the electron density in this bond decreases. For the normal-electron-demand Diels-Alder reaction, the better dienophile is hypothesized to be the more electron deficient one. Therefore, the lengthening of the $C_1=C_2$ bond (for electronegative X) hypothetically should stabilize the normal-electron-demand Diels-Alder reaction. This is not the case. The evaluated $\Delta E_{isodesmic}$ for the isodesmic reactions pictured in Figure 4.7 for *endo-anti* and *exo-anti* addition indicated that electronegative X's destabilize these TS's.

Further support for the destabilization of the TS by an electronegative X is the rough correlation between incipient bond length *versus* Ξ_{CX} for all four modes of addition of CprX and Bdiene (Figure 4.16; $r^2 = 0.88, 0.87, 0.71$ and 0.81 for *endo-anti*, *endo-syn*, *exo-anti* and *exo-syn* additions, respectively). The incipient bond length increases as Ξ_{CX} increases, and the $C_1=C_2$ bond length decreases. A longer incipient bond indicates an earlier, and thus more favourable, TS. On this basis, electronegative X destabilize the TS for all four modes of addition in a systematic way.

Alternatively, this reaction may proceed through the inverse-electron-demand mechanism. Figure 4.17 displays a plot of HOMO and LUMO energies of CprX, *versus* Ξ_{CX} . There is a rough correlation between the HOMO energy of CprX and Ξ_{CX} ($r^2 = 0.75$). As electronegativity increases, the HOMO energy decreases, thus an electronegative X would destabilize an inverse-electron-demand Diels-Alder TS. This is consistent with the observed trends in geometry.

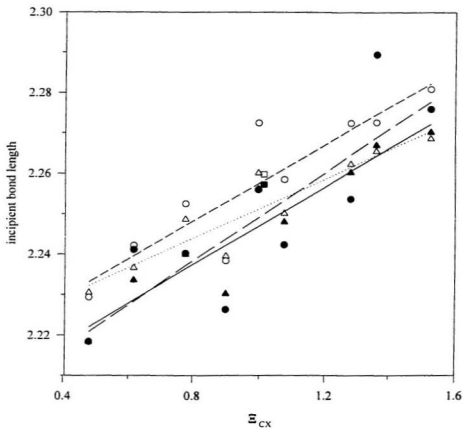


Figure 4.16 Incipient bond length (Å) versus Ξ_{CX} for *endo-anti* (▲, solid line), *endo-syn* (●, long-dashed line), *exo-anti* (△, dotted line) and *exo-syn* (○, short-dashed line) additions of CprX with Bdiene, and *endo* (■) and *exo* (□) addition of CprH and Bdiene.

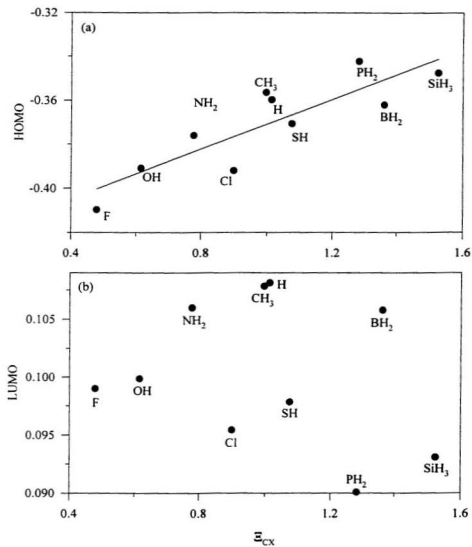


Figure 4.17 (a) π_S -HOMO and (b) π_A^* -LUMO of CprX (Hartrees), versus Σ_{CX} .

If reaction of CprX and Bdiene involves the inverse-electron-demand Diels-Alder route, which is based on an MO argument, then the corresponding MO which depicts a mixing between the π_5 -HOMO of the dienophile and the π_5^* -LUMO of the diene must exist in the TS. This MO was not found. Figures 4.8 and 4.9 (Section 4.4) display MO's which are very similar to the ones displayed in Figures 2.3 to 2.13 in Section 2.4. These MO's are of the π_A/π_A^* , π_5/π_5 bonding and π_5/π_5 antibonding MO types which belong to the TS's for the reactions of CpX and ethene, ethyne, maleimide and TAD. Like the TS's involving TAD, the π_A/π_A^* MO's for *endo* and *exo* addition exhibit significant components throughout the cyclopropene ring.

In the TS for *endo* addition of CprH and Bdiene, there are five other MO's which have significant mixing between the diene and the dienophile. These are low-lying MO's: MO 18, MO 17, MO 15, MO 13 and MO 11 (HOMO is MO 26). They involve a mixing between the σ -MO's of Bdiene and either the π_5 -MO or the σ -MO's of CprH. As was concluded in Section 2.4, there are too many MO's which depict an interaction between the diene and the dienophile that could be important in determining the observed trends. As a predictive tool, one MO cannot be studied in isolation from the other MO's. Thus, *the nature of the inverse-electron-demand behavior of CprX cannot be accounted for by the MO's.*

The trend in incipient bond length does explain the correlations between ΔE_{act} and ΔE_{diene}^{def} for *endo-anti* and *exo-anti* additions. An earlier TS (*i.e.*, longer incipient bond length) would result in less geometric change in the diene, and therefore less ΔE_{diene}^{def} . Figure 4.19 displays

a plot of ΔE_{act} versus Ξ_{CX} for *endo-anti* and *exo-anti* additions. The correlation is better for *endo-anti* addition than for *exo-anti* addition ($r^2 = 0.94$ and 0.73 , respectively), as was the case in the plot of ΔE_{act} versus ΔE_{diene}^{def} (Figures 4.2 and 4.5a). A decrease in Ξ_{CX} corresponds to an increase in ΔE_{act} and a decrease in incipient bond length. A rationale for why there exists a correlation between ΔE_{act} and ΔE_{diene}^{def} has been provided.

Ξ_{CX} measures a substituent effect in the GS. The correlations with incipient bond length and ΔE_{act} imply that this property measured in the GS can predict stereoselectivity in these reactions. $\Delta E_{isodesmic}$ for the isodesmic reaction pictured in Figure 4.18 is an energetic quantification of the substituent effect on CprX. Table 4.9 lists $\Delta E_{isodesmic}$ for the reaction in Figure 4.18. For all CprX except CprSiH₃, X has a stabilizing effect relative to H. Figure 4.20 presents a plot of ΔE_{act} for the four modes of addition of CprX and Bdiene, versus $\Delta E_{isodesmic}$ for the reaction in Figure 4.18. There is a good correlation between ΔE_{act} and $\Delta E_{isodesmic}$ for *endo-anti* addition and for *exo-anti* addition ($r^2 = 0.97$ and 0.89 , and slope = -0.44 and -0.20 , respectively), but no correlation for *endo-syn* and *exo-syn* additions.

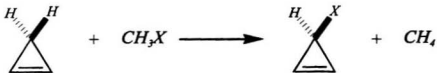


Figure 4.18 The isodesmic process defined to quantify energetically the substituent effect on CprX.

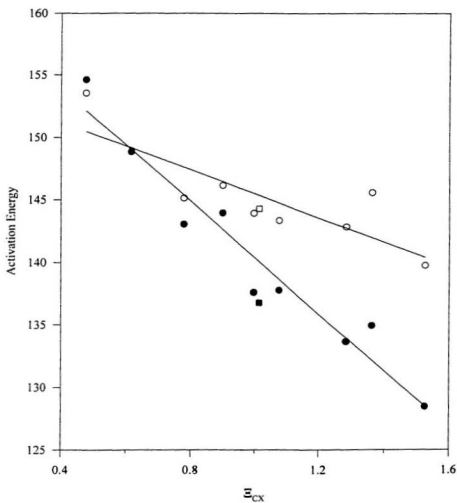


Figure 4.19 ΔE_{act} (kJ·mol⁻¹) versus Σ_{CX} for *endo-anti* (●) and *exo-anti* (○) addition of CprX and Bdiene, and *endo* (■) and *exo* (□) addition of CprH and Bdiene.

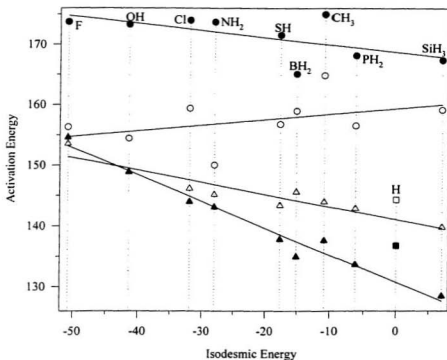


Figure 4.20 ΔE_{act} for the *endo-anti* (\blacktriangle), *endo-syn* (\bullet), *exo-anti* (\triangle) and *exo-syn* (\circ) additions of CprX and Bdiene, and the *endo* (\blacksquare) and *exo* (\square) additions of CprH and Bdiene, versus $\Delta E_{isodesmic}$ ($\text{kJ}\cdot\text{mol}^{-1}$) for the reaction pictured in Figure 4.16.

Table 4.9 $\Delta E_{isodesmic}$ ($\text{kJ}\cdot\text{mol}^{-1}$) for the reaction pictured in Figure 4.16.

X	$\Delta E_{isodesmic}$	X	$\Delta E_{isodesmic}$	X	$\Delta E_{isodesmic}$
H	0	OH	-41.4	PH ₂	-6.3
BH ₂	-15.1	F	-50.8	SH	-17.6
CH ₃	-10.8	SiH ₃	7	Cl	-32.0
NH ₂	-28.0				

Given the correlation between incipient bond and Ξ_{CX} , $\Delta E_{\text{isodesmic}}$ would be expected to correlate similarly with ΔE_{act} for all four modes of addition if ΔE_{act} was determined by the same combination of factors for every mode of addition. ΔE_{act} for *endo-anti* addition is most dependent on $\Delta E_{\text{isodesmic}}$ (steeper slope). This is because the substituent affects both the primary orbital interaction between the diene and the dienophile, and the SOI between the methylene hydrogen of CprX and the π_5 -MO of Bdiene. On the other hand, the substituent affects only the primary orbital interaction between the addends for *exo-anti* addition, thus there is a lesser dependence on $\Delta E_{\text{isodesmic}}$ (smaller slope). The same dependence should exist for *endo-syn* and *exo-syn* additions. Steric hindrance between X and the diene raises ΔE_{act} , but not uniformly for all X. The steric effect of X increases from left to right in Figure 4.20. Thus, ΔE_{act} for CprSiH₃ is raised more due to steric hindrance than it is for CprF. Thus, what would have been a dependence similar to that of *exo-anti* addition between ΔE_{act} and $\Delta E_{\text{isodesmic}}$ is flattened by steric hindrance for *endo-syn* and *exo-syn* additions. This is further evidence of the electronic nature of *endo/exo* stereoselectivity and the steric nature of *syn/anti* facial selectivity in the reaction of CprX and Bdiene.

5. Conclusions and Future Work

A rationale based on steric hindrance has been proposed to explain facial selectivity in the Diels-Alder reaction of CpX. It is possible that an electronic effect may contribute to facial selectivity in these reactions. However, orbital mixing arguments and TS hyperconjugation have been shown to have an insignificant effect on facial selectivity. Such arguments are frequently used in the literature to explain the stereoselectivity of numerous reactions and to account for the conformational preferences of molecules (*e.g.*, the Cieplak effect used to explain facial selectivity of nucleophilic additions to cyclohexanones,²⁹ and hyperconjugation arguments used to explain the anomeric effect⁷⁹). Systematic studies using the methodologies developed in this thesis could be employed to determine the relative importance of such effects in other systems.

Stereoselectivity in the Diels-Alder reaction of CprX and Bdiene was studied. It was determined that a favourable interaction between the methylene hydrogen of CprH and Bdiene in the *endo* TS led to the experimentally observed preference for *endo* addition of CprH. As well, it was proposed that steric hindrance between X and the diene resulted in the higher ΔE_{act} for *endo-syn* and *exo-syn* additions.

The study of the reaction of CprX and Bdiene followed our work with CpX. Therefore, it was initially hypothesized that the stereoselectivity for this reaction could be explained largely by steric arguments. Figure 5.1 displays the TS's for the reaction of CpH and ethene, ethyne, maleimide (*endo* and *exo*) and TAD (*endo* and *exo*), and the *endo* and *exo* TS's for the reaction of CprH and Bdiene. The geometries of the TS's are remarkably alike. For all of the TS's, the angle of approach of the dienophile is similar. For *endo* addition, the plane of the dienophile is directed away from the plane of the diene, but for *exo* addition, the diene and the dienophile lie in "parallel planes." In the TS for the reaction of CpH and ethene, the orientation of the planes containing the *endo* and *exo* hydrogen atoms in the dienophile is similar to the *endo* and *exo* orientations of the planes of the larger dienophiles. It is hypothesized that most Diels-Alder TS have *endo* and *exo* geometries similar to those in Figure 5.1. If this is the case, then several conjectures can be made.

First, the orientation of the diene and the dienophile in the *endo* TS's for the reactions of CpH with maleimide and TAD does not appear to be able to facilitate well the SOO suggested by Woodward and Hoffman.⁷ A survey of the MO's for these TS's (Figures 2.9 to 2.13) indicates that SOI's exist in both the *endo* and the *exo* TS's. The differences between *endo* and *exo* additions are more pronounced for the reaction with TAD, and could be the basis of some to the minor secondary effects observed for this reaction (Section 2). The relative importance of SOO or SOI's in determining the stereoselectivity of Diels-Alder reactions is uncertain.

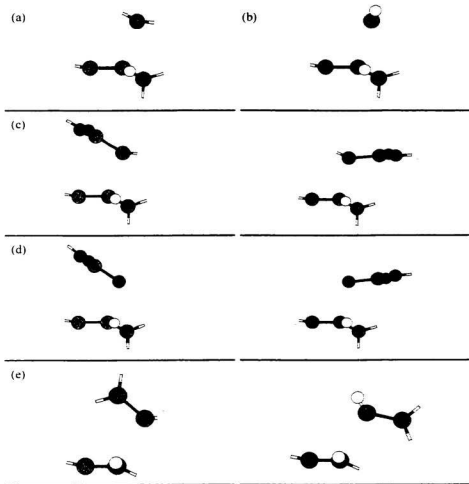


Figure 5.1 TS's for the reactions of CpH with (a) ethene, (b) ethyne, (c) maleimide (*endo* and *exo*) and (d) TAD (*endo* and *exo*), and (e) for the reaction of CpH and Bdiene (*endo* and *exo*).

A Diels-Alder TS can be separated into two sides: the *endo*-side and the *exo*-side (Figure 5.2). The part of the dienophile that resides in the *exo*-side of the TS is closer to the diene, and in the case of CpX, is closer to the *syn* face C₃-substituent. Thus, the more sterically hindering part of the dienophile would prefer to reside in the *endo* side of the TS.

The reaction of CprH and Bdiene may be unique. Unlike the other *endo* TS's which have the bulk of the dienophile directed away from the diene, the methylene hydrogen of CprH is directed towards the diene in the *endo* addition TS of CprH and Bdiene. Ironically, the orientation of CprH in the *endo* TS may be more likely to lead to a significant SOI than the *endo* orientation of maleimide or TAD. It is predicted that the reaction of CpH and CprH should produce a higher proportion of *endo* addition product due to both the favourable SOI and an increase in steric hindrance in the *exo* TS.

More work is required to quantify the relative importance of SOI's and steric hindrance in determining *endo/exo* stereoselectivity in the Diels-Alder reaction, and thus confirm or invalidate the hypotheses presented in this thesis.

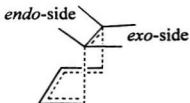


Figure 5.2 Definition of the *endo* side and the *exo* side of a Diels-Alder TS.

Ξ_{CX} was defined in Section 2.7 as a measure of steric hindrance, and then it was used as a measure of electronegativity in Section 4.5. Ξ_{CX} can be thought of as a more general substituent factor, that may measure any number of effects that X has on the molecule to which it is attached. It was hypothesized in Section 2.8 that a more general factor Ξ_{YX} would be a useful measure of electronegativity for any group X attached to atom Y. This factor could have more applications beyond measuring electronegativity.

The definition of Ξ_{CX} is somewhat arbitrary because there are many possible localized sets of MO's. It may be possible to evaluate Ξ_{CX} at X or at the bond critical point (*i.e.*, where $\nabla\rho = 0$ along a bond). As well, it may be possible to define a general measure of the steric hindrance, Ξ_M , for a whole molecular structure. One proposed definition was:

$$\Xi_M = \sum_A \sum_{B \neq A} \frac{S_A S_B}{R_{AB}}$$

where A and B are the set of non-core LMO's. For several systems, Ξ_M was consistently inversely proportional to steric hindrance. More exploration into this phenomenon, and into other definitions of Ξ_{CX} and Ξ_M would likely be very interesting.

References

1. (S)-(+)-ibuprofen exerts its effect in twelve minutes, while the racemic mixture requires thirty-eight minutes. Bruice, P. Y. In *Organic Chemistry*; Prentice-Hall, Inc.: New Jersey, 1995, 209.
2. Sepracor Inc. is a company which specializes in the development and commercialization of single-isomer or active-metabolite versions of other companies' leading drugs. Recently, Sepracor signed a \$90 million licencing agreement with Eli Lilly that gives Lilly exclusive rights to develop and market Sepracor's (R)-fluoxetine, the active single isomer of Lilly's drug Prozac. (a) Rogers, R. S. In *Chemical & Engineering News*; November 30, 1998, 11. (b) Rogers, R. S. In *Chemical & Engineering News*; December 14, 1998, 14.
3. Diels, O.; Alder, K. *Justus Liebigs Ann. Chem.* **1928**, 460, 98.
4. Houk, K. N.; González, J.; Li, Y. *Acc. Chem. Res.* **1995**, 28, 81, and references therein.
5. Fleming, I. In *Frontier Orbitals and Organic Chemistry Reactions*; Wiley: New York, 1976.
6. Liu, C.; Burnell, D. J. *J. Am. Chem. Soc.* **1997**, 119, 9584.
7. Woodward, R. B.; Hoffman, R. *J. Am. Chem. Soc.* **1965**, 89, 4388.
8. Franck-Neumann, M.; Sedrati, M. *Tetrahedron Lett.* **1983**, 24, 1391.
9. Breslow, R.; Hoffman, J. M.; Perchonock, C. *Tetrahedron Lett.* **1973**, 3723.
10. Corey, E. J.; Weinshenker, N. M.; Schaat, T. K.; Huber, W. *J. Am. Chem. Soc.* **1969**, 91, 5675.
11. Ishida, M.; Aoyama, T.; Kato, S. *Chem. Lett.* **1989**, 663.
12. Fleming, I.; Michael, J. P. *J. Chem. Soc., Chem. Commun.* **1978**, 245.
13. Weinstein, M.; Shatavsky, C.; Norton, C.; Woodward, R. B. *J. Am. Chem. Soc.* **1955**, 77, 4183.
14. McClinton, M. A.; Sik, V. *J. Chem. Soc., Perkin Trans. I* **1992**, 1891.
15. For example: Jones, D. W. *J. Chem. Soc., Chem. Commun.* **1980**, 739.

16. Macaulay, J. B.; Fallis, A. G. *J. Am. Chem. Soc.* **1990**, *112*, 1136.
17. Williamson, K. L.; Hsu, Y. L.; Lacko, R.; Young, C. H. *J. Am. Chem. Soc.* **1969**, *91*, 6129.
18. Burnell, D. J.; Valenta, Z. *J. Chem. Soc., Chem. Commun.* **1985**, 1247.
19. Williamson, K. L.; Hsu, Y. L.; Lacko, R.; Youn, C. H. *J. Am. Chem. Soc.* **1969**, *91*, 6129.
20. Anh, N. T. *Tetrahedron* **1973**, *29*, 3227.
21. Inagaki, S.; Fujimoto, H.; Fukui, K. *J. Am. Chem. Soc.* **1976**, *98*, 4054.
22. Gleiter, R.; Paquette, L. A. *Acc. Chem. Res.* **1983**, *16*, 328.
23. Brown, F. K.; Houk, K. N. *J. Am. Chem. Soc.* **1985**, *107*, 1971.
24. Brown, F. K.; Houk, K. N.; Burnell, D. J.; Valenta, Z. *J. Org. Chem.* **1987**, *52*, 3050.
25. Coxon, J. M.; Fong, S. T.; McDonald, D. Q.; Steel, P. J. *Tetrahedron Lett.* **1993**, *34*, 163.
26. Kahn, S. D.; Hehre, W. J. *J. Am. Chem. Soc.* **1987**, *109*, 663.
27. Ishida, M.; Aoyama, T.; Kato, S. *Chem. Lett.* **1989**, 663.
28. Ishida, M.; Aoyama, T.; Beniya, Y.; Yamabe, S.; Kato, S.; Inagaki, S. *Bull. Chem. Soc. Jpn.* **1993**, *66*, 3430.
29. Cieplak, A. S. *J. Am. Chem. Soc.* **1981**, *103*, 4540.
30. Epiotis, N. D.; Cherry, W. R.; Shaik, S.; Yates, R. L.; Bernardi, F. *Topics in Current Chemistry* **1977**, *70*, 1.
31. Werstiuk, N. H.; Ma, J.; Macaulay, J. B.; Fallis, A. G. *Can. J. Chem.* **1992**, *70*, 2798.
32. Werstiuk, N. H.; Ma, J. *Can. J. Chem.* **1994**, *72*, 2493.
33. Sauer, J. *Angew. Chem., Int. Ed.* **1967**, *6*, 16. (b) Sauer, J. *Angew. Chem., Int. Ed.* **1966**, *5*, 211.
34. Halterman, R. L.; McCarthy, B. A.; McEvoy, M. A. *J. Org. Chem.* **1992**, *57*, 5585.

35. (a) Ishida, M.; Kakita, S.; Inagaki, S. *Chem. Lett.* **1995**, 469. (b) Ishida, M.; Tomohiro, S.; Minako, S.; Inagaki, S. *Chem. Lett.* **1995**, 739. (c) Ishida, M.; Kobayashi, H.; Tomohiro, S.; Wasada, H.; Inagaki, S. *Chem. Lett.* **1998**, 41.
36. (a) Hickey, E. R.; Paquette, L. A. *Tetrahedron Lett.* **1994**, 35, 2309. (b) Hickey, E. R.; Paquette, L. A. *Tetrahedron Lett.* **1994**, 35, 2313.
37. Alder, K.; Stein, G. *Angew. Chem.* **1937**, 50, 510.
38. Ginsburg, D. *Tetrahedron* **1983**, 39, 2095, and references therein.
39. Gleiter, R.; Böhm, M. C. *Pure Appl. Chem.* **1983**, 55, 237.
40. Apeloig, Y.; Matzner, E. *J. Am. Chem. Soc.* **1995**, 117, 5375.
41. Jursic, B. S. *J. Org. Chem.* **1997**, 62, 3046.
42. Sodupe, M.; Rios, R.; Branchadell, V.; Nicholas, T. Oliva, A.; Dannenberg, J. J. *J. Am. Chem. Soc.* **1997**, 119, 4232.
43. For example: (a) Mellor, J. M.; Webb, C. F. *J. Chem. Soc., Perkins Trans. II* **1974**, 17. (b) Cantello, B. C. C.; Mellor, J. M.; Webb, C. F. *J. Chem. Soc., Perkins Trans. II* **1974**, 22. (c) Mellor, J. M.; Webb, C. F. *J. Chem. Soc., Perkins Trans. II* **1974**, 26.
44. Fox, M. A.; Cardona, R.; Kiwiet, N. J. *J. Org. Chem.* **1987**, 52, 1469.
45. Sodupe, M.; Dannenberg, J. J.; Oliva, A.; Bertrán, J. J. *J. Org. Chem.* **1989**, 54, 2488.
46. (a) Burry, L. C. Ph.D. Thesis, Memorial University of Newfoundland, St. John's, Newfoundland, Canada, 1998. (b) Burry, L. C.; Bridson, J. N.; Burnell, J. D. *J. Org. Chem.* **1995**, 60, 5931.
47. (a) Letourneau, J. E. M.Sc. Thesis, Memorial University of Newfoundland, St. John's, Newfoundland, Canada, 1996. (b) Letourneau, J. E.; Wellman, M. A.; Burnell, D. J. *J. Org. Chem.* **1997**, 62, 7272.
48. (a) Wellman, M. A. M.Sc. Thesis, Memorial University of Newfoundland, St. John's, Newfoundland, Canada, 1996. (b) Wellman, M. A.; Burry, L. C.; Letourneau, J. E.; Bridson, J. N.; Miller, D. O.; Burnell, D. J. *J. Org. Chem.* **1997**, 62, 939.
49. The first calculations for the computational study of facial selectivity in the Diels-Alder reaction of CpX were performed by Cory Pye. This consisted of some of the early TS structures evaluated at STO-3G, and substantial work with the GS CpX, though most of the

6-31G(d) results presented in this thesis were calculated by myself. His work with GS CpX is summarized in his thesis: (a) Pye, C. C. Ph.D. Thesis, Memorial University of Newfoundland, St. John's, Newfoundland, Canada, 1997. Pye was also involved in the early analysis and the discussions leading to the communication and full paper published by our group on this topic: (b) Poirier, R. A.; Pye, C. C.; Xidos, J. D.; Burnell, D. J. *J. Org. Chem.* **1995**, *60*, 2328. (c) Xidos, J. D.; Poirier, R. A.; Pye, C. C.; Burnell, D. J. *J. Org. Chem.* **1998**, *63*, 105.

50. Fringuelli, F.; Taticchi, A. In *Dienes in the Diels-Alder Reaction*; John Wiley & Sons, Inc.: Toronto, 1990, and references therein.

51. The reaction of *cis*-cyclohexa-3,5-diene-1,2-diol with NPM was performed in seven solvents of different polarity. Facial selectivity ranged from 88% *syn* addition to the hydroxides to 95% *syn* addition. Gillard, J. R.; Burnell, D. J. *Can. J. Chem.* **1991**, *70*, 1296.

52. For example: Goldstein, E.; Beno, B.; Houk, K. N. *J. Am. Chem. Soc.* **1996**, *118*, 6036.

53. Hehre, W. J.; Radom, L.; Schleyer, P. v. R.; Pople, J. A. In *Ab Initio Molecular Orbital Theory*; John Wiley & Sons, Inc.: Toronto, 1986.

54. Francl, M. M.; Pietro, W. J.; Hehre, W. J.; Binkley, J. S.; Gordon, M. S.; Defrees, D. J.; Pople, P. A. *J. Chem. Phys.* **1982**, *77*, 3654, and references therein.

55. (43321/4321/41) and (433321/43321/431) are the split valence forms of the (4333/433/4) and (43333/4333/43) basis sets, respectively, augmented by a set of d-polarization functions. Each digit in the basis set name signifies the number of primitive gaussians used to describe each basis function. The forward-slashes separate the AO types (s/p/d). Huzinaga, S.; Andzelm, J.; Klobukowski, M.; Radzio-Andzelm, E.; Sakai, Y.; Tatewaki, H. In *Gaussian Basis Sets for Molecular Calculations*; Huzinaga, S., Ed.; Elsevier Science: Amsterdam, 1984.

56. (a) Poirier, R.A.; Peterson, M.R. MUNGAUSS V0.0; **1990**, Chemistry Department, Memorial University of Newfoundland, St. John's, Newfoundland, Canada. (b) Poirier, R. A.; Wang, Y.; Pye, C. C. MUNGAUSS V1.0; Chemistry Department, Memorial University of Newfoundland, St. John's, Newfoundland, Canada. (c) Colonna, F.; Jolly, L. -H.; Poirier, R. A.; Angyan, J. G.; Jansen, G. *Comput. Phys. Commun.* **1994**, *81*, 293.

57. Davidson, W. C. *Math. Prog.* **1975**, *9*, 1.

58. Powell, M. J. D. Subroutine VA05, A. E. R. E. Subroutine Library, Harwell; Didcott, Berkshire, U. K.

59. Csaszar, P.; Pulay, P. *J. Mol. Struct.* **1984**, *114*, 31.
60. (a) Gaussian 92, Revision A: Frisch, M. J.; Trucks, G. W.; Head-Gordon, M.; Gill, P. M. W.; Wong, M. W.; Foresman, J. B.; Johnson, B. G.; Schlegel, H. B.; Robb, M. A.; Replogle, E. S.; Gomperts, R.; Andres, J. L.; Raghavachari, K.; Binkley, J. S.; Gonzalez, C.; Martin, R. L.; Fox, D. J.; Defrees, D. J.; Baker, J.; Stewart, J. J.; Pople, J. A.; Gaussian, Inc., Pittsburgh, PA, 1992. (b) Gaussian 94, Revision B.3: Frisch, M. J.; Trucks, G. W.; Schlegel, H. B.; Gill, P. M. W.; Johnson, B. G.; Robb, M. A.; Cheeseman, J. R.; Keith, T.; Petersson, G. A.; Montgomery, J. A.; Raghavachari, K.; Al-Laham, M. A.; Zakrzewski, V. G.; Ortiz, J. V.; Foresman, J. B.; Peng, C. Y.; Ayala, P. Y.; Chen, M.; Wong, W.; Andres, J. L.; Replogle, E. S.; Gomperts, R.; Martin, R. L.; Fox, D. J.; Binkley, J. S.; Defrees, D. J.; Baker, J.; Stewart, J. P.; Head-Gordon, M.; Gonzalez, C.; Pople, J. A. Gaussian, Inc., Pittsburgh PA, 1995.
61. Spartan version 4.1. Wavefunction, Inc., 18401 Von Karman Ave., #370, Irvine, CA 92715.
62. Mulliken, R. S. *J. Chem. Phys.* **1955**, *23*, 1833, 1841, 2338, 2345.
63. Mayer, I. *Chem. Phys. Lett.* **1983**, *97*, 270.
64. Bader, R. F. W. In *Atoms in Molecules: A Quantum Theory*; Clarendon Press: Oxford, 1990.
65. Boyd, R. J.; Edgecombe, K. E. *J. Am. Chem. Soc.* **1988**, *110*, 4182.
66. Allred, A. L.; Rochow, E. G. *J. Inorg. Nucl. Chem.* **1958**, *5*, 264.
67. (a) Bondi, A. *J. Phys. Chem.* **1964**, *68*, 441-451. (b) Cotton, F. A.; Wilkinson, G. In *Basic Inorganic Chemistry*; John Wiley & Sons, Inc.: Toronto, 1976.
68. (a) Bragg, W. L. *Phil. Mag.* **1920**, *40*, 169. (b) Slater, J. C. *J. Chem. Phys.* **1964**, *41*, 3199.
69. Hirsch, J. *Top. Stereochem.* **1967**, *1*, 199.
70. Förster, H.; Vögtle, F. *Angew. Chem., Int. Ed. Engl.* **1977**, *16*, 429.
71. Anderson, J. E.; Pearson, H. J. *Chem. Soc., Chem. Commun.* **1971**, 871.
72. Unger, S. H.; Hansch, C. In *Progress in Physical Organic Chemistry*; Taft, R. W., Ed.; John Wiley & Sons: Toronto, 1976; Vol. 12, 91, and references therein.

73. (a) Robb, M. A.; Haines, W. J.; Csizmadia, I. G. *J. Am. Chem. Soc.* **1973**, *95*, 42. (b) Csizmadia, I. G. In *Localization and Delocalization in Quantum Chemistry*; Chalvet, O. et al., Eds.; D. Reidel Publishing Company: Dordrecht, Holland, 1975; Vol. 1, 349.

74. Edmiston, C.; Ruedenberg, K. *Rev. Mod. Phys.* **1963**, *35*, 457.

75. (a) Boys, S. F. In *Quantum Theory of Atoms, Molecules and the Solid State*; Löwdin, P. O., Ed.; Academic Press: New York, 1966, 253. (b) Foster, J. M.; Boys, S. F. *Rev. Mod. Phys.* **1960**, *32*, 300.

76. Gillespie, R. J.; Hargittai, I. In *The VSEPR Model of Molecular Geometry*; Allyn and Bacon: Toronto, 1991.

77. The 6-31++G(d) basis set adds a diffuse s function for first period elements, and a set of diffuse sp functions on all other elements. Clark, T.; Chandrasekhar, J.; Spitznagel, G. W.; Schleyer, P. v. R. *J. Comp. Chem.* **1983**, *4*, 294.

78. Halton, B.; Banwell, M. G. In *The Chemistry of the Cyclopropyl group*; Rappoport, Z. Ed. Wiley: New York, 1997; Chapter 21, and references therein.

79. For example: Salzner, U.; Schleyer, P. v. R. *J. Org. Chem.* **1994**, *59*, 2138.

Appendix

Table A.1 Total energies (Hartrees) for CpX.

6-31G(d)//6-31G(d)		6-31++G(d)//6-31++G(d)	
X (conform.)	E _{Total}	X (conform.)	E _{Total}
H	-192.791723	H	-192.798325
BH ₂ (gau)	-218.041547	NH ⁻ (stag)	-247.167359
CH ₃ (stag)	-231.826583	NH ₂ (gau)	-247.819509
NH ₂ (gau)	-247.809306	NH ₃ ⁻ (stag)	-248.185244
OH (stag)	-267.636724	O ⁻	-267.034071
F	-291.634395	OH (stag)	-267.647484
SiH ₃ (stag)	-482.872605	OH ₂ ⁻ (gau)	-267.957226
PH ₂ (gau)	-534.084601	F	-291.647726
SH (stag)	-590.298721	PH ⁻ (stag)	-533.496364
Cl	-651.689894	PH ₂ (gau)	-534.091653
GeH ₃ (stag)	-2267.374437	PH ₃ ⁻ (stag)	-534.436324
AsH ₂ (stag)	-2425.516566	S ⁻	-589.741690
SeH (stag)	-2590.471889	SH (stag)	-590.305541
Br	-2762.354209	SH ₂ ⁻ (gau)	-590.614451
SnH ₃ (stag)	-6212.428784	Cl	-651.696189
SbH ₂ (stag)	-6502.212655		
TeH (gau)	-6799.790430		
I	-7105.257602		
CH=CH ₂ (ecli)	-269.669213		
C≡CH	-268.458787		
C≡N	-284.521535		
CF ₃ (stag)	-528.415855		
NO ₂ (stag)	-396.257794		

Table A.2 Total energies (Hartrees) for the syn addition TS for the reaction of CpX and ethene, evaluated at 6-31G(d)/6-31G(d).

X (conform.)	E _{Total} (TS)	E _{Total} (TS diene)	E _{Total} (TS dphile)
H	-270.760244	-192.754024	-78.013407
BH ₂ (stag)	-296.003977	-217.998830	-78.011869
CH ₃ (stag)	-309.791434	-231.785479	-78.014185
NH ₂ (gau)	-325.779164	-247.771665	-78.014494
OH (gau)	-345.609648	-267.599090	-78.016450
F	-369.613297	-291.601755	-78.016300
SiH ₃ (stag)	-560.828758	-482.823983	-78.012548
PH ₂ (stag)	-612.045350	-534.038918	-78.013670
SH (gau)	-668.263484	-590.255138	-78.014649
Cl	-729.659357	-651.649975	-78.015853
GeH ₃ (stag)	-2345.330235	-2267.325576	-78.012866
AsH ₂ (stag)	-2503.475282	-2425.469298	-78.013348
SeH (ecli)	-2668.434702	-2590.426603	-78.014141
Br	-2840.320548	-2762.311592	-78.015669
SnH ₃ (stag)	-6290.380542	-6212.376517	-78.012174
SbH ₂ (stag)	-6580.166670	-6502.161849	-78.012623
TeH (ecli)	-6877.750588	-6799.743599	-78.013520
I	-7183.219653	-7105.211721	-78.015206
CH=CH ₂ (ecli)	-347.634287	-269.628049	-78.014131
C≡CH	-346.428776	-268.420028	-78.014889
C≡N	-362.491979	-284.482401	-78.014416
CF ₃ (stag)	-606.377994	-528.370370	-78.014680
NO ₂ (stag)	-474.231080	-396.219929	-78.014889

Table A.3 Total energies (Hartrees) for the anti addition TS for the reaction of CpX and ethene, evaluated at 6-31G(d)//6-31G(d).

X (conform.)	E_{Total} (TS)	E_{Total} (TS diene)	E_{Total} (TS dophile)
BH ₂ (gau)	-296.009037	-218.005452	-78.012006
CH ₃ (stag)	-309.792755	-231.788529	-78.013271
NH ₂ (gau)	-325.776433	-247.770979	-78.014067
OH (stag)	-345.605648	-267.598881	-78.014682
F	-369.603671	-291.596719	-78.014598
SiH ₃ (stag)	-560.838928	-482.835521	-78.011693
PH ₂ (stag)	-612.051707	-534.047985	-78.012669
SH (stag)	-668.265440	-590.260885	-78.013274
Cl	-729.658519	-651.652932	-78.013809
GeH ₃ (stag)	-2345.340926	-2267.337575	-78.011514
AsH ₂ (stag)	-2503.484216	-2425.480871	-78.012217
SeH (gau)	-2668.438574	-2590.434304	-78.012842
Br	-2840.323019	-2762.317922	-78.013353
SnH ₃ (stag)	-6290.395156	-6212.392008	-78.010842
SbH ₂ (stag)	-6580.180191	-6502.177179	-78.011548
TeH (gau)	-6877.758351	-6799.754489	-78.012422
I	-7183.226517	-7105.221986	-78.012934
CH=CH ₂ (ecli)	-347.636974	-269.631887	-78.013462
C≡CH	-346.425905	-268.419549	-78.013730
C≡N	-362.490061	-284.482561	-78.014010
CF ₃ (stag)	-606.381293	-528.377012	-78.013249
NO ₂ (stag)	-474.225411	-396.218392	-78.014197

Table A.4 Total energies (Hartrees) for the TS's for the reaction of CpX and ethyne, evaluated at 6-31G(d)//6-31G(d).

X (conform.)	E _{Total} (TS)	E _{Total} (TS diene)	E _{Total} (TS dphile)
H	-269.541072	-192.753537	-76.793447
<i>syn</i>			
CH ₃ (stag)	-308.572855	-231.785321	-76.794360
NH ₂ (gau)	-324.562559	-247.772322	-76.794459
OH (stag)	-344.395118	-267.601995	-76.794186
F	-368.391138	-291.600933	-76.796348
SiH ₃ (ecli)	-559.612426	-482.824050	-76.792685
PH ₂ (gau)	-610.827988	-534.039334	-76.793577
SH (ecli)	-667.045539	-590.255957	-76.794627
Cl	-728.438200	-651.649591	-76.796122
Br	-2839.099632	-2762.311426	-76.796004
I	-7181.999715	-7105.211887	-76.795527
C≡CH	-345.207678	-268.419733	-76.795021
C≡N	-361.271660	-284.482176	-76.794885
<i>anti</i>			
CH ₃ (stag)	-308.573697	-231.787883	-76.793401
NH ₂ (gau)	-324.557926	-247.770792	-76.794546
OH (stag)	-344.387477	-267.598975	-76.795432
F	-368.385815	-291.596909	-76.795345
SiH ₃ (stag)	-559.619251	-482.834526	-76.791628
PH ₂ (stag)	-610.832205	-534.047075	-76.792712
SH (stag)	-667.046657	-590.260320	-76.793556
Cl	-728.439953	-651.652627	-76.794269
Br	-2839.104362	-2762.317529	-76.793719
I	-7182.007588	-7105.221476	-76.793194
C≡CH	-345.206921	-268.419116	-76.794065
C≡N	-361.271121	-284.482114	-76.794471

Table A.5 Total energies (Hartrees) for the *endo* addition TS's for the reaction of CpX and maleimide, evaluated at 6-31G(d)//6-31G(d).

X (conform.)	E _{Total} (TS)	E _{Total} (TS diene)	E _{Total} (TS dophile)
H	-550.149923	-192.755944	-357.386963
<i>syn</i>			
CH ₃ (stag)	-589.180758	-231.787146	-357.387859
NH ₂ (stag)	-605.169121	-247.770570	-357.389777
OH (gau)	-624.999144	-267.600714	-357.390137
F	-649.000714	-291.603281	-357.389849
SiH ₃ (stag)	-840.217042	-482.825405	-357.385688
PH ₂ (stag)	-891.433268	-534.040048	-357.386606
SH (gau)	-947.650818	-590.256425	-357.387782
Cl	-1009.045563	-651.651145	-357.388934
Br	-3119.706443	-2762.312722	-357.388635
I	-7462.604422	-7105.212749	-357.388078
C=CH	-625.817004	-268.421604	-357.388393
C=N	-641.876480	-284.483435	-357.387734
<i>anti</i>			
CH ₃ (stag)	-589.182560	-231.790258	-357.387073
NH ₂ (gau)	-605.165110	-247.772558	-357.387833
OH (stag)	-624.992561	-267.600450	-357.388769
F	-648.989664	-291.597866	-357.388682
SiH ₃ (stag)	-840.227983	-482.837225	-357.384880
PH ₂ (stag)	-891.439765	-534.049176	-357.385829
SH (stag)	-947.652492	-590.261906	-357.386672
Cl	-1009.043731	-651.653639	-357.387435
Br	-3119.707106	-2762.318305	-357.386738
I	-7462.610616	-7105.222135	-357.386138
C=CH	-625.813433	-268.421415	-357.387630
C=N	-641.873947	-284.484114	-357.387767

Table A.6 Total energies (Hartrees) for the *endo* addition TS's for the reaction of CpX and TAD, evaluated at 6-31G(d)//6-31G(d).

X (conform.)	E _{Total} (TS)	E _{Total} (TS diene)	E _{Total} (TS dphile)
H	-582.111259	-192.758789	-389.344334
<i>syn</i>			
CH ₃ (stag)	-621.145366	-231.792501	-389.345230
NH ₂ (gau)	-637.134063	-247.778911	-389.345567
OH (stag)	-656.964592	-267.607913	-389.345735
F	-680.953443	-291.604918	-389.346348
SiH ₃ (stag)	-872.183033	-482.831681	-389.344263
PH ₂ (gau)	-923.397802	-534.047105	-389.344990
SH (s'tag)	-979.613836	-590.263407	-389.345517
Cl	-1041.000461	-651.654661	-389.346264
Br	-3151.661539	-2762.316651	-389.346156
I	-7494.562171	-7105.217740	-389.345907
C≡CH	-657.773142	-268.424927	-389.345590
C≡N	-673.831760	-284.486467	-389.345772
<i>anti</i>			
CH ₃ (stag)	-621.144619	-231.793270	-389.344321
NH ₂ (gau)	-637.126199	-247.775393	-389.344930
OH (stag)	-656.951852	-267.602781	-389.345503
F	-680.949116	-291.599989	-389.345492
SiH ₃ (stag)	-872.189467	-482.839551	-389.343013
PH ₂ (gau)	-923.400554	-534.050666	-389.343567
SH (stag)	-979.613015	-590.264144	-389.344170
Cl	-1041.002860	-651.655313	-389.344630
Br	-3151.666039	-2762.319459	-389.344064
I	-7494.569216	-7105.222924	-389.343612
C≡CH	-657.774396	-268.424228	-389.344665
C≡N	-673.832950	-284.486246	-389.345057

Table A.7 Total energies (Hartrees) for the *exo* addition TS's for the reaction of CpX and maleimide, evaluated at 6-31G(d)//6-31G(d).

X (conform.)	E _{Total} (TS)	E _{Total} (diene)	E _{Total} (dophile)
H	-550.145268	-192.756140	-357.385151
<i>syn</i>			
F	-648.990675	-291.601854	-357.384591
Cl	-1009.028930	-651.647324	-357.381768
Br	-3119.676320	-2762.300210	-357.381762
<i>anti</i>			
F	-648.982218	-291.597933	-357.385696
Cl	-1009.037255	-651.653815	-357.384818
Br	-3119.689886	-2762.311284	-357.384898

Table A.8 Total energies (Hartrees) for the *exo* addition TS's for the reaction of CpX and TAD, evaluated at 6-31G(d)//6-31G(d).

X (conform.)	E _{Total} (TS)	E _{Total} (diene)	E _{Total} (dophile)
H	-582.093404	-192.754405	-389.342719
<i>syn</i>			
F	-680.938031	-291.599148	-389.343654
Cl	-1040.976380	-651.644789	-389.343239
Br	-3151.625624	-2762.297339	-389.342943
<i>anti</i>			
F	-680.925914	-291.595061	-389.343280
Cl	-1040.980832	-651.650366	-389.342531
Br	-3151.635334	-2762.307353	-389.342094

Table A.9 Total energies (Hartrees) for the TS's for the reaction of CpX and ethene, evaluated at 6-31++G(d)/6-31++G(d).

X (conform.)	E _{Total} (TS)	E _{Total} (TS diene)	E _{Total} (TS dophile)
H	-270.768122	-192.760879	-78.017772
<i>syn</i>			
NH ⁺ (stag)	-325.141927	-247.131991	-78.020202
NH ₂ (gau)	-325.790540	-247.782180	-78.018861
NH ₃ ⁺ (stag)	-326.156275	-248.143770	-78.016948
O ⁺	-345.017062	-267.003378	-78.021403
OH (stag)	-345.621586	-267.610218	-78.020811
OH ₂ ⁺ (gau)	-345.931079	-267.916661	-78.017094
F	-369.626413	-291.614700	-78.020759
PH ⁺ (stag)	-611.458881	-533.451764	-78.018918
PH ₂ (gau)	-612.053758	-534.046326	-78.018037
PH ₃ ⁺ (stag)	-612.398600	-534.388330	-78.016238
S ⁺	-667.711483	-589.701286	-78.020287
SH (stag)	-668.271862	-590.262306	-78.019012
SH ₂ ⁺ (gau)	-668.582275	-590.568875	-78.017581
Cl	-729.667203	-651.656694	-78.020264
<i>anti</i>			
NH ⁺ (stag)	-325.134458	-247.130192	-78.016935
NH ₂ (gau)	-325.787370	-247.781161	-78.018471
NH ₃ ⁺ (stag)	-326.162716	-248.147448	-78.019590
O ⁺	-345.000629	-266.995052	-78.018064
OH (stag)	-345.617234	-267.609586	-78.019088
OH ₂ ⁺			
F	-369.617876	-291.610328	-78.019021
PH ⁺ (stag)	-611.460765	-533.458896	-78.014134
PH ₂ (gau)	-612.059064	-534.054608	-78.017080
PH ₃ ⁺ (stag)	-612.412512	-534.398669	-78.018586
S ⁺	-667.706723	-589.704005	-78.015499
SH (stag)	-668.273094	-590.267640	-78.017722
SH ₂ ⁺ (gau)	-668.593685	-590.578610	-78.018894
Cl	-729.665454	-651.659136	-78.018337

Table A.10 Total energies (Hartrees) for GS dienophiles.

dienophile	6-31G(d)//6-31G(d) E_{Total}	6-31++G(d)//6-31++G(d) E_{Total}
ethene	-78.031719	-78.035902
ethyne	-76.817826	
maleimide	-357.407644	
TAD	-389.355711	

Table A.11 Total energies (Hartrees), for the products of the given reactions,evaluated at 6-31G(d)//6-31G(d).

Reaction	E_{Total} (<i>syn</i> product)	E_{Total} (<i>anti</i> product)
CpH + ethene	-270.861856	
CpF + ethene	-369.719306	-369.713792
CpCl + ethene	-729.767706	-729.764417
CpBr + ethene	-2840.429355	-2840.426353
CpI + ethene	-7183.328669	-7183.326931
CpH + maleimide	-550.240625	
CpCl + maleimide	-1009.143806	-1009.139660
CpH + TAD	-582.196728	
CpCl + TAD	-1041.093259	-1041.091965

Table A.12 Total energies (Hartrees) for CprX, evaluated at 6-31++G(d)//6-31++G(d).

X	E_{Total}
H	-115.826496
BH ₂ (ecli)	-141.079177
CH ₃ (stag)	-154.864463
NH ₂ (gau)	-170.855863
OH (stag)	-190.687648
F	-214.694330
SiH ₃ (stag)	-405.902267
PH ₂ (stag)	-457.120699
SH (gau)	-513.338964
Cl	-574.737199

Table A.13 Total energies (Hartrees) for the *endo* addition TS's for the reaction of CprX and Bdiene, evaluated at 6-31++G(d)/6-31++G(d).

X (conform.)	E _{Total} (TS)	E _{Total} (diene)	E _{Total} (dphile)
H	-270.695774	-154.892933	-115.807375
<i>syn</i>			
BH ₂ (stg)	-295.937681	-154.895420	-141.048839
CH ₃ (stag)	-309.719186	-154.889787	-154.838561
NH ₂ (stag)	-325.711083	-154.890123	-170.829201
OH (stag)	-345.543023	-154.887916	-190.662237
F	-369.549536	-154.888399	-214.666599
SiH ₃ (stag)	-560.759890	-154.892664	-405.875229
PH ₂ (stag)	-611.978034	-154.891067	-457.094578
SH (gau)	-668.195000	-154.890516	-513.310851
Cl	-729.592305	-154.889759	-574.707021
<i>anti</i>			
BH ₂ (ecli)	-295.949155	-154.893746	-141.059001
CH ₃ (stag)	-309.733428	-154.892820	-154.845513
NH ₂ (gau)	-325.722749	-154.891421	-170.837157
OH (gau)	-345.552325	-154.890389	-190.667829
F	-369.556811	-154.888929	-214.673046
SiH ₃ (stag)	-560.774718	-154.894388	-405.883330
PH ₂ (stag)	-611.991164	-154.893414	-457.101148
SH (gau)	-668.207858	-154.892215	-513.319437
Cl	-729.603744	-154.890539	-574.716835

Table A.14 Total energies (Hartrees) for the *exo* addition TS's for the reaction of CprX and Bdiene, evaluated at 6-31++G(d)//6-31++G(d).

X (conform.)	E _{Total} (TS)	E _{Total} (diene)	E _{Total} (dophile)
H	-270.692912	-154.893938	-115.806142
<i>syn</i>			
BH ₂ (ecli)	-295.940014	-154.894159	-141.053866
CH ₃ (stag)	-309.723065	-154.893636	-154.839332
NH ₂ (stag)	-325.720113	-154.894153	-170.830937
OH (gau)	-345.550202	-154.893060	-190.661831
F	-369.556169	-154.891770	-214.667714
SiH ₃ (stag)	-560.763035	-154.894453	-405.877168
PH ₂ (stag)	-611.982460	-154.893767	-457.095327
SH (gau)	-668.200634	-154.893646	-513.312079
Cl	-729.597878	-154.892661	-574.708263
<i>anti</i>			
BH ₂ (ecli)	-295.945110	-154.894066	-141.057683
CH ₃ (stag)	-309.731020	-154.894084	-154.844411
NH ₂ (gau)	-325.721960	-154.893503	-170.836065
OH (stag)	-345.552329	-154.892646	-190.666339
F	-369.557217	-154.891591	-214.671824
SiH ₃ (stag)	-560.770407	-154.894834	-405.882016
PH ₂ (stag)	-611.987669	-154.894270	-457.099849
SH (stag)	-668.205738	-154.893742	-513.318017
Cl	-729.602911	-154.892687	-574.715462

Table A.15 Bond lengths (Å) for CpX, evaluated at 6-31G(d)//6-31G(d).

X (conform.)	C ₂ -C ₃	C ₁ -C ₂ C ₃ -C ₄	C ₁ -C ₅ C ₄ -C ₅	C ₃ -H ₃	C ₅ -X
H	1.4764	1.3285	1.5064	1.0890	1.0890
BH ₂ (gau)	1.4606	1.3355 1.3380	1.4940 1.5100	1.0856	1.5869
CH ₃ (stag)	1.4771	1.3277	1.5101	1.0911	1.5346
NH ₂ (gau)	1.4826	1.3256 1.3259	1.5118 1.5187	1.0897	1.4558
OH (stag)	1.4862	1.3248	1.5158	1.0864	1.4014
F	1.4877	1.3235	1.5093	1.0865	1.3694
SiH ₃ (stag)	1.4647	1.3345	1.4995	1.0891	1.9084
PH ₂ (gau)	1.4729	1.3296 1.3297	1.5072 1.5031	1.0891	1.8776
SH (stag)	1.4797	1.3267	1.5078	1.0867	1.8300
Cl	1.4828	1.3247	1.5062	1.0822	1.8027
GeH ₃ (stag)	1.4648	1.3351	1.4956	1.0867	1.9922
AsH ₂ (stag)	1.4687	1.3326	1.4982	1.0831	2.0052
SeH (stag)	1.4781	1.3279	1.5030	1.0851	1.9784
Br	1.4815	1.3257	1.5022	1.0797	1.9755
SnH ₃ (stag)	1.4576	1.3403	1.4872	1.0848	2.2134
SbH ₂ (stag)	1.4620	1.3372	1.4909	1.0825	2.2158
TeH (gau)	1.4708	1.3310 1.3312	1.4959 1.5001	1.0817	2.1987
I	1.4780	1.3276	1.4992	1.0794	2.2004
CH=CH ₂ (ecli)	1.4772	1.3276	1.5138	1.0894	1.5099
C≡CH	1.4776	1.3258	1.5150	1.0904	1.4732
C≡N	1.4776	1.3254	1.5150	1.0885	1.4743
CF ₃ (stag)	1.4780	1.3261	1.5107	1.0882	1.5105
NO ₂ (stag)	1.4839	1.3241	1.5087	1.0866	1.4936

Table A.16 Angles (degrees) for CpX, evaluated at 6-31G(d)//6-31G(d).

X (conform.)	C ₁ -C ₂ -C ₃ C ₂ -C ₃ -C ₄	C ₂ -C ₁ -C ₅ C ₃ -C ₄ -C ₅	C ₁ -C ₅ -C ₄	C ₁ -C ₅ -H ₅ C ₄ -C ₅ -H ₅	C ₁ -C ₅ -X C ₄ -C ₅ -X	H ₅ -C ₅ -X
H	109.1726	109.5942	102.4664	111.9416	111.9416	106.7240
BH ₂ (gau)	108.8869 109.4677	110.0627 109.0760	102.2650	115.1715 113.9355	112.7409 97.7673	113.1625
CH ₃ (stag)	109.0419	110.0683	101.7794	109.3628	113.8116	108.4994
NH ₂ (gau)	109.1689 109.1127	110.0238 109.8380	101.8127	108.4799 108.6322	112.5412 117.9449	107.0842
OH (stag)	109.2344	109.6225	102.1893	109.2081	115.3949	105.3419
F	109.3073	109.0333	103.0244	110.0675	113.4214	106.8462
SiH ₃ (stag)	109.1073	109.5810	102.4696	113.3515	109.9432	107.7166
PH ₂ (gau)	109.2116 109.0831	109.5725 109.7719	102.3460	111.0626 111.5021	110.9252 115.4857	105.6434
SH (stag)	109.2479	109.4200	102.6571	110.7112	114.6513	103.6543
Cl	109.3423	109.0232	103.1733	111.5658	112.7822	105.1783
GeH ₃ (stag)	109.0615	109.4991	102.7447	114.1400	109.6427	106.4899
AsH ₂ (stag)	109.0788	109.5480	102.6835	113.8351	109.1520	108.0098
SeH (stag)	109.2271	109.2657	103.0129	112.0566	113.6790	102.7086
Br	109.3381	108.8808	103.5076	113.0740	111.8094	103.8394
SnH ₃ (stag)	109.0302	109.2505	103.2410	116.2222	106.9303	106.6573
SbH ₂ (stag)	109.0585	109.3162	103.1114	115.6586	107.6070	106.7476
TeH (gau)	109.1123 109.2833	109.3733 109.1292	103.0930	114.1814 113.6857	112.2233 108.4552	105.2674
I	109.3347	108.8309	103.6515	113.9585	111.3566	102.8253
CH=CH ₂ (ecli)	109.1407	110.0114	101.6957	110.0088	112.9763	108.9966
C=CH	109.3704	109.5405	102.1380	109.2206	114.0308	108.0112
C=N	109.5465	109.1408	102.5851	110.3636	113.1299	107.2744
CF ₃ (stag)	109.4106	109.2254	102.6844	110.4419	113.7500	105.8597
NO ₂ (stag)	109.6567	108.3291	103.8154	111.0387	113.9289	103.3090

Table A.17 Bond lengths (Å) for CpX, evaluated at 6-31++G(d)//6-31++G(d).

X (conform.)	C ₂ -C ₃	C ₁ -C ₂ C ₃ -C ₄	C ₁ -C ₃ C ₄ -C ₅	C ₃ -H ₃	C ₅ -X
H	1.4760	1.3320	1.5064	1.0889	1.0889
NH ⁺ (stag)	1.4827	1.3343	1.5303	1.1012	1.4331
NH ₂ (gau)	1.4824	1.3291 1.3289	1.5188 1.5121	1.0896	1.4547
NH ₃ ⁺ (stag)	1.4861	1.3273	1.5102	1.0833	1.5197
O ⁻	1.4829	1.3333	1.5364	1.1289	1.3255
OH (stag)	1.4861	1.3280	1.5157	1.0861	1.4015
OH ₂ ⁺ (gau)	1.4955	1.3264 1.3262	1.5023 1.5016	1.0782	1.5575
F	1.4881	1.3263	1.5095	1.0856	1.3739
PH ⁺ (stag)	1.4722	1.3387	1.4988	1.0910	1.9316
PH ₂ (gau)	1.4728	1.3330 1.3329	1.5034 1.5071	1.0893	1.8774
PH ₃ ⁺ (stag)	1.4731	1.3322	1.5132	1.0868	1.8218
S ⁻	1.4764	1.3350	1.5055	1.0912	1.8445
SH (stag)	1.4795	1.3299	1.5082	1.0870	1.8281
SH ₂ ⁺ (gau)	1.4829	1.3288 1.3285	1.5064 1.5115	1.0840	1.8642
Cl	1.4827	1.3276	1.5066	1.0822	1.8010

Table A.18 Angles (degrees) for CpX, evaluated at 6-31++G(d)//6-31++G(d).

X (conform.)	C ₁ -C ₂ -C ₃ C ₂ -C ₃ -C ₄	C ₂ -C ₁ -C ₃ C ₃ -C ₄ -C ₅	C ₁ -C ₃ -C ₄	C ₁ -C ₃ -H ₅ C ₄ -C ₃ -H ₅	C ₁ -C ₃ -X C ₄ -C ₃ -X	H ₃ -C ₃ -X
H	109.1489	109.5973	102.5076	111.8965	111.8965	106.8523
NH ⁺ (stag)	108.6463	111.5965	99.5015	105.1214	119.1462	107.2668
NH ₂ (gau)	109.0876 109.1660	109.8266 109.9964	101.8671	108.5289 108.3408	117.9540 112.6815	107.1004
NH ₃ ⁺ (stag)	109.6020	108.4709	103.7838	113.0919	110.4926	105.9819
O ⁺	108.8247	111.3992	99.3961	101.9951	118.6863	113.3458
OH (stag)	109.2247	109.5726	102.2889	109.1926	115.4258	105.2125
OH ₂ ⁺ (gau)	109.6630 109.6860	107.5532 107.5735	105.3414	116.5890 115.7837	110.7733 107.0683	100.9429
F	109.3161	108.9522	103.1695	110.5091	113.1166	106.4903
PH ⁺ (stag)	108.5688	110.5580	101.7082	110.4765	116.0983	102.1750
PH ₂ (gau)	109.0491 109.1774	109.7915 109.6001	102.3706	111.3269 110.9265	115.6242 111.1038	105.6062
PH ₃ ⁺ (stag)	109.7422	108.6117	103.2868	114.0906	108.3122	108.4517
S ⁺	108.6340	110.6771	101.3734	108.5524	115.1572	107.7124
SH (stag)	109.2222	109.4389	102.6667	110.4955	114.8299	103.6861
SH ₂ ⁺ (gau)	109.7504 109.7567	108.2110 108.0695	104.1784	114.7772 114.1564	112.4628 107.5307	103.7480
Cl	109.3251	109.0204	103.2009	111.4053	112.9011	105.2234

Table A.19 Bond lengths (Å) for the *syn* TS structure for the reaction of CpX and ethene, evaluated at 6-31G(d)//6-31G(d).

X (conform.)	C ₂ -C ₃	C ₁ -C ₂ C ₃ -C ₄	C ₁ -C ₅ C ₄ -C ₅	C ₅ -H ₅	C ₅ -X	C ₁ -C ₆ C ₄ -C ₇	C ₆ -C ₇
H	1.3919	1.3894	1.5060	1.0915	1.0805	2.1935	1.3824
BH ₂ (stag)	1.3887	1.3920	1.5092	1.1035	1.5716	2.1917	1.3850
CH ₃ (stag)	1.3908	1.3901	1.5099	1.0940	1.5235	2.2104	1.3802
NH ₂ (gau)	1.3935	1.3880 1.3873	1.5176 1.5078	1.0911	1.4423	2.2095 2.2103	1.3800
OH (gau)	1.3967	1.3852 1.3847	1.5125 1.5036	1.0934	1.3936	2.2064 2.2131	1.3772
F	1.3982	1.3841	1.5029	1.0876	1.3622	2.2081	1.3779
SiH ₂ (stag)	1.3874	1.3926	1.5109	1.0974	1.8950	2.2054	1.3826
PH ₂ (stag)	1.3893	1.3911	1.5098	1.0903	1.8677	2.2125	1.3809
SH (gau)	1.3927	1.3893 1.3877	1.5098 1.5063	1.0873	1.8215	2.1958 2.2273	1.3802
Cl	1.3956	1.3866	1.5040	1.0838	1.7881	2.2170	1.3781
GeH ₂ (stag)	1.3881	1.3926	1.5085	1.0945	1.9722	2.2053	1.3822
AsH ₂ (stag)	1.3891	1.3918	1.5074	1.0884	1.9843	2.2101	1.3813
SeH (ecli)	1.3923	1.3893	1.5062	1.0854	1.9667	2.2079	1.3812
Br	1.3953	1.3874	1.5026	1.0820	1.9566	2.2174	1.3784
SnH ₂ (stag)	1.3872	1.3936	1.5079	1.0943	2.1865	2.2049	1.3827
SbH ₂ (stag)	1.3880	1.3931	1.5068	1.0894	2.1906	2.2091	1.3819
TeH (ecli)	1.3911	1.3907	1.5060	1.0865	2.1758	2.2076	1.3817
I	1.3941	1.3886	1.5032	1.0821	2.1771	2.2181	1.3788
CH=CH ₂ (ecli)	1.3908	1.3893	1.5131	1.0920	1.5031	2.2099	1.3805
C≡CH	1.3922	1.3878	1.5125	1.0919	1.4677	2.2060	1.3804
C≡N	1.3924	1.3873	1.5113	1.0900	1.4691	2.2101	1.3810
CF ₃ (stag)	1.3915	1.3896	1.5071	1.0906	1.5111	2.2212	1.3801
NO ₂ (stag)	1.3949	1.3872	1.5012	1.0880	1.4840	2.2099	1.3812

Table A.20 Angles (degrees) for the diene portion of the *syn* TS structure for the reaction of CpX and ethene, evaluated at 6-31G(d)//6-31G(d).

X (conform.)	C ₁ -C ₂ -C ₃ C ₂ -C ₃ -C ₄	C ₂ -C ₁ -C ₅ C ₃ -C ₄ -C ₅	C ₁ -C ₅ -C ₄	C ₁ -C ₃ -H ₅ C ₄ -C ₅ -H ₅	C ₁ -C ₅ -X C ₄ -C ₅ -X	H ₅ -C ₅ -X
H	108.9615	106.3701	99.2598	108.3266	115.9877	108.3884
BH ₂ (stag)	108.9112	106.8809	98.7604	105.6451	120.9201	103.4121
CH ₃ (stag)	108.9018	106.2921	98.7138	104.0745	120.7363	106.3875
NH ₂ (gau)	109.0151 109.0463	105.8365 106.2118	98.8806	104.9080 104.5771	123.0252 117.6637	105.9224
OH (gau)	109.0115 109.1389	105.5187 105.7943	99.4967	106.2549 106.0225	119.4803 115.1133	109.2646
F	109.1967	104.9927	100.3456	108.4227	116.4248	106.4201
SiH ₃ (stag)	108.9348	106.4855	98.6215	104.4797	122.0636	102.9341
PH ₂ (stag)	108.9660	105.9846	98.8444	105.2088	119.4035	107.2110
SH (gau)	109.0448 109.1437	105.2673 105.4979	99.4515	106.2820 105.8205	120.8393 117.1300	106.0879
Cl	109.2310	104.4465	100.2828	107.2862	118.5867	104.0815
GeH ₃ (stag)	108.9278	106.3158	98.8492	105.0411	121.6648	102.6765
AsH ₂ (stag)	108.9512	105.9206	99.0407	105.8890	119.4179	105.8900
SeH (ecli)	109.0977	105.2770	99.6331	106.8219	119.0438	104.5526
Br	109.2519	104.2012	100.4771	107.8624	118.7654	102.5444
SnH ₃ (stag)	108.9011	106.4029	98.8108	105.1748	121.4560	102.9606
SbH ₂ (stag)	108.9313	106.0275	99.0181	105.8216	120.3217	104.1402
TeH (ecli)	109.0831	105.3224	99.5981	106.7533	119.8552	103.0108
I	109.2596	104.1740	100.4245	107.5965	119.5670	101.3599
CH=CH ₂ (ecli)	108.9674	106.1796	98.5855	104.6018	120.1223	106.9537
C=CH	109.1231	105.7087	99.0698	105.5795	119.1213	106.9738
C=N	109.2593	105.1880	99.5427	106.8989	118.0055	106.6112
CF ₃ (stag)	109.2096	104.8644	99.8149	104.9202	121.6174	101.9450
NO ₂ (stag)	109.4143	104.0238	101.0205	108.5491	117.8224	102.7683

Table A.21 Dienophile angles and angles of approach (degrees) for the *syn* TS for the reaction of CpX and ethene, evaluated at 6-31G(d)/6-31G(d).

X (conform.)	C ₂ -C ₁ -C ₆ C ₃ -C ₄ -C ₇	C ₅ -C ₁ -C ₆ C ₅ -C ₄ -C ₇	C ₇ -C ₆ -H _{6x} C ₆ -C ₇ -H _{7x}	C ₇ -C ₆ -H _{6en} C ₆ -C ₇ -H _{7n}	H _{6n} -C ₆ -H _{6x} H _{7n} -C ₇ -H _{7x}
H	100.6303	89.9456	119.7248	120.1623	114.6903
BH ₂ (stag)	99.3833	90.4850	119.8354	120.1109	114.1864
CH ₃ (stag)	98.7219	92.1351	120.2615	120.0402	114.4897
NH ₂ (gau)	99.5516 99.5821	91.6218 91.4762	120.4283 120.5085	120.1600 120.0879	114.1837
OH (gau)	101.5319 101.1847	90.3117 90.2057	119.4558 119.6268	120.3415 120.2501	115.5723
F	102.0664	89.8690	119.6292	120.3090	115.5434
SiH ₃ (stag)	98.1542	92.1940	119.8425	120.0574	114.3612
PH ₂ (stag)	98.5299	92.5663	119.5565	120.1831	114.8548
SH (gau)	99.5866 99.3467	92.7054 91.4609	119.6811 119.8654	120.0157 120.3571	115.2191
Cl	100.0032	92.2418	119.8597	120.1782	115.2823
GeH ₃ (stag)	98.2390	92.2313	119.9202	120.0399	114.4056
AsH ₂ (stag)	98.4398	92.5787	119.6830	120.1471	114.6661
SeH (ecli)	99.3071	92.1920	120.0594	120.1234	114.6369
Br	99.6534	92.6645	119.9083	120.1317	115.2224
SnH ₃ (stag)	97.9756	92.3599	119.8942	120.0306	114.2019
SbH ₂ (stag)	98.0184	92.7437	119.7738	120.1097	114.3703
TeH (ecli)	98.8127	92.5164	120.2207	120.0591	114.3333
I	99.0659	93.1367	119.9641	120.1009	115.0383
CH=CH ₂ (ecli)	98.8727	92.2041	120.3093	120.0464	114.4357
C≡CH	100.0661	91.3764	119.6155	120.1879	115.2437
C≡N	100.3242	91.3839	119.6163	120.1756	115.1009
CF ₃ (stag)	98.1750	93.2822	120.0826	119.9475	114.9389
NO ₂ (stag)	100.5673	91.4906	120.0677	120.0798	114.9613

Table A.22 Bond lengths (Å) for the *anti* TS structure for the reaction of CpX and ethene, evaluated at 6-31G(d)//6-31G(d).

X (conform.)	C ₂ -C ₃	C ₁ -C ₂ C ₃ -C ₄	C ₁ -C ₅ C ₄ -C ₅	C ₅ -H ₅	C ₅ -X	C ₁ -C ₆ C ₄ -C ₇	C ₆ -C ₇
BH ₂ (gau)	1.3809	1.3991 1.4031	1.5009 1.5112	1.0811	1.5910	2.1743 2.1767	1.3852
CH ₃ (stag)	1.3931	1.3875	1.5142	1.0813	1.5410	2.1931	1.3829
NH ₂ (gau)	1.3999	1.3824 1.3828	1.5261 1.518	1.0792	1.4619	2.1989 2.1965	1.3816
OH (stag)	1.4044	1.3801	1.5231	1.0764	1.4064	2.2005	1.3807
F	1.4026	1.3778	1.5159	1.0765	1.3783	2.2063	1.3813
SiH ₃ (stag)	1.3830	1.3992	1.5018	1.0834	1.9144	2.1762	1.3859
PH ₂ (stag)	1.3865	1.3935	1.5061	1.0783	1.8883	2.1868	1.3844
SH (stag)	1.3951	1.3860	1.5110	1.0777	1.8426	2.1953	1.3838
Cl	1.3964	1.3823	1.5093	1.0726	1.8228	2.2038	1.3835
GeH ₃ (stag)	1.3827	1.3994	1.4985	1.0811	1.9958	2.1771	1.3865
AsH ₂ (stag)	1.3850	1.3960	1.5004	1.0768	2.0102	2.1834	1.3856
SeH (gau)	1.3897	1.3885 1.3906	1.5038 1.5055	1.0743	1.9963	2.1988 2.1883	1.3850
Br	1.3939	1.3846	1.5041	1.0711	1.9997	2.2023	1.3849
SnH ₃ (stag)	1.3795	1.4043	1.4928	1.0805	2.2124	2.1699	1.3878
SbH ₂ (stag)	1.3815	1.4011	1.4947	1.0773	2.2170	2.1766	1.3869
TeH (gau)	1.3868	1.392 1.3946	1.4981 1.5014	1.0747	2.2105	2.1987 2.1808	1.3859
I	1.3908	1.3878	1.5002	1.0711	2.2267	2.1996	1.3860
CH=CH ₂ (ecli)	1.3926	1.3883	1.5160	1.0802	1.5150	2.1926	1.3826
C≡CH	1.3934	1.3853	1.5183	1.0800	1.4799	2.2002	1.3820
C≡N	1.3938	1.3853	1.5169	1.0790	1.4822	2.2021	1.3817
CF ₃ (stag)	1.3929	1.3868	1.5127	1.0795	1.5212	2.1927	1.3836
NO ₂ (stag)	1.3998	1.3804	1.5124	1.0778	1.5081	2.2067	1.3825

Table A.23 Angles (degrees) for the diene portion of the *anti* TS structure for the reaction of CpX and ethene, evaluated at 6-31G(d)//6-31G(d).

X (conform.)	C ₁ -C ₂ -C ₃ C ₂ -C ₃ -C ₄	C ₂ -C ₁ -C ₃ C ₃ -C ₄ -C ₅	C ₁ -C ₃ -C ₄	C ₁ -C ₃ -H ₅ C ₂ -C ₃ -H ₅	C ₁ -C ₃ -X C ₂ -C ₃ -X	H ₃ -C ₃ -X
BH ₂ (gau)	108.6643 108.8554	106.9836 106.2533	98.5166	115.0237 114.1094	113.9074 102.6345	111.3862
CH ₃ (stag)	108.8445	106.9774	98.2232	113.1502	112.3149	107.6330
NH ₂ (gau)	108.8642 109.0825	106.8953 106.9959	98.0910	113.1790 113.4355	115.4586 110.4388	106.3310
OH (stag)	109.0788	106.7375	98.4377	114.2993	112.7682	104.6147
F	109.2355	106.5861	99.2969	115.5844	110.2127	105.9167
SiH ₃ (stag)	108.7415	106.5847	98.8924	114.4403	111.3195	106.4778
PH ₂ (stag)	108.8575	106.8101	98.8124	114.6106	109.8325	108.7811
SH (stag)	109.0471	106.8085	99.1096	114.4324	113.6022	102.2761
Cl	109.2314	106.8138	99.6820	115.9547	110.8929	103.6911
GeH ₃ (stag)	108.7421	106.6286	99.1793	115.0069	110.9558	105.8158
AsH ₂ (stag)	108.8135	106.7413	99.2080	115.5046	109.2962	107.7054
SeH (gau)	108.9660 109.0718	107.0138 106.7163	99.4140	115.8800 115.4171	112.3858 108.3803	105.3599
Br	109.2389	106.7985	100.1170	116.8558	110.4661	102.2803
SnH ₃ (stag)	108.6637	106.5995	99.4788	115.7384	109.4596	106.7516
SbH ₂ (stag)	108.7361	106.7011	99.5027	116.0748	108.9616	106.9403
TeH (gau)	108.9451 108.9893	107.0062 106.6519	99.6922	116.3036 115.9082	112.1674 108.3231	104.4823
I	109.2120	106.8251	100.3371	117.1818	110.4530	101.4437
CH=CH ₂ (ecli)	108.9150	106.8407	98.2537	113.7812	111.2716	108.2905
C≡CH	109.1350	106.7221	98.5663	113.7796	111.5343	107.5779
C≡N	109.2619	106.3855	99.0504	114.7826	110.6096	106.9380
CF ₃ (stag)	109.1272	106.5586	99.0620	114.1742	112.9917	103.8796
NO ₂ (stag)	109.4316	106.1465	100.0691	116.0163	111.3021	102.4892

Table A.24 Dienophile angles and angles of approach (degrees) for the *anti* TS for the reaction of CpX and ethene, evaluated at 6-31G(d)//6-31G(d).

X (conform.)	C ₂ -C ₁ -C ₆ C ₂ -C ₄ -C ₇	C ₅ -C ₁ -C ₆ C ₅ -C ₄ -C ₇	C ₇ -C ₆ -H _{6x} C ₆ -C ₇ -H _{7x}	C ₇ -C ₆ -H _{6n} C ₆ -C ₇ -H _{7n}	H _{6n} -C ₆ -H _{6x} H _{7n} -C ₇ -H _{7x}
BH ₂ (gau)	99.7701 100.0324	91.2653 91.1325	119.5164 119.6707	119.9811 120.0189	114.5312 114.6105
CH ₃ (stag)	100.2993	90.3486	119.7714	120.1186	114.6607
NH ₂ (gau)	101.1606 100.8878	89.5112 89.8163	119.7940 119.8767	120.2119 120.1586	114.7731 114.7925
OH (stag)	101.7387	88.9135	119.8734	120.2366	114.8900
F	102.3929	87.5512	119.8655	120.2593	114.8743
SiH ₃ (stag)	99.5871	91.1626	119.5849	119.9966	114.5016
PH ₂ (stag)	100.2802	90.0852	119.6907	120.0767	114.6262
SH (stag)	100.5304	89.0947	119.7739	120.1392	114.6918
Cl	101.4671	87.3817	119.8016	120.1993	114.7983
GeH ₃ (stag)	99.5084	90.8639	119.5434	119.9947	114.5044
AsH ₂ (stag)	100.0597	90.0819	119.6002	120.0613	114.6127
SeH (gau)	100.4186 100.7414	88.5647 88.9428	119.6789 119.6798	120.1599 120.0887	114.6850 114.6922
Br	101.2443	87.0936	119.7233	120.1875	114.7829
SnH ₃ (stag)	99.0932	91.0836	119.4494	119.9414	114.4587
SbH ₂ (stag)	99.5757	90.3767	119.5129	120.0034	114.5640
TeH (gau)	99.8631 100.4157	88.6649 89.2779	119.6639 119.5835	120.1558 120.0398	114.6648 114.6437
I	100.8307	87.1656	119.6701	120.1637	114.7519
CH=CH ₂ (ecli)	100.5622	90.2064	119.7812	120.1359	114.6923
C≡CH	100.7873	89.4408	119.7950	120.1734	114.7207
C≡N	101.3025	88.9201	119.8086	120.1983	114.7783
CF ₃ (stag)	100.9551	89.1383	119.7669	120.1307	114.6826
NO ₂ (stag)	101.9079	87.4708	119.8324	120.2470	114.8257

Table A.25 Bond lengths (Å) for the TS structures for the reaction of CpX and ethene, evaluated at 6-31++G(d)/6-31++G(d).

X	C ₂ -C ₃	C ₁ -C ₂ C ₃ -C ₄	C ₁ -C ₅ C ₄ -C ₅	C ₅ -H ₅	C ₃ -X	C ₁ -C ₆ C ₄ -C ₇	C ₆ -C ₇
H	1.3928	1.3926	1.5067	1.0806	1.0917	2.1892	1.3865
<i>syn</i>							
NH ⁺	1.3965	1.3927	1.5421	1.1018	1.4069	2.1850	1.3857
NH ₂	1.3945	1.3910	1.5178	1.0910	1.4423	2.2069	1.3839
		1.3905	1.5085			2.2048	
NH ₃ ⁺	1.3943	1.3901	1.5039	1.0855	1.5047	2.2306	1.3841
O ⁺	1.3978	1.3913	1.5440	1.1215	1.3131	2.1760	1.3843
OH	1.3977	1.3884	1.5130	1.0923	1.3952	2.2019	1.3813
		1.3877	1.5043			2.2091	
OH ₂ ⁺	1.3983	1.3895	1.4964	1.0805	1.5252	2.2297	1.3844
		1.3890	1.4937			2.2297	
F	1.3993	1.3871	1.5031	1.0867	1.3666	2.2070	1.3813
PH ⁺	1.3917	1.3978	1.5151	1.0973	1.8935	2.1823	1.3877
PH ₂	1.3901	1.3943	1.5103	1.0907	1.8670	2.2081	1.3847
PH ₃ ⁺	1.3908	1.3915	1.5131	1.0924	1.8179	2.2244	1.3852
S ⁺	1.3934	1.3962	1.5147	1.0941	1.8182	2.1835	1.3855
SH	1.3937	1.3922	1.5104	1.0876	1.8204	2.1916	1.3840
		1.3906	1.5072			2.2218	
SH ₂ ⁺	1.3943	1.3900	1.5065	1.0843	1.8527	2.2336	1.3833
Cl	1.3964	1.3895	1.5046	1.0840	1.7870	2.2132	1.3817
<i>anti</i>							
NH ⁺	1.3999	1.3878	1.5473	1.0848	1.4285	2.1829	1.3912
NH ₂	1.4014	1.3848	1.5266	1.0790	1.4616	2.1968	1.3856
		1.3853	1.5188			2.1909	
NH ₃ ⁺	1.4043	1.3847	1.5122	1.0758	1.5389	2.2119	1.3840
O ⁺	1.4015	1.3832	1.5597	1.1015	1.3257	2.1952	1.3890
OH	1.4052	1.3826	1.5235	1.0759	1.4074	2.1970	1.3846
F	1.4035	1.3804	1.5159	1.0757	1.3842	2.2038	1.3853
PH ⁺	1.3845	1.4006	1.5027	1.0820	1.9345	2.1725	1.3967
PH ₂	1.3875	1.3959	1.5068	1.0785	1.8888	2.1827	1.3883
PH ₃ ⁺	1.3930	1.3946	1.5118	1.0805	1.8412	2.1974	1.3855
S ⁺	1.3875	1.3945	1.5108	1.0783	1.8528	2.1846	1.3942
SH	1.3960	1.3885	1.5117	1.0779	1.8411	2.1923	1.3876
SH ₂ ⁺	1.3964	1.3892	1.5049	1.0745	1.9103	2.2080	1.3868
Cl	1.3973	1.3846	1.5101	1.0725	1.8215	2.2013	1.3869

Table A.26 Angles (degrees) for the diene portion for the TS structures for the reaction of CpX and ethene, evaluated at 6-31++G(d)/6-31++G(d).

X	C ₁ -C ₂ -C ₃ C ₂ -C ₃ -C ₄	C ₂ -C ₁ -C ₅ C ₃ -C ₄ -C ₅	C ₁ -C ₃ -C ₄	C ₁ -C ₃ -H ₅ C ₂ -C ₃ -H ₅	C ₁ -C ₃ -X C ₂ -C ₃ -X	H ₅ -C ₃ -X
H	108.9227	106.3977	99.2706	108.3778	115.9359	108.3908
<i>syn</i>						
NH ⁻	108.6921	108.2007	95.8446	101.0637	124.0723	106.6392
NH ₂	108.9587	105.8314	98.9153	105.0280	122.7412	105.9176
	109.0284	106.1579		104.6476	117.7795	
NH ₃ ⁻	109.4557	103.5928	100.9646	109.0042	116.5070	104.6806
O ⁻	108.7720	108.3620	95.9130	100.9477	121.0770	113.1015
OH	108.9813	105.4704	99.5423	106.4853	119.1922	109.1716
	109.1058	105.7480		106.1603	115.1475	
OH ₂ ⁻	109.6248	102.1194	102.5028	112.9220	116.2702	100.7273
	109.6471	102.2470		112.9449	111.9081	
F	109.1775	104.8384	100.4621	108.6537	116.3637	106.0373
PH ⁻	108.5505	107.5183	97.6628	102.7882	124.6995	100.4921
PH ₂	108.9229	106.0115	98.8548	105.2547	119.3758	107.1835
PH ₃ ⁻	109.5291	104.1070	100.1693	107.7071	118.5683	103.5229
S ⁻	108.5564	107.2397	97.7574	103.0140	121.9128	106.4809
SH	109.0064	105.3191	99.4391	106.3475	120.6185	106.0954
	109.0938	105.5366		105.9133	117.2326	
SH ₂ ⁻	109.5852	103.0217	101.0750	110.1503	115.1242	105.2645
Cl	109.1907	104.4754	100.2777	107.3549	118.5103	104.1281
<i>anti</i>						
NH ⁻	108.6956	108.4194	95.4378	110.1723	117.1258	106.4991
NH ₂	108.8206	107.0073	98.1140	113.1121	115.5246	106.1615
	109.0548	107.0737		113.3558	110.6941	
NH ₃ ⁻	109.3146	106.0381	100.2045	117.2449	108.4715	104.8605
O ⁻	108.9511	108.3881	95.0065	108.3881	114.7235	112.4675
OH	109.0594	106.8335	98.4925	114.2901	112.9227	104.3110
F	109.2401	106.6312	99.4552	115.8189	110.2383	105.2894
PH ⁻	108.4716	107.5868	98.2173	112.7042	116.3322	101.2144
PH ₂	108.8197	106.8478	98.7970	114.4853	110.1318	108.5138
PH ₃ ⁻	109.2796	106.0032	99.8625	116.7684	108.1987	106.5747
S ⁻	108.6135	107.9504	97.8427	112.3264	113.9920	106.4528
SH	109.0125	106.8560	99.0946	114.3084	113.7863	102.1851
SH ₂ ⁻	109.4652	106.0628	100.9929	119.0609	105.6320	105.1569
Cl	109.1988	106.8699	99.6639	115.8581	111.0713	103.5807

Table A.27 Dienophile angles and angles of approach (degrees) for the TS's for the reaction of CpX and ethene, evaluated at 6-31++G(d)/6-31++G(d).

X	C ₂ -C ₁ -C ₆ C ₃ -C ₄ -C ₇	C ₂ -C ₁ -C ₆ C ₃ -C ₄ -C ₇	C ₇ -C ₆ -H _{6a} C ₆ -C ₇ -H _{7a}	C ₇ -C ₆ -H _{6b} C ₆ -C ₇ -H _{7b}	H _{6a} -C ₆ -H _{6b} H _{7a} -C ₇ -H _{7b}
H	100.5606	90.0216	120.1148	119.6721	114.7689
<i>syn</i>					
NH ⁺	99.2978	91.3628	120.0669	120.0005	115.4093
NH ₂	99.3742	91.7979	120.0982	120.4438	114.2300
	99.5732	91.6313	120.0378	120.4592	114.5474
NH ₃ ⁺	99.7916	92.8182	120.2310	120.6544	113.3557
O ⁺	101.3685	89.2459	120.3453	118.6138	116.9391
OH	101.3892	90.5283	120.2762	119.3977	115.6954
	101.1342	90.3426	120.2328	119.5442	115.8373
OH ₂ ⁺	100.7905	92.7003	120.2965	120.7774	113.2191
	100.6666	92.7091	120.2245	120.9353	113.2351
F	101.8043	90.2598	120.2663	119.6068	115.6046
PH ⁺	97.8216	92.2555	119.9535	119.6258	115.4752
PH ₂	98.4531	92.6534	120.1381	119.5067	114.9168
PH ₃ ⁺	98.9892	93.0330	120.0573	120.4885	113.4444
S ⁺	98.7894	91.9823	120.1873	118.8258	116.4785
SH	99.5213	92.7396	119.9753	119.6625	115.2357
	99.3234	91.5355	120.3081	119.8612	114.7985
SH ₂ ⁺	99.8202	93.3427	120.2432	119.9597	114.1621
Cl	99.9076	92.3473	120.1499	119.7870	115.3669
<i>anti</i>					
NH ⁺	99.4150	91.3199	119.9577	119.8017	114.7135
NH ₂	101.0181	89.4201	120.1869	119.7699	114.8409
	100.8497	89.7899	120.1180	119.8221	114.8492
NH ₃ ⁺	102.9086	87.1387	120.2705	119.7610	115.1270
O ⁺	99.9034	90.8563	120.0307	119.9027	114.8724
OH	101.6371	88.7924	120.1969	119.8338	114.9591
F	102.3202	87.3363	120.2392	119.8128	114.9467
PH ⁺	98.0597	91.7575	119.8265	119.5135	114.3261
PH ₂	100.2142	90.1676	120.0463	119.6308	114.6986
PH ₃ ⁺	101.7246	88.4654	120.1547	119.6556	115.0151
S ⁺	98.5605	90.7533	119.9307	119.6379	114.5016
SH	100.4124	89.1890	120.1164	119.7214	114.7594
SH ₂ ⁺	103.0607	85.8019	120.2336	119.6475	115.1377
Cl	101.3499	87.4557	120.1904	119.7506	114.8702

Table A.28 Bond lengths (Å) for the TS structures for the reaction of CpX and ethyne, evaluated at 6-31G(d)//6-31G(d).

X	C ₂ -C ₃	C ₁ -C ₂ C ₃ -C ₄	C ₁ -C ₅ C ₄ -C ₅	C ₅ -H ₅	C ₅ -X	C ₁ -C ₆ C ₄ -C ₇	C ₆ -C ₇
H	1.3929	1.3878	1.5071	1.0918	1.0782	2.1874	1.2256
<i>syn</i>							
CH ₃	1.3919	1.3884	1.5111	1.0938	1.5230	2.1996	1.2244
NH ₂	1.3947	1.3861 1.3851	1.5195 1.5084	1.0910	1.4399	2.1911 2.2087	1.2249
OH	1.3962	1.3843	1.5127	1.0879	1.3833	2.2012	1.2257
F	1.3990	1.3826	1.5040	1.0878	1.3566	2.1975	1.2220
SiH ₃	1.3889	1.3903	1.5123	1.0942	1.9030	2.1899	1.2270
PH ₂	1.3912	1.3885 1.3888	1.5087 1.5114	1.0916	1.8686	2.2055 2.1794	1.2257
SH	1.3942	1.3862	1.5081	1.0871	1.8226	2.1925	1.2246
Cl	1.3960	1.3853	1.5046	1.0837	1.7838	2.2000	1.2222
Br	1.3958	1.3860	1.5032	1.0820	1.9523	2.1995	1.2223
I	1.3945	1.3873	1.5039	1.0822	2.1723	2.1982	1.2229
<i>anti</i>							
CH ₃	1.3942	1.3859	1.5156	1.0788	1.5412	2.1858	1.2258
NH ₂	1.4017	1.3803 1.3804	1.5285 1.5195	1.0767	1.4614	2.1869 2.1916	1.2247
OH	1.4065	1.3775	1.5253	1.0740	1.4062	2.1906	1.2238
F	1.4049	1.3749	1.5180	1.0740	1.3794	2.1958	1.2241
SiH ₃	1.3837	1.3983	1.5027	1.0813	1.9145	2.1709	1.2278
PH ₂	1.3873	1.3923	1.5073	1.0761	1.8892	2.1780	1.2268
SH	1.3961	1.3844	1.5123	1.0755	1.8423	2.1851	1.2261
Cl	1.3977	1.3802	1.5109	1.0705	1.8246	2.1917	1.2256
Br	1.3951	1.3825	1.5057	1.0691	2.0023	2.1899	1.2265
I	1.3919	1.3860	1.5017	1.0692	2.2298	2.1872	1.2272

Table A.29 Angles (degrees) for the diene portion of the TS structures for the reaction of CpX and ethyne, evaluated at 6-31G(d)//6-31G(d).

X	C ₁ -C ₂ -C ₃ C ₂ -C ₃ -C ₄	C ₂ -C ₁ -C ₅ C ₃ -C ₄ -C ₅	C ₁ -C ₅ -C ₄	C ₁ -C ₅ -H ₅ C ₄ -C ₅ -H ₅	C ₁ -C ₅ -X C ₄ -C ₅ -X	H ₅ -C ₅ -X
H	108.8218	106.5562	98.7839	108.2191	116.0738	108.8156
<i>syn</i>						
CH ₃	108.7516	106.5557	98.2102	104.1169	120.8674	106.5285
NH ₂	108.8464 108.9270	106.1777 106.5880	98.3845	104.9819 104.8066	123.0134 117.6140	106.2225
OH	109.0025	106.0359	98.8382	106.2110	119.6332	105.1151
F	109.0467	105.1507	99.8313	107.9385	117.1478	106.3021
SiH ₃	108.7381	107.0597	97.9707	105.5279	119.5367	107.2299
PH ₂	108.8955 108.7333	106.5739 106.5321	98.4418	105.9627 105.2919	121.9882 118.0502	105.6058
SH	108.9247	105.9376	98.9865	106.5138	118.6633	106.4474
Cl	109.0622	104.7737	99.7431	107.1444	118.9595	104.0822
Br	109.0759	104.5715	99.9213	107.7942	119.0385	102.6541
I	109.0767	104.5969	99.8384	107.6770	119.6145	101.7325
<i>anti</i>						
CH ₃	108.7074	107.1306	97.7481	113.2377	112.2341	108.0177
NH ₂	108.7523 108.9523	107.0333 107.1923	97.6218	113.3734 113.5794	115.2673 110.2890	106.7307
OH	108.9661	106.9216	97.9714	114.5516	112.5157	105.0173
F	109.1237	106.7626	98.8426	115.9720	109.8377	106.2371
SiH ₃	108.5837	106.7567	98.3930	114.3519	111.5213	106.7242
PH ₂	108.7054	106.9807	98.2984	114.6223	109.9137	109.0528
SH	108.9100	106.9921	98.6225	114.5538	113.5396	102.6248
Cl	109.1038	107.0172	99.1937	116.2356	110.6853	103.9746
Br	109.1109	107.0085	99.6167	117.1597	110.2689	102.5155
I	109.0758	107.0440	99.8284	117.4371	110.3677	101.5933

Table A.30 Dienophile angle and angles of approach (degrees) for the TS's for the reaction of CpX and ethyne, evaluated at 6-31G(d)//6-31G(d).

X	C ₂ -C ₁ -C ₆ C ₃ -C ₄ -C ₇	C ₂ -C ₁ -C ₆ C ₃ -C ₄ -C ₇	C ₇ -C ₆ -H ₆ C ₆ -C ₇ -H ₇
H	99.2532	89.1449	154.1741
<i>syn</i>			
CH ₃	97.4729	91.1503	154.6407
NH ₂	98.5387	90.5810	154.4451
	98.1186	90.1651	155.0578
OH	98.9462	89.8678	154.6575
F	100.0363	89.5596	155.7241
SiH ₃	98.0918	90.0826	153.8272
PH ₂	97.9140	89.9022	154.4600
	98.6331	90.5309	154.0815
SH	98.9425	90.0382	154.8381
Cl	98.6581	91.1959	155.5930
Br	98.4282	91.4843	155.5271
I	98.1026	91.7336	155.2679
<i>anti</i>			
CH ₃	98.8148	89.6797	154.1649
NH ₂	99.4798	89.0407	154.6473
	99.2971	89.0046	154.9329
OH	100.0239	88.2568	155.2832
F	100.6883	86.8887	155.2514
SiH ₃	98.4236	90.2818	153.2495
PH ₂	98.9908	89.3034	153.8241
SH	99.0391	88.3694	154.2939
Cl	99.8818	86.6648	154.6998
Br	99.7208	86.3305	154.4314
I	99.4100	86.3410	154.1686

Table A.31 Bond lengths (Å) for the TS structures for the reaction of CpX and maleimide, evaluated at 6-31G(d)//6-31G(d).

X	C ₂ -C ₃	C ₁ -C ₂ C ₃ -C ₄	C ₁ -C ₅ C ₄ -C ₅	C ₅ -H ₅	C ₅ -X	C ₁ -C ₆ C ₄ -C ₇	C ₆ -C ₇
H	1.3913	1.3905	1.5066	1.0904	1.0804	2.1969	1.3874
<i>syn</i>							
CH ₃	1.3906	1.3908	1.5116	1.0929	1.5244	2.2141	1.3850
NH ₂	1.3938	1.3877	1.5109	1.0958	1.4465	2.2130	1.3813
OH	1.3966	1.3860 1.3854	1.5150 1.5059	1.0917	1.3907	2.2048 2.2133	1.3817
F	1.3980	1.3850	1.5048	1.0865	1.3598	2.2075	1.3824
SiH ₃	1.3869	1.3939	1.5116	1.0966	1.9024	2.2070	1.3876
PH ₂	1.3886	1.3924	1.5111	1.0895	1.8730	2.2126	1.3856
SH	1.3921	1.3907 1.3888	1.5118 1.5080	1.0866	1.8215	2.1927 2.2286	1.3852
Cl	1.3948	1.3880	1.5060	1.0834	1.7839	2.2134	1.3832
Br	1.3944	1.3889	1.5046	1.0817	1.9524	2.2133	1.3836
I	1.3930	1.3902	1.5051	1.0819	2.1739	2.2135	1.3842
<i>anti</i>							
CH ₃	1.3928	1.3888	1.5144	1.0812	1.5417	2.1961	1.3878
NH ₂	1.3995	1.3834 1.3839	1.5269 1.5189	1.0793	1.4583	2.2025 2.2013	1.3864
OH	1.4043	1.3813	1.5245	1.0765	1.4013	2.2041	1.3851
F	1.4032	1.3787	1.5176	1.0767	1.3723	2.2113	1.3852
SiH ₃	1.3822	1.4008	1.5013	1.0834	1.9200	2.1756	1.3914
PH ₂	1.3859	1.3949	1.5064	1.0785	1.8929	2.1865	1.3897
SH	1.3941	1.3880	1.5112	1.0782	1.8386	2.1962	1.3888
Cl	1.3961	1.3839	1.5111	1.0734	1.8109	2.2049	1.3878
Br	1.3933	1.3865	1.5060	1.0720	1.9848	2.2024	1.3893
I	1.3897	1.3901	1.5019	1.0722	2.2095	2.1982	1.3905

Table A.32 Angles (degrees) for the diene portion of the TS structures for the reaction of CpX and maleimide, evaluated at 6-31G(d)//6-31G(d).

X	C ₁ -C ₂ -C ₃ C ₂ -C ₃ -C ₄	C ₂ -C ₁ -C ₅ C ₃ -C ₄ -C ₅	C ₁ -C ₃ -C ₄	C ₁ -C ₅ -H ₅ C ₄ -C ₅ -H ₅	C ₁ -C ₅ -X C ₄ -C ₅ -X	H ₅ -C ₅ -X
H	109.0149	106.6122	99.3604	108.2971	116.0828	108.1707
<i>syn</i>						
CH ₃	108.9556	106.5502	98.7302	103.8299	120.9983	106.2034
NH ₂	108.9910	106.2780	98.9510	104.5519	117.7169	111.5434
OH	109.0887	105.7623	99.4757	106.2887	119.2456	109.6653
	109.1909	106.0559		105.9784	114.9626	
F	109.2559	105.2040	100.3605	108.4832	116.2239	106.6933
SiH ₃	108.9580	106.7854	98.6309	104.1749	122.5824	102.2382
PH ₂	108.9946	106.2404	98.8194	104.9010	119.8293	106.8579
SH	109.1021	105.5271	99.3932	106.0528	120.9742	106.0592
	109.1554	105.8012		105.5339	117.4920	
Cl	109.2636	104.7119	100.1959	107.0945	118.6961	104.2636
Br	109.2714	104.5106	100.3575	107.5875	118.9669	102.7108
I	109.2678	104.5343	100.2718	107.2268	119.9302	101.3647
<i>anti</i>						
CH ₃	108.8823	107.1899	98.3408	113.2618	112.2037	107.5300
NH ₂	108.9402	107.0628	98.1923	113.1899	115.5228	106.3014
	109.1262	107.1780		113.3875	110.3406	
OH	109.1346	106.9230	98.5003	114.2097	112.8019	104.6604
F	109.2786	106.6882	99.3265	115.5775	110.0026	106.2628
SiH ₃	108.7603	106.8143	99.0043	114.5635	111.3958	106.0231
PH ₂	108.8735	107.0136	98.8495	114.6092	109.9692	108.5206
SH	109.0696	106.9568	99.1657	114.3544	113.6570	102.2667
Cl	109.2393	106.9487	99.5897	115.7057	110.9507	104.1480
Br	109.2296	106.9357	99.9589	116.4922	110.6239	102.8660
I	109.1855	106.9763	100.1314	116.7131	110.7633	102.0267

Table A.33 Dienophile angle and angles of approach (degrees) for the TS's for the reaction of CpX and maleimide, evaluated at 6-31G(d)//6-31G(d).

X	C ₂ -C ₁ -C ₆ C ₃ -C ₄ -C ₇	C ₃ -C ₁ -C ₆ C ₃ -C ₄ -C ₇	C ₇ -C ₆ -H ₆ C ₆ -C ₇ -H ₇	C ₇ -C ₆ -C ₈ C ₆ -C ₇ -C ₉	C ₈ -C ₆ -H ₆ C ₈ -C ₇ -H ₇
H	101.2520	88.8943	125.9783	107.9403	119.2116
<i>syn</i>					
CH ₃	99.5846	91.0063	126.5597	107.9629	118.8657
NH ₂	101.0879	90.1191	125.6114	108.0378	120.3586
OH	102.1234	89.3628	125.7118	108.0798	120.2483
	101.7438	89.2485	125.8536	107.9915	120.4849
F	102.5758	89.0249	125.8486	108.0174	120.2036
SiH ₃	99.1969	90.9324	126.0982	107.9151	118.5593
PH ₂	99.5497	91.4355	125.7658	107.9528	119.1078
SH	100.5548	91.6397	125.7943	107.8578	119.5579
	100.1197	90.4164	126.1775	108.0651	119.1750
Cl	100.7834	91.3151	126.0216	107.9815	119.6894
Br	100.4418	91.7264	126.0684	107.9692	119.5472
I	99.9093	92.1399	126.1059	107.9563	119.3148
<i>anti</i>					
CH ₃	100.8782	89.3972	126.0783	107.9413	119.2034
NH ₂	101.6106	88.6976	126.1021	107.9969	119.3495
	101.3507	88.9632	126.1584	107.9342	119.3709
OH	102.0540	88.1877	126.2463	107.9908	119.5440
F	102.8225	86.9605	126.2214	107.9872	119.5328
SiH ₃	100.3967	90.0898	125.7554	107.8620	118.8363
PH ₂	101.0340	89.1579	125.8673	107.8904	118.9935
SH	101.0487	88.3877	126.0029	107.9171	119.1501
Cl	101.9308	86.9068	126.0806	107.9334	119.3062
Br	101.7012	86.7352	125.9678	107.9078	119.2196
I	101.3203	86.8538	125.8870	107.8858	119.1189

Table A.34 Bond lengths (Å) for the TS structures for the reaction of CpX and TAD, evaluated at 6-31G(d)//6-31G(d).

X	C ₂ -C ₃	C ₁ -C ₂ C ₃ -C ₄	C ₁ -C ₃ C ₄ -C ₅	C ₅ -H ₅	C ₅ -X	C ₁ -C ₆ C ₄ -C ₇	C ₆ -C ₇
H	1.3929	1.3916	1.5031	1.0893	1.0774	2.0845	1.2936
<i>syn</i>							
CH ₃	1.3937	1.3903	1.5085	1.0928	1.5221	2.1039	1.2893
NH ₂	1.3972	1.3882 1.3853	1.5210 1.5063	1.0908	1.4298	2.0811 2.1423	1.2881
OH	1.3990	1.3853	1.5132	1.0880	1.3707	2.1116	1.2880
F	1.4005	1.3852	1.5053	1.0873	1.3426	2.0835	1.2862
SiH ₃	1.3888	1.3942	1.5062	1.0944	1.9108	2.0894	1.2935
PH ₂	1.3924	1.3949 1.3878	1.5093 1.5060	1.0915	1.8676	2.0520 2.1387	1.2906
SH	1.3952	1.3890	1.5082	1.0888	1.8035	2.0981	1.2890
Cl	1.3974	1.3878	1.5055	1.0841	1.7650	2.0824	1.2865
Br	1.3968	1.3888	1.5039	1.0824	1.9317	2.0811	1.2870
I	1.3952	1.3902	1.5036	1.0825	2.1532	2.0812	1.2880
<i>anti</i>							
CH ₃	1.3947	1.3899	1.5102	1.0782	1.5408	2.0871	1.2935
NH ₂	1.4017	1.3844 1.3852	1.5236 1.5160	1.0765	1.4543	2.0934 2.0883	1.2913
OH	1.4057	1.3827	1.5224	1.0741	1.3982	2.0873	1.2896
F	1.4043	1.3798	1.5173	1.0740	1.3682	2.0904	1.2900
SiH ₃	1.3837	1.4021	1.4961	1.0812	1.9212	2.0633	1.2990
PH ₂	1.3891	1.3953 1.3957	1.5003 1.5038	1.0794	1.8880	2.0772 2.0684	1.2970
SH	1.3951	1.3901	1.5077	1.0766	1.8312	2.0762	1.2950
Cl	1.3965	1.3859	1.5100	1.0722	1.7988	2.0798	1.2938
Br	1.3932	1.3889	1.5050	1.0711	1.9688	2.0750	1.2961
I	1.3896	1.3929	1.5007	1.0715	2.1914	2.0713	1.2979

Table A.35 Angles (degrees) for the diene portion of the TS structures for the reaction of CpX and TAD, evaluated at 6-31G(d)//6-31G(d).

X	C ₁ -C ₂ -C ₃ C ₂ -C ₃ -C ₄	C ₂ -C ₁ -C ₅ C ₃ -C ₄ -C ₅	C ₁ -C ₃ -C ₄	C ₁ -C ₅ -H ₅ C ₄ -C ₅ -H ₅	C ₁ -C ₃ -X C ₄ -C ₅ -X	H ₅ -C ₅ -X
H	108.7430	107.5243	99.0744	108.5302	115.3166	109.4592
<i>syn</i>						
CH ₃	108.6945	107.6761	98.4643	104.1959	120.0612	107.8454
NH ₂	108.8228 108.9194	107.1365 107.8195	98.5587	104.5704 104.7704	122.8456 116.6980	107.5356
OH	108.9996	107.1082	98.9781	105.8744	119.2851	106.2449
F	109.0213	105.9625	99.8284	107.6866	116.6385	107.7192
SiH ₃	108.6404	108.1228	98.3799	105.3498	120.7329	104.6687
PH ₂	108.7902 108.7114	107.3418 107.9390	98.6579	105.3008 105.1898	123.3353 117.8383	104.8225
SH	108.9113	106.8861	99.1067	105.2602	121.1774	103.1254
Cl	108.9763	105.8959	99.6094	106.5242	118.7708	105.6281
Br	108.9620	105.8059	99.7189	107.0914	118.9113	104.2932
I	108.9340	105.9923	99.6298	106.9798	119.5733	103.1952
<i>anti</i>						
CH ₃	108.6259	108.0446	98.1759	112.4771	112.2161	109.0197
NH ₂	108.7658 108.8786	107.8239 107.9667	98.0663	112.6148 112.4972	115.3010 110.2523	107.9490
OH	108.9413	107.6204	98.3060	113.5763	112.5834	106.3435
F	109.0946	107.4312	98.9756	115.1240	109.5898	108.1141
SiH ₃	108.4373	107.6957	98.7194	113.5532	112.0378	106.9778
PH ₂	108.5884 108.6163	107.9218 107.7094	98.7128	113.4381 112.8783	115.0813 111.4931	105.4543
SH	108.8090	107.7116	98.9177	113.4773	113.6373	104.1139
Cl	108.9984	107.7117	99.1380	114.8606	110.8538	106.2979
Br	108.9664	107.6903	99.4227	115.5785	110.5692	105.2012
I	108.8904	107.7294	99.5437	115.6494	110.9202	104.3498

Table A.36 Dienophile angle and angles of approach (degrees) for the TS's for the reaction of CpX and TAD, evaluated at 6-31G(d)//6-31G(d).

X	C ₂ -C ₁ -N ₆ C ₃ -C ₄ -N ₇	C ₂ -C ₁ -N ₆ C ₂ -C ₄ -N ₇	C ₇ -N ₆ -C ₈ C ₆ -N ₇ -C ₉
H	98.7193	87.7560	109.5029
<i>syn</i>			
CH ₃	97.4219	89.1898	109.5734
NH ₂	98.7460 97.4527	89.4145 87.6992	109.6318 109.5825
OH	98.8156	88.0016	109.6322
F	99.7996	88.3926	109.5524
SiH ₃	97.2874	88.6037	109.5350
PH ₂	97.2968 97.6341	90.7812 86.8504	109.6601 109.4937
SH	97.5503	89.3493	109.5844
Cl	98.5059	89.7336	109.5604
Br	98.2447	89.9977	109.5571
I	97.8839	90.0829	109.5569
<i>anti</i>			
CH ₃	98.3404	88.2496	109.5150
NH ₂	98.8772 98.4884	87.6046 88.0443	109.5580 109.5326
OH	99.2607	87.3103	109.5603
F	100.1333	86.0058	109.5547
SiH ₃	98.1600	88.9915	109.4336
PH ₂	97.9499 98.4159	88.2323 88.3608	109.4753 109.4542
SH	98.4345	87.4852	109.4951
Cl	99.3276	86.0932	109.5056
Br	99.1234	86.0695	109.4775
I	98.7931	86.3134	109.4541

Table A.37 Bond lengths (Å) and angles (degrees) for CprX, evaluated at 6-31++G(d)//6-31++G(d).

X	C ₁ -C ₃ C ₂ -C ₃	C ₁ -C ₂	C ₁ -H ₁ C ₂ -H ₂	C ₃ -H ₃	C ₃ -X	C ₂ -C ₁ -C ₃ C ₁ -C ₂ -C ₃	C ₁ -C ₃ -C ₂	C ₁ -C ₃ -H ₃ C ₂ -C ₃ -H ₃	C ₁ -C ₃ -X C ₂ -C ₃ -X	X-C ₃ -H ₃
H	1.4974	1.2777	1.0680	1.0826	1.0826	64.7437	50.5125	119.8641	119.8641	113.1868
BH ₂	1.5350	1.2638	1.0669	1.0843	1.5490	65.6906	48.6188	115.5588	120.4956	117.9062
CH ₃	1.4960	1.2803	1.0689	1.0851	1.5194	64.6652	50.6695	117.8320	122.3574	112.5883
NH ₂	1.4914 1.4768	1.2871	1.0699 1.0698	1.0811	1.4447	63.7215 64.8867	51.3918	119.7971 119.7023	123.9392 120.9747	109.9632
OH	1.4726	1.2915	1.0700	1.0768	1.3966	63.9904	52.0191	122.0737	122.4572	107.1167
F	1.4550	1.2899	1.0686	1.0755	1.3811	63.6875	52.6251	125.2935	118.5914	107.6007
SiH ₃	1.5153	1.2729	1.0678	1.0875	1.8834	65.1655	49.6691	116.3671	122.6688	114.2031
PH ₂	1.5031	1.2744	1.0678	1.0833	1.8518	64.9182	50.1637	117.9237	120.7403	114.5070
SH	1.4856 1.4838	1.2784	1.0678 1.0679	1.0793	1.8198	64.4285 64.5697	51.0019	120.4727 119.9198	122.1195 119.8673	111.2819
Cl	1.4607	1.2853	1.0679	1.0746	1.8142	63.8985	52.2030	124.3464	120.1502	107.0695

Table A.38 Bond lengths (Å) for the *endo-syn* and *endo-anti* addition TS's for the reaction of CprX and Bdiene.

X	C ₁ -C ₃ C ₂ -C ₃	C ₁ -C ₂	C ₁ -H ₁ C ₂ -H ₂	C ₃ -H ₃	C ₃ -X	C ₁ -C ₄ C ₂ -C ₇	C ₄ -C ₅ C ₆ -C ₇	C ₅ -C ₆
H	1.4808	1.3373	1.0683	1.0870	1.0825	2.2573	1.3688	1.4089
<i>endo-syn</i>								
BH ₂	1.4877	1.3349	1.0689	1.0993	1.5777	2.2895	1.3669	1.4139
CH ₃	1.4939	1.3428	1.0703	1.0888	1.5186	2.2560	1.3710	1.4036
NH ₂	1.4856	1.3426	1.0699	1.0892	1.4441	2.2402	1.3701	1.4018
OH	1.4787	1.3529	1.0712	1.0801	1.3888	2.2411	1.3739	1.4031
F	1.4599	1.3542	1.0700	1.0782	1.3764	2.2184	1.3723	1.4001
SiH ₃	1.5020	1.3293	1.0687	1.0901	1.8993	2.2759	1.3679	1.4083
PH ₂	1.4953	1.3363	1.0691	1.0858	1.8618	2.2537	1.3700	1.4041
SH	1.4834	1.3417	1.0695	1.0818	1.8254	2.2323	1.3705	1.4034
	1.4795		1.0694			2.2523	1.3700	
Cl	1.4621	1.3491	1.0695	1.0764	1.8186	2.2263	1.3709	1.4025
<i>endo-anti</i>								
BH ₂	1.5105	1.3209	1.0676	1.0881	1.5529	2.2670	1.3679	1.4097
CH ₃	1.4805	1.3401	1.0694	1.0887	1.5185	2.2562	1.3691	1.4088
NH ₂	1.4810	1.3491	1.0706	1.0844	1.4410	2.2360	1.3711	1.4070
	1.4672		1.0703			2.2439	1.3703	
OH	1.4720	1.3480	1.0693	1.0840	1.3951	2.2306	1.3722	1.4056
	1.4597		1.0690			2.2365	1.3715	
F	1.4554	1.3524	1.0687	1.0782	1.3726	2.2184	1.3734	1.4034
SiH ₃	1.4922	1.3315	1.0685	1.0929	1.8804	2.2702	1.3674	1.4108
PH ₂	1.4851	1.3336	1.0683	1.0874	1.8499	2.2603	1.3686	1.4093
SH	1.4742	1.3394	1.0682	1.0832	1.8125	2.2426	1.3703	1.4077
	1.4718		1.0685			2.2534	1.3695	
Cl	1.4583	1.3467	1.0682	1.0782	1.7953	2.2302	1.3718	1.4053

Table A.39 Angles (degrees) for the *endo-syn* and *endo-anti* addition TS's for the reaction of CprX and Bdiene.

X	C ₂ -C ₁ -C ₃ C ₁ -C ₂ -C ₃	C ₁ -C ₃ -C ₂	C ₁ -C ₃ -H ₃ C ₂ -C ₃ -H ₃	C ₁ -C ₃ -X C ₂ -C ₃ -X	X-C ₃ -H ₃	C ₁ -C ₄ -C ₅ C ₂ -C ₄ -C ₆	C ₄ -C ₅ -C ₆ C ₂ -C ₅ -C ₆
H	63.1566	53.6868	117.6135	120.9003	113.5631	100.9916	122.4032
<i>endo-syn</i>							
BH ₂	63.3441	53.3118	116.1932	129.3146	105.2558	100.9958	122.6485
CH ₃	63.2929	53.4142	115.4936	125.8346	110.2489	104.9479	122.6699
NH ₂	63.1348	53.7304	116.6477	121.7027	113.7244	103.4477	122.5990
OH	62.7772	54.4456	119.2561	124.8415	106.6848	105.2446	122.5396
F	62.3670	55.2660	122.6702	120.9453	106.9805	103.3688	122.4390
SiH ₃	63.7350	52.5301	114.4088	129.6453	107.2037	102.8620	122.7556
PH ₂	63.4580	53.0840	115.7962	125.4303	110.5017	103.6947	122.6723
SH	62.9233	53.8520	117.9351	126.4956	108.4011	103.7086	122.6375
	63.2247		117.5387	123.5290		103.4437	122.6241
Cl	62.5247	54.9505	121.1584	124.5492	104.5923	103.3396	122.5593
<i>endo-anti</i>							
BH ₂	64.0716	51.8568	114.0464	121.3518	117.7114	100.6075	122.4562
CH ₃	63.0913	53.8173	115.4518	123.2914	113.1970	101.1856	122.4324
NH ₂	63.2911	54.4629	116.9993	124.9344	110.9618	101.9515	122.4080
	62.2461		117.1529	121.7766		101.5321	122.3862
OH	62.1663	54.7445	118.6472	121.3822	112.9164	102.4070	122.3621
	63.0892		118.7449	118.6838		102.0670	122.3481
F	62.3158	55.3684	122.3145	119.4809	109.1037	102.5267	122.2822
SiH ₃	63.5015	52.9969	114.5044	123.6937	114.0832	100.3766	122.4892
PH ₂	63.3222	53.3555	115.8964	121.5218	114.9288	100.8097	122.4555
SH	62.8653	54.0841	118.2526	122.6838	112.2751	101.5262	122.4551
	63.0506		117.7364	120.2073		101.1783	122.3730
Cl	62.5015	54.9970	121.4706	120.7727	108.7198	101.9206	122.3455

Table A.40 Bond lengths (Å) for the *exo-syn* and *exo-anti* addition TS's for the reaction of CprX and Bdiene.

X	C ₁ -C ₃ C ₂ -C ₃	C ₁ -C ₂	C ₁ -H ₁ C ₂ -H ₂	C ₃ -H ₃	C ₃ -X	C ₁ -C ₄ C ₂ -C ₇	C ₄ -C ₅ C ₆ -C ₇	C ₅ -C ₆
H	1.4910	1.3348	1.0680	1.0852	1.0840	2.2598	1.3684	1.4084
<i>exo-syn</i>								
BH ₂	1.5315	1.3222	1.0676	1.0880	1.5487	2.2726	1.3697	1.4076
CH ₃	1.4974	1.3403	1.0692	1.0890	1.5196	2.2724	1.3698	1.4073
NH ₂	1.4878	1.3393	1.0688	1.0881	1.4489	2.2525	1.3710	1.4065
OH	1.4814	1.3460	1.0694	1.0839	1.4037	2.2434	1.3716	1.4052
	1.4693		1.0690			2.2409	1.3720	
F	1.4600	1.3518	1.0689	1.0775	1.3871	2.2293	1.3729	1.4036
SiH ₃	1.5109	1.3314	1.0681	1.0930	1.8830	2.2809	1.3687	1.4085
PH ₂	1.5025	1.3340	1.0682	1.0864	1.8512	2.2724	1.3699	1.4072
SH	1.4883	1.3380	1.0685	1.0819	1.8220	2.2440	1.3710	1.4066
	1.4867		1.0681			2.2730	1.3700	
Cl	1.4646	1.3467	1.0685	1.0764	1.8259	2.2383	1.3716	1.4051
<i>exo-anti</i>								
BH ₂	1.5221	1.3190	1.0673	1.0868	1.5551	2.2655	1.3682	1.4085
CH ₃	1.4909	1.3374	1.0691	1.0871	1.5192	2.2601	1.3684	1.4086
NH ₂	1.4910	1.3467	1.0704	1.0830	1.4396	2.2428	1.3695	1.4078
	1.4762		1.0701			2.2545	1.3690	
OH	1.4758	1.3516	1.0701	1.0786	1.3918	2.2366	1.3703	1.4064
F	1.4615	1.3506	1.0682	1.0777	1.3749	2.2305	1.3713	1.4049
SiH ₃	1.5043	1.3293	1.0683	1.0900	1.8853	2.2686	1.3675	1.4096
PH ₂	1.4958	1.3314	1.0680	1.0854	1.8543	2.2623	1.3682	1.4086
SH	1.4775	1.3438	1.0690	1.0825	1.8170	2.2501	1.3690	1.4079
Cl	1.4647	1.3454	1.0677	1.0766	1.8049	2.2395	1.3702	1.4036

Table A.41 Angles (degrees) for the *endo-syn* and *endo-anti* addition TS's for the reaction of CprX and Bdiene.

X	C ₂ -C ₁ -C ₁ C ₁ -C ₂ -C ₃	C ₁ -C ₃ -C ₂	C ₁ -C ₃ -H ₃ C ₂ -C ₃ -H ₃	C ₁ -C ₃ -X C ₂ -C ₃ -X	X-C ₃ -H ₃	C ₁ -C ₄ -C ₅ C ₂ -C ₇ -C ₆	C ₄ -C ₅ -C ₆ C ₇ -C ₆ -C ₇
H	63.4090	53.1821	118.7954	120.9218	112.3323	100.3903	122.4603
<i>endo-syn</i>							
BH ₂	64.4258	51.1485	114.9616	123.1063	114.8391	97.7972	122.5850
CH ₃	63.4142	53.1717	116.6254	124.9983	110.0305	98.2734	122.7724
NH ₂	63.2506	53.4987	118.2042	120.2810	113.6655	99.2263	122.3562
OH	62.4009	54.2779	120.9063	121.3243	110.5520	99.3355	122.4001
	63.3212		120.6439	118.8687		99.1439	122.4983
F	62.4214	55.1573	124.5590	119.3554	106.6327	98.9780	122.5121
SiH ₃	63.8572	52.2857	115.4296	127.6437	108.5522	98.0565	122.6683
PH ₂	63.6435	52.7130	117.1196	122.9384	112.0610	97.8832	122.5449
SH	63.2112	53.4558	119.0847	124.7173	109.2265	98.6250	122.5337
	63.3330		118.7950	121.8269		98.1377	122.5262
Cl	62.6285	54.7430	122.7972	122.9652	104.6267	98.6786	122.6023
<i>exo-anti</i>							
BH ₂	64.3232	51.3537	115.0294	121.5003	116.5689	100.5573	122.4579
CH ₃	63.3507	53.2986	116.6958	123.0369	112.2366	100.2579	122.4972
NH ₂	62.4471	53.9836	118.3141	124.5481	110.0263	99.8129	122.5174
	63.5693		118.4925	121.4081		99.6296	122.4926
OH	62.7477	54.5046	120.4650	123.1314	107.2899	99.3811	122.4842
F	62.4799	55.0402	123.5916	119.2915	107.9194	99.0964	122.4578
SiH ₃	63.7795	52.4410	115.6988	123.5229	113.0969	100.4380	122.5152
PH ₂	63.5732	52.8568	117.1315	121.3800	113.8319	100.1486	122.5201
SH	62.9504	54.0993	119.8847	123.7955	107.3330	99.5566	122.5253
Cl	62.6596	54.6807	123.0297	120.4835	107.3226	99.0896	122.5063

Table A-42 Electronegativity and measures of size. Radii are in pm, A-value, P-value, P-value, and E_s are in $\text{kJ}\cdot\text{mol}^{-1}$.

X	group/atomic (*) electronegativity	van der Waals radius	Bragg- Slater radius	A-value	P-value	n-value	molar refractivity	Taft's E_s	van der Waals volume
H	2.20*	120	25	0.0	0.0		1.0	0.0	1.20
BH ₃	1.93		85						
CH ₃	2.56	170	77	7.1		8.5	5.7	-1.24	13.67
NH ₃	3.10	155	65	5.0		7.2	4.4	-0.61	10.54
OH	3.64	152	60	2.2		6.3	2.6	-0.55	8.04
F	4.00	147	50	0.6	4.6	5.1	0.8	-0.46	6.20
SiH ₃	1.91	210	110						
PH ₃	2.17	180	100						
SH	2.63	180	100				8.8	-1.07	14.80
Cl	3.05	175	100	1.8	14.7	8.1	5.8	-0.97	12.24
GeH ₃	2.05	219	125						
AsH ₃	2.26	185	115						
SeH	2.47	190	115						
Br	2.75	185	115	1.6	15.9	9.2	8.7	-1.16	14.60
SnH ₃	1.72*	217	145						
SbH ₃	1.82*	206	149						
TeH	2.01*	198	140						
I	2.21*			1.8	17.6	9.9	14.0	-1.40	20.35
CH=CH ₂	2.61						9.8	-2.84	
C≡CH	2.66			0.7		8.9	5.5	-0.51	
C≡N	2.69					7.9	5.0	-2.40	
CF ₃				4.6			6.7	-1.01	
NO ₂	3.25								



